NAVAL POSTGRADUATE SCHOOL

MONTEREY, CALIFORNIA

THESIS

THE USE OF AGENT BASED SIMULATION FOR COOPERATIVE SENSING OF THE BATTLEFIELD

by

Lawrence A.H. Liang

December 2005

Thesis Advisor:	Susan M. Sanchez
Second Reader:	David W. Netzer

Approved for public release; distribution is unlimited.

THIS PAGE INTENTIONALLY LEFT BLANK

REPORT DOCUMENTATION PAGE		Form Approved OMB No. 0704-0188

1. AGENCY USE ONLY *(Leave blank)*	2. REPORT DATE December 2005	3. REPORT TYPE AND DATES COVERED Master's Thesis

4. TITLE AND SUBTITLE: The Use of Agent-Based Simulation for Cooperative Sensing of the Battlefield	5. FUNDING NUMBERS
6. AUTHOR(S) Lawrence A.H. Liang	
7. PERFORMING ORGANIZATION NAME(S) AND ADDRESS(ES) Naval Postgraduate School Monterey, CA 93943-5000	8. PERFORMING ORGANIZATION REPORT NUMBER
9. SPONSORING /MONITORING AGENCY NAME(S) AND ADDRESS(ES) N/A	10. SPONSORING/MONITORING AGENCY REPORT NUMBER

11. SUPPLEMENTARY NOTES The views expressed in this thesis are those of the author and do not reflect the official policy or position of the Department of Defense or the U.S. Government.

12a. DISTRIBUTION / AVAILABILITY STATEMENT Approved for public release; distribution is unlimited.	12b. DISTRIBUTION CODE

13. ABSTRACT (maximum 200 words)

Many military Intelligence Surveillance and Reconnaissance (ISR) operations would benefit greatly from a fleet of disparate sensor-bearing UAVs that are tightly integrated via a communications network, work cooperatively for a common operational objective, enhance situation awareness of the areas of operation, and increase persistence of sensor dwell time on strategic targets. This would enable continuity in the entire target acquisition cycle, from detection to classification to identification and finally localization of targets, in a diverse and dynamic environment. The integration of sensors and development of tactics in a cooperative sensing environment is one of the current focuses among the military intelligence community, and hence motivates this thesis effort. By building models with an existing agent-based simulation platform and using an extremely efficient experimental design methodology, numerous factors which could potentially affect the effectiveness of a cooperative sensing network against two arrays of targets are explored. The factors considered include UAV airspeed, reliability, detection/classification coverage and probability, network latency and degradation, UAV configurations and responsiveness, as well as air space separation. The two arrays of targets are mobile armor concentrations and time critical targets; these vary in their deployment profiles, vulnerability constraints and ease of detectability. Factors characterizing these targets, such as the shoot-and-scoot behavior of time critical targets, are also investigated. The study provides operational insights pertaining to the design and effective use of cooperative sensing for ISR purposes. These include the importance of having good UAV sensor capabilities, the need for a suite of sensors to aid in locating well-camouflaged time-critical targets, and the need for "intelligent" application of UAV cooperation tactics based on the characteristics of recently-classified targets.

14. SUBJECT TERMS Cooperative Sensing Network, Intelligence Surveillance and Reconnaissance (ISR), Unmanned Aerial Vehicle (UAV), Agent Based Modeling (ABM), Map Aware Non-uniform Automata (MANA), Nearly Orthogonal Latin Hypercube, Design of Experiment	15. NUMBER OF PAGES 121
	16. PRICE CODE

17. SECURITY CLASSIFICATION OF REPORT	18. SECURITY CLASSIFICATION OF THIS PAGE	19. SECURITY CLASSIFICATION OF ABSTRACT	20. LIMITATION OF ABSTRACT
Unclassified	Unclassified	Unclassified	UL

NSN 7540-01-280-5500

Standard Form 298 (Rev. 2-89)
Prescribed by ANSI Std. 239-18

THIS PAGE INTENTIONALLY LEFT BLANK

Approved for public release; distribution is unlimited.

THE USE OF AGENT-BASED SIMULATION FOR COOPERATIVE SENSING OF THE BATTLEFIELD

Lawrence A.H. Liang
Ministry of Defence, Republic of Singapore
B.A.Sc. (Computer Engineering), Nanyang Technological University, 1998
M.Phil. (Computer Engineering), Nanyang Technological University, 2000

Submitted in partial fulfillment of the
requirements for the degree of

MASTER OF SCIENCE IN OPERATIONS RESEARCH

from the

NAVAL POSTGRADUATE SCHOOL
December 2005

Author: Lawrence A.H. Liang

Approved by: Susan M. Sanchez
Thesis Advisor

David W. Netzer
Second Reader

James N. Eagle
Chair, Department of Operations Research

THIS PAGE INTENTIONALLY LEFT BLANK

ABSTRACT

Many military Intelligence Surveillance and Reconnaissance (ISR) operations would benefit greatly from a fleet of disparate sensor-bearing UAVs that are tightly integrated via a communications network, work cooperatively for a common operational objective, enhance situation awareness of the areas of operation, and increase persistence of sensor dwell time on strategic targets. This would enable continuity in the entire target acquisition cycle, from detection to classification to identification and finally localization of targets, in a diverse and dynamic environment. The integration of sensors and development of tactics in a cooperative sensing environment is one of the current focuses among the military intelligence community, and hence motivates this thesis effort. By building models with an existing agent-based simulation platform and using an extremely efficient experimental design methodology, numerous factors which could potentially affect the effectiveness of a cooperative sensing network against two arrays of targets are explored. The factors considered include UAV airspeed, reliability, detection/classification coverage and probability, network latency and degradation, UAV configurations and responsiveness, as well as air space separation. The two arrays of targets are mobile armor concentrations and time critical targets; these vary in their deployment profiles, vulnerability constraints and ease of detectability. Factors characterizing these targets, such as the shoot-and-scoot behavior of time critical targets, are also investigated. The study provides operational insights pertaining to the design and effective use of cooperative sensing for ISR purposes. These include the importance of having good UAV sensor capabilities, the need for a suite of sensors to aid in locating well-camouflaged time-critical targets, and the need for “intelligent” application of UAV cooperation tactics based on the characteristics of recently-classified targets.

THIS PAGE INTENTIONALLY LEFT BLANK

THESIS DISCLAIMER

The reader is cautioned that computer programs developed in this research may not have been exercised for all cases of interest. While every effort has been made, within the time available, to ensure that the programs are free of computational and logic errors, they cannot be considered validated. Any application of these programs without additional verification is at the risk of the user.

THIS PAGE INTENTIONALLY LEFT BLANK

TABLE OF CONTENTS

LIST OF FIGURES

LIST OF ACRONYMS AND ABBREVIATIONS

ADA	Air Defense Artillery
AGL	Above Ground Level
CCD	Concealment, Camouflage and Deception
DMSO	Defense Modeling and Simulation Office
DO	Distributed Operations
DoD	Department of Defense
EO	Electro-optics
FOPEN	Foliage Penetration
FOV	Field Of View
IPB	Intelligence Preparation of the Battlefield
IR	Infra-Red
ISR	Intelligence, Surveillance and Reconnaissance
LADAR	Laser Radar
LAE	Low Altitude and Endurance
LOS	Line Of Sight
MAE	Medium Altitude and Endurance
MANA	Map Aware Non-uniform Automata
MCWL	Marine Corps Warfighting Lab
MEB	Marine Expeditionary Brigade
MHPCC	Maui High Performance Computing Center
MLRS	Multiple Launched Rocket System

MOE	Measure Of Effectiveness
M&S	Modeling and Simulation
NCW	Network Centric Warfare
NOLH	Nearly Orthogonal Latin Hypercube
OLH	Orthogonal Latin Hypercube
SA	Situation Awareness
SAM	Surface-to-Air Missile
SAR	Synthetic Aperture Radar
SEAD	Suppression of Enemy Air Defense
SV04	Sea Viking 2004
SV06	Sea Viking 2006
TCT	Time Critical Target or Time Critical Targeting
UAV	Unmanned Aerial Vehicle
UCAV	Unmanned Combat Aerial Vehicle
VTOL	Vertical Takeoff and Landing

ACKNOWLEDGMENTS

The completion of this thesis would not have been possible without the knowledge, encouragement and support from many people surrounding me. Below are a few of those important people in the creation of this thesis.

I begin by thanking Professor Susan Sanchez for taking me as an advisee and for introducing me to agent-based simulation and design of experiment methodologies which have proven appropriate for the analysis of a large dimensional problem like cooperative sensing for military Intelligence, Surveillance and Reconnaissance operations. Her interest and dedication to her profession are unparalleled.

I cannot forget to mention Professor Dave Netzer for his guidance and expertise throughout all of the aspects of producing the thesis. He has been instrumental in turning operational ideas and concepts into modeling and analytical approaches.

I am grateful to the Project Albert team: Dr. Gary Horne, Mr. Matthew Koehler and Mr. Steve Upton for their precious time and dedication to conduct the mini workshop in NPS to get us onboard our thesis quickly. The sharing of their experience and expertise has saved us many weeks of self exploring of the Project Albert tools.

I must also acknowledge my fellow students for their earnest help, and in many occasions, inspired me to greater heights. I have learnt a great deal from those times of quality discussion. Friends like Rick, Kok Meng and Victor, amongst many others, are worth mentioning.

Finally and most importantly, I appreciate my wife, Christina, for her unceasing encouragement and support. In those valleys of this academic journey, she never stopped cheering me forward. Without her, I would have to actually think about administering my life. We have shared many great moments together in Monterey, those sweet memories will last us a long way.

THIS PAGE INTENTIONALLY LEFT BLANK

EXECUTIVE SUMMARY

As a result of combat operations during Operation Iraqi Freedom, a major lesson learned indicates that the success of a battle is increasingly reliant on more accurate and timely collection of the battle-space intelligence. Unmanned systems, and certainly Unmanned Aerial Vehicles (UAVs), are widely used in today's military ISR operations, and will be even more prevalent in the next generation military as warfighting concepts such as Network Centric Warfare and Distributed Operation emerge. A number of significant military Intelligence Surveillance and Reconnaissance (ISR) operations would benefit greatly from a fleet of disparate sensor-bearing UAVs that are integrated via a communications network, work in a cooperative manner for a common operational objective, enhance situation awareness of the areas of operation, and increase persistence of sensor time on strategic targets. Furthermore, the cooperative sensing network enables continuity in the entire target acquisition cycle, from detection to classification to identification and finally localization of interested targets, in a diverse and dynamic environment. The integration and tactics development in a cooperative sensing environment are currently key focuses among the military intelligence community, and serve as the motivation for this thesis.

The objective of the thesis is to explore the enhancement in detection and classification capabilities for mission critical and time critical targets, should the capability of a cooperative sensing network becomes available to the Marine Expeditionary Brigade commander. Two types of UAVs are considered: the Low Altitude and Endurance (LAE) and the Medium Altitude and Endurance (MAE). The two target types in the study include the time critical targets and the mobile armor concentrations; they represent the two main arrays of targets characterized by their deployment profiles, vulnerability constraints and ease of detectability. The study measures the proportion of the enemy's mobile targets and Time Critical Targets (TCTs) classified over a four-hour period for Intelligence Preparation of the Battlefield prior to a Marine Expeditionary

amphibious assault. In doing so, the author applies suitable analytical methodologies to gain insights into questions as these:

- What are good cooperative sensing network configurations?
- Are there diminishing returns with increasing UAVs allocated?
- What are good UAV responses in a cooperative sensing environment?
- What are the effects of degraded communications and increasing latency?
- What are the effects of UAV failure in the presence of cooperative sensing?

A number of models are developed with reference to the Marine Corps Warfighting Laboratory's Sea Viking 2004 scenario using the agent-based simulation platform *Map Aware Non-uniform Automata* (MANA). The computing resource requirements for these models are much lower than for most conventional simulation models, and can be executed over tens of thousands repetitions to explore many possible representations of real-life situations Time and cost considerations would preclude running even a fraction of these situations in a field experiment, so the simulation results provide useful insights regarding overall system effectiveness. A total of 20 factors varying over 1290 design points are considered. Controllable factors pertaining to the number of LAEs, UAV characteristics such as airspeed, detection range, classification range and probability of classification, network parameters including link reliability and message latency, as well as air-space separation are explored. Factors uncontrollable in real-world settings, such as enemy concealment, counter detection sensor range and period of vulnerability, are also varied in the simulation runs. The 1290 excursions with 50 repetitions each, amounting to 64,500 MANA runs, are submitted to the MAUI High Performance Computing Center for computation. Another set of models and excursions are also generated to study the effects of an LAE failure at specific time periods during the four-hour operation.

The data collected from the simulations is analyzed using several graphical and statistical tools. Multiple Linear Regression and Data Partitioning are used in conjunction with the results from other statistical techniques to draw useful insights and operational guidance relevant to the employment of cooperative sensing for military ISR purposes.

The results show approximately 9.8% of the TCTs and 27.2% of the armor targets are classified with the configuration of an MAE and four LAEs at the end of the four-hour operation. The relatively low classification measures are attributed to the relatively small coverage area extended throughout the entire duration of operation as compared to the considerably large area of interest. The analysis leads to the observation that the classification effectiveness depends on the UAV routings, and is an important consideration when preparing an intelligence collection plan. Prior knowledge of the enemy's courses of action, target's profiles and terrain information is beneficial. An LAE should be more responsive to the MAE cueing to achieve higher classification performance against TCTs and less responsive to the MAE cueing when acquiring armor targets. However, an LAE should tend to follow a new classified enemy contact when searching out armor targets as they are generally deployed in formations.

While much is discussed about the behaviors of the UAVs in a cooperative sensing environment with shared situation awareness, many fundamental sensor characteristics like longer classification range and higher classification probability also have impacts on the overall classification effectiveness. However, an LAE classification range that is larger than 5 km easily distracts the LAE; more clutter appears in the sensor view and penalizes the overall classification performance. An increase in number of LAEs generally improves the target classification proportions, but the proportion of armor classification seems to taper off at four LAEs for this scenario.

Link reliability and message latency are shown to have no significant effects on the classification outcome. Air-space separations also do not matter. High TCT concealment capabilities and counter-detection sensor ranges

significantly hinder good classification performance of the sensing network. A UAV equipped solely with an electro-optics sensor may not be effective against the well-camouflage TCTs. Against such targets, other sensors or radars may be a more viable option.

There is some indication showing that cooperative sensing does provide a more robust solution in some scenarios in terms of the classification performance should an LAE fail or be shot down during the four-hour operation. Following a fixed set of standard operating tactics regardless of the targets of interest and enemy's courses of action is not the way forward in employing a cooperative sensing network.

I. INTRODUCTION

A. OVERVIEW

Unmanned Aerial Vehicles (UAVs) are remotely piloted or self-piloted aircraft that carry cameras, sensors, communication equipment or other payloads. They have been used primarily in Intelligence, Surveillance and Reconnaissance (ISR) roles since the 1950s. Since 1964 the Department of Defense (DoD), having realized the potential of UAVs as a key component in ISR missions, had 11 different types of UAV developed. However, due to acquisition and development problems, only three entered production. The U.S. Navy has also studied the feasibility of operating Vertical Takeoff and Landing (VTOL) UAVs since the early 1960s to overcome the limitation of short takeoff distance from surface vessels, the QH-50 Gyrodyne torpedo-delivery drone being an early example. Nonetheless, high cost and technological immaturity precluded acquiring and fielding operational VTOL UAV systems at that time. By the early 1990s, DoD sought UAVs capable of satisfying surveillance requirements in Close Range, Short Range or Endurance categories, where persistence, dynamic re-tasking capability and real-time imagery are critical to the mission. By the late 1990s, the Close and Short Range categories were combined, and a separate Shipboard category emerged. The current classes of these vehicles are the Tactical UAV and the Long Endurance UAV, however, both classes are still predominately employed for ISR purposes (Federation of American Scientists Intelligence Resource Program website, 2005).

The use of UAVs evolved rapidly over the last two decades to conduct air-to-ground strike missions with the development of the Unmanned Combat Aerial Vehicles (UCAVs). The operational UCAV system is envisioned as a force enabler for the U.S. Air Force that will conduct Suppression of Enemy Air Defense (SEAD) and strike missions in support of post-2010 manned strike packages. This SEAD/Strike mission will be the first instantiation of an UCAV vision that will evolve into a broader range of combat missions as the concept

and technologies mature, and the UCAV affordability potential is realized. The DARPA/Air Force/Boeing X-45A technology demonstration aircraft completed its first flight on 22 May 2002. Multi-aircraft testing began in 2003 when a second X-45A became operational, leading to joint UCAV and manned exercises in 2006 (Federation of American Scientists Military Analysis Network website, 2005). As technology advances and the importance of unmanned vehicles as a force enabler is realized by the military, the Stealth UAV becomes the current class of UAV to be researched and developed.

Being an unmanned platform and generally smaller in size, the UAV is preferred over manned aircraft for strategic deployment into the airspace deep behind the adversary line of operations which is often protected by heavy air defense elements. Today UAVs are widely deployed in Time Critical Targeting (TCT) operations, where long endurance and dynamic re-tasking capabilities are imperative to the success of acquiring of high value targets and eventually executing the kill chain in prosecuting these targets. The concept of cooperative sensing soon evolved to offer the ability to cue available and suitable joint sensors networked together in the theatre of war to extend the persistence of sensor time on target. This is currently drawing great attention of military strategists and technologists. Medium Altitude Endurance (MAE) UAVs have the capability of extended flight duration, typically 6-12 hours or longer. These are supplemented with the tactical Low Altitude Endurance (LAE) UAVs which enable near-real-time imagery and local tracking of targets. While the MAE UAVs have long-range deployment and wide-area surveillance or long sensor dwell over the target area to provide initial detections, the close-in LAE UAVs allow the identification, localization and tracking of interested targets with high accuracy.

Today there are some 50 U.S. companies, academic institutions, and government organizations developing over 150 UAV designs. Forty of these companies have some 115 of these designs flying, i.e., at least one working prototype built. Fifteen of these companies have 26 models of UAVs in, or ready for, production (UAV Forum website, 2005). With recent emphasis in Network

Centric Warfare (NCW) which extensively exploits UAVs as an indispensable part of the sensor grid, the development of UAVs will definitely be an important part of military development and a future force multiplier.

B. MOTIVATION

As a result of combat operations during Operation Iraqi Freedom, a major lesson learned indicates that a better asset to collect battle-space intelligence is crucial to the way forward (U.S. Joint Forces Command, 2004). A number of significant military operations would benefit greatly from a fleet of disparate sensor-bearing UAVs that are integrated via a communications network, work in a cooperative manner for a common operational objective, enhance situation awareness of the areas of operation, and increase persistence of sensor time on strategic targets. Figure 1 depicts a cooperative sensing network employed in a Time Critical Targeting operation. Multiple UAVs allow sensing to be performed in parallel, thereby reducing the amount of time required to gather data. If a vehicle becomes disabled, the remaining vehicles can continue sensing, although at a reduced collection rate. Most importantly, the cooperative sensing network enables continuity in the entire target acquisition cycle, from detection to classification to identification and finally localization of interested targets, in a diverse and dynamic environment. The success of cooperative sensing depends significantly on two key technological emphases: the development of state-of-art imaging sensors and the integration of sensor and ISR systems in a seamless and cooperative manner. The ensuing paragraphs provide further discussion on these technologies.

Perhaps the need for a complementary suite of sensors is of greater importance for surveillance on land than for a maritime environment. The richness of terrain variation and coverage on the ground mean that targets moving across land surfaces could employ effective Concealment, Camouflage and Deception (CCD) tactics to prevent being detected by the adversary. The entire battle of ground search and detection revolves around the ability to employ

sensing equipments and technologies that are superior to the adversary's CCD capability. Over the last two decades, the development of air-to-ground sensor technologies has improved by leaps and bounds. Conventional microwave radar is now able to detect longer and perform better in a wider range of operating environments. Many Electro-Optics (EO) and Infra-Red (IR) imaging sensors can achieve astonishing spatial resolutions of less than one meter, the Foliage Penetration (FOPEN) Radar and Synthetic Aperture Radar (SAR) allow detection of targets hidden under concealment and camouflage, Laser Radar (LADAR) imaging is achievable with higher spatial resolution and precision up a tenth of a meter, and the "through-the-wall" imaging radar is under research and development to provide the capability to look into buildings at standoff distances and build a picture of the tactical situation. The availability of a diverse range of air-to-ground radars and imaging sensors makes it possible for a fleet of UAVs, each mounted with disparate sensors, to be integrated to form a cooperative sensing network to collect data in a parallel, coordinated and optimal manner.

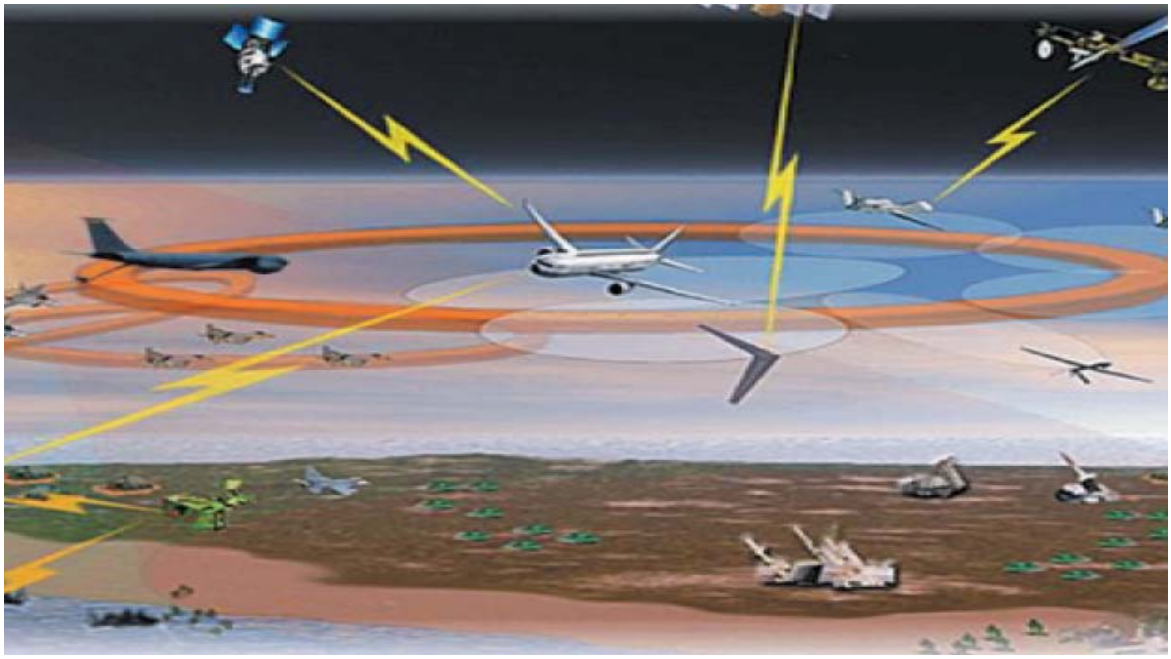

Figure 1. A Cooperative Sensing Network Deployed for Time Critical Targeting Operation [Best Viewed in Color]

The greater challenge of cooperative sensing, in the author's opinion, does not lie on the employment of advanced sensors as one could expect these sensors to be widely available in the near future given the amazing rate at which technology advances. The greater challenge involves seamless integration of all the sensors in the theatre of operations and tactics development to provide high-quality, uninterrupted information over the entire target life to the commander for making battle decisions effectively. This involves an intelligent sensing system that is able to efficiently task suitable and available sensors on-the-fly given various tactical situations. The sensing system should also be capable of prioritizing conflicting sensing requirements, if any should occur. The development of such a smart system is by no means trivial; it is not uncommon to have overwhelming ISR requests beyond the availability of the sensors. The tight integration amongst sensor systems has prompted the need for developing a high throughput and robust communications network. Obviously, the availability of such a sensing network would not be effective without restructuring the military ISR processes, just as adopting the Network Centric Warfare paradigm would not be effective without changing the traditional ways of fighting a war.

C. BACKGROUND WORK

There have been a number of preceding theses at the Naval Postgraduate School (NPS) that use an agent-based modeling approach to explore the use of UAVs for military intelligence gathering missions. Each thesis focuses on a different aspect of using UAVs on a targeted ISR operational scenario. Below are brief summaries of some of these works.

Raffetto (2004) analyzes the impact various UAV capabilities have on intelligence gathering missions for a Marine Expeditionary Brigade (MEB) commander's 2015 UAV to support rapid planning and decision making for multiple concurrent operations. This facilitates maneuver and precision engagement based on the UAV operations in the Sea Viking 2004 (SV04) scenario provided by Marine Corps Warfighting Lab (MCWL). He explores the

validity of current requirements and provides insights into the importance of various UAV characteristics, such as airspeed, endurance, sweep width, and sensor capability for a single UAV. The analysis seeks to measure the proportion of the enemy's entities detected over time, hence the ability to gain superiority in situation awareness (Raffetto, 2004).

Berner (2004) explores the effective use of multiple UAVs for the Navy's Surface Search and Control mission based on a coastal environment scenario with dense shipping traffic and sparse enemy contacts. In addition to the impacts various UAV parameters have on the detection and classification effectiveness of the enemy contacts, he also shows the ISR effectiveness for different UAV tactics and combinations (Berner, 2004). However, although the contacts acquired by each UAV are routed to a central command, this has no influence on the collection plan of the other UAVs as would occur within a cooperative sensing network.

McMindes (2005) looks at how UAV survivability is affected by UAV speed, stealth, altitude, and sensor range, as well as enemy force sensor ranges, probability of kill, array of forces, and numerical strength. The analysis, which is based upon the SV04 scenario of Raffetto (2004), concludes that a UAV is highly survivable with fast speed, with the exception that stealth becomes more important than speed alone when the enemy has extremely high-capability assets (McMindes, 2005).

D. THE PROBLEM

The Sea Viking Division of the MCWL is responsible for experiment planning and design of the ongoing Sea Viking live experimentation campaign. Sea Viking is planned and executed in two-year segments. The current focus for Sea Viking 2006 (SV06) is to conduct live experimentation that will assist in the development of operational maneuver from the sea/ship to objective maneuver tactics, techniques and procedures and to develop and assess experimental

capabilities that support these concepts. Additionally, SV06 will examine the emerging Distributed Operations (DO) concept which will deploy for operations in the Global War on Terror (Marine Corps Warfighting Laboratory Sea Viking website, 2005). General Hagee, Commandant of the Marine Corps, highlights the required capabilities for enhanced intelligence capabilities to collect, report, and exploit intelligence for small units employing DO. These include employment or direction of unmanned ground or air vehicles, or the ability to access command and control networks for the purpose of extracting specific intelligence pertinent to the unit's local situation (Hagee, 2005). A cooperative sensing capability will indeed provide the required strategic and tactical ISR requirements for the emerging DO concept.

The objective of this study is to explore the enhancement in the effectiveness on detection and classification capabilities of mission critical and time critical targets, should the capability of a cooperative sensing network become available to the MEB commander. These targets are deemed to have significant implications for subsequent battle developments, and hence warrant elaborate sensing requirements directed toward them. The study aims to measure the proportion of the enemy's mobile and time critical targets classified over a four-hour period for Intelligence Preparation of the Battlefield (IPB) prior to an amphibious assault, thus offering insights about the effectiveness of the cooperative sensing network for ISR missions against these target types.

E. SCOPE AND ASSUMPTIONS

The research focuses primarily on formulating and building models to capture essential characteristics of UAVs in an IPB operation. These models are explored extensively to uncover how the effectiveness of cooperative sensing capability is affected by ISR processes and structures as well as UAV responses to shared Situation Awareness (SA). An existing agent-based distillation called *Map Aware Non-uniform Automata* (MANA) is used to construct the scenario. The scenario is modified from Raffetto's SV04 base scenario to eliminate the red

infantry elements and include high value targets such as the Air Defense Artillery (ADA) elements, Surface-to-Air Missile (SAM) launchers, armor concentrations and Multiple Launched Rocket Systems (MLRS). To further evaluate the effects of cooperative sensing, communications models are incorporated into the network of UAVs, and various mixes of MAE and LAE UAVs are introduced.

The model exploration uses a very efficient experimental design methodology to capture a large number of factors and their interactions which potentially affect the scenario outcomes. The controllable factors to be considered include UAV parameters (airspeed, reliability, detection/classification coverage and probability), network parameters (latency and degradation), ISR configurations (number of LAEs to one MAE), UAV behaviors (reactivity to other UAVs' Situation Awareness, reactivity to spontaneous enemy contacts) and airspace deconfliction rules (minimum tactical separation in time and space). The uncontrollable factors to explore, which are often ignored in other studies, include the enemy Time Critical Target's parameters (concealment, detection range and vulnerability duration) that characterize the shoot-and-scoot behaviors.

The experiment consists of running the agent-based models over a large combination of design points (i.e., settings for the controllable and uncontrollable factors) and collecting the measures of effectiveness. Regression and other statistical analysis techniques are then used to analyze the data and to provide insights to the following questions:

- What are good cooperative sensing network configurations?
- Are there diminishing returns with increasing UAVs allocated?
- What are good UAV responses in a cooperative sensing environment?
- What are the effects of degraded communications and increasing latency?
- What are the effects of UAV failure in the presence of cooperative sensing?

Furthermore, the analysis allows identification of main effects and interactions which may have significance impacts on ISR effectiveness for a cooperative sensing network, thus providing areas of focus for more detailed experiments and analysis.

One should be aware that the employment of a disparate suite of sensors is an important consideration for cooperative sensing. However, it is not the focus of this thesis to model detailed sensor performances against a wide spectrum of terrains and targets. The sensors in the agent-based model, though they consider factors of detection degradation imposed by the different terrain features, are subjected to the same degradation on each terrain feature irrespective of the types of sensors and targets. The range of sensors explored is broadly classified into two main categories: the stand-off wide area sensors on board the MAE and the close-in small area sensors on board the LAE.

F. AGENT-BASED SIMULATION

Reductions in military operating budgets and improvements in computer technology have driven the increasing use of simulations throughout the military. Simulations are being employed in a wide variety of military applications including training, mission rehearsal, system analysis, system acquisition and tactical decision aiding. Furthermore, high complexity and nonlinearities in combat, where outcomes are highly correlated to battlefield conditions and events, make it too complicated and costly - if not impossible - to explore a full range of possibilities for any useful study in field experiments. In most of these cases, simulations are used for initial exploration to bound complex problems and tease out areas of emphasis relevant to the questions at hand that can then be expounded more meaningfully using methods such as field experiments and live tests and evaluations. The mission of the Defense Modeling and Simulation Office (DMSO) is to support the war-fighter by leading a defense-wide team in fostering interoperability, reuse, and affordability of Modeling and Simulation (M&S), as well as the responsive application of these tools to provide

revolutionary war-fighting capabilities and improve aspects of DoD operations. As a catalyst organization for the DoD, DMSO ensures that M&S technology development is consistent with other related initiatives by performing key corporate level functions necessary to encourage cooperation, synergism, and cost-effectiveness among the M&S activities of the DoD Components (Defense Modeling and Simulation Office website, 2005).

The traditional (and widely used) modeling technique in the DoD uses differential equations to calculate casualties and changes in the frontlines. These equations are called Lanchester equations and were originally published in 1914. Many modern simulation models use variants of the Lanchester equations to predict the attrition rates of opposed forces massed in parallel strips across the battlefront. According to a RAND study, “these models were developed when computers had much more limited capabilities, making it necessary to reduce the number of simulation entities and to use aggregation techniques” (Gonzales, et al., 2001). The aggregated Lanchester equation-based models are beginning to fall out of favor in some DoD agencies for several reasons. Tighe cites a paper by Battilega and Grange that shows that the equations “do not accurately model many historical battles” (Tighe, 1999). This is surprising given that many of these battles follow the massive force-on-force attrition warfare formula for which the equations are designed. With modern warfare increasingly reliant on C4ISR systems, the old models break down even further. Gonzales points out that the legacy models cannot model individual C4ISR effects, and can only be represented by adjusting parameters. He continues by highlighting the fact that these models cannot take into account how information is used to support command decision-making processes. This severely limits their utility for assessing many Information Superiority concepts, such as force synchronization, that may be enhanced or enabled by advanced C4ISR systems (Gonzales, et al., 2001). In other words, what good is C4ISR when your forces’ movements are scripted?

These problems have been addressed by a new generation of models that attempt to model complex adaptive systems. Forces are made up of individual "agents" that are programmed to follow a rough set of rules. "The individual agents are then responsible for making their own decisions as to how they should prosecute the battle" (Tighe, 1999). Hence they are adaptive. While the rules that govern an individual agent may be simple, a collection of agents interacting with one another (and the synthetic environment) will exhibit complex behaviors. These agent-based models, which are better suited for the analysis of modern concepts such as Network Enabled Warfare and Effects Based Operations, have begun to catch on in the DoD M&S community (Bjorkman and Sheldon, 2002; North, et al., 2003).

G. MAP AWARE NON-UNIFORM AUTOMATA (MANA)

The benefits of agent-based simulation models are greatly harnessed by the combat researchers and analysts in the Marine Corps Warfighting Laboratory (MCWL). The MCWL's Project Albert is the research and development effort whose goal is to develop the process and capabilities of Data Farming. Data Farming is a method to address decision-maker's questions by applying high-performance computing to relatively simple models in order to examine and understand the landscape of potential simulated outcomes, enhance intuition, find surprises and outliers, and identify potential options. Data Farming is the method by which potentially millions of data points are explored and captured. This process is made possible, in part, by the exploitation of High Performance Computing assets and methods, and the project is fully supported by the Maui High Performance Computing Center (MHPCC). The Project Albert modeling approach is achieved through the development of a suite of models, sometimes called *distillations*, to drive home the point that these models are produced as an intentional complement to the very highly-detailed simulations being developed and used within the DoD, which by the very fact that they are so highly-detailed and encumbered, do not permit the examination of a very wide range of

possibilities and outcomes. By virtue of distillations being much easier to run and understand, they are proving to be effective tools that help capture and scientifically reproduce the ideas of subject matter experts, such as those thinking about tomorrow's concepts, doctrine, and requirements. This suite of entity-based models allow for rapid and highly tailorable changes in entity characteristics and behaviors, quite amenable to, and intentionally designed for rapid, repeatable concept exploration. Project Albert develops a suite of modeling platforms, rather than a single realization of a model. This has the added benefit of allowing the robustness of observations across modeling platforms to be examined. Also, each model has inherent strengths and unique capabilities with regard to each aspect of modeling how entities think, decide, shoot, move, and communicate (Marine Corps Warfighting Laboratory Project Albert website, 2005).

The MANA software, developed by the New Zealand Defense Technology Agency, is one of the distillation modeling platforms extensively used by the Project Albert Team to answer real world questions. The authors of the MANA User Manual (Galligan, et al., 2004) present a powerful illustration, "…the world is far more complicated than Newton's equations (laws of motion)… Therefore, to rely on models built "on a bedrock of physics" is to deceive ourselves. It is a myth that a more detailed model is necessarily a better model, because it is impossible to capture accurately every aspect of nature". They further their arguments by noting that the non-linear nature of equations describing many real world phenomena makes them extremely sensitive to initial conditions. This means that even infinitesimal errors in describing the real world initial conditions will cause the model to make predictions that are almost uncorrelated with actual events. The illustration provides a clear motivation for the design of MANA as what they refer as a scenario-exploring model.

MANA is in a general class of models called agent-based models (ABMs), which have the characteristics of containing entities that are controlled by internal decision-making algorithms. Hence, an ABM combat model contains entities

representing military units that make their own decisions as they react to their surroundings, as opposed to the modeler explicitly determining their behaviors in advance. Models built in MANA, like those built using other Project Albert modeling platforms, are sometimes called agent-based distillations because their common intention is to model the essence of a problem rather than to describe every aspect of a military operation. MANA is designed to explore key concepts such as Situation Awareness, Communications, Terrain Features, Waypoints and Event-Driven Personality Changes. In MANA, agents can exhibit a surprisingly wide set of behaviors as long as careful configurations are given to sets of parameters that determine the agents' propensities, move constraints, basic capabilities (such as sensors, weapons, interactions and movement speed) and movement characteristics (Galligan, et al., 2004).

The model is designed to analyze the value of things such as situation awareness, command and control, and the informational edge that enhanced sensors provide. These features are limited in those models which purport to be detailed, highly physics based and rigorous where these aspects of combat can only be represented within the model in a completely arbitrary way by the modeler (Galligan, et al., 2004). These strengths of MANA as an agent-based model ties in closely to Gonzales' (2001) presentation about the limitations of DoD legacy models as discussed in Section F. These are also the strengths that attracted the author to selecting MANA as a modeling tool for the analysis of cooperative sensing.

H. THESIS ORGANIZATION

Chapter II begins by painting the modified Sea Viking scenario which includes the area of operation and the two sided force deployments and objectives. The chapter also describes the model development and in particular the modeling parameters and techniques used to achieve the desired agent behaviors.

Chapter III covers a detailed discussion of the controllable and uncontrollable factors of interest in the analysis and their operational significance and tradeoffs. It also provides a brief contrast of various possible designs of experiments and concludes that a Nearly Orthogonal Latin Hypercube design is the most efficient choice for running the experiments.

In Chapter IV, the data analysis process is presented and followed by a meticulous exploration of the simulation results using regression and statistical analysis techniques.

Chapter V concludes the thesis with a presentation of operational insights and recommendations from the results of the analysis. It also presents suggestions for follow-on work that the author considers worthwhile exploring.

II. SCENARIO AND MODEL DEVELOPMENT

A. THE SCENARIO

The IPB scenario prior to the Marine's amphibious assault depicted in Figure 2 provides the basis for the study of the effectiveness of a cooperative sensing network. The area of operation extends across the Los Angeles and San Diego city areas represented in the map as light orange regions. The Red target types included in this scenario represent two main arrays of targets characterized by their deployment profiles, vulnerability constraints and ease of detectability.

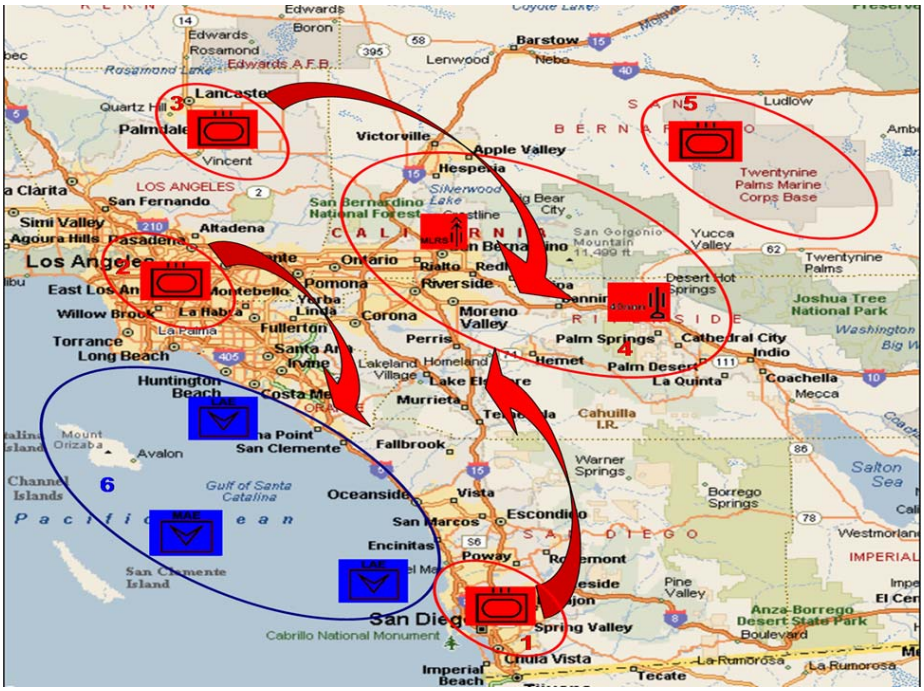

Figure 2. IPB Scenario for Marine Amphibious Assault [Best Viewed in Color]

Area 5 at the upper right corner shows the Twenty-nine Palms encompassing the Red objective and their senior leadership, and is protected by an armored battalion. Area 4 in the central region defines the deployment ground of the multiple launched rocket systems and the anti-aircraft artillery elements for the defense of the Red objective. These targets are commonly deployed in isolation in a small fighting unit. They are usually well-concealed and have limited

windows of vulnerability, which makes detection and prosecution of these targets very challenging. The three armor battalions concentrated in Areas 1, 2 and 3 move along the axis as shown in the map to stage a barrier patrol line against the coastal assault. The armor concentrations represent target arrays that are commonly deployed in formations and are “noisy” from the electronic and visual detection perspectives, hence making them easier targets for detection and prosecution. Area 6 represents the Blue MAE and LAEs supporting the IPB operation for the MEB. Each LAE has a pre-assigned area of responsibility to provide classification of enemy contacts, while the single MAE sweeps through the whole area of operation to provide wide area sensor coverage.

B. MODEL DEVELOPMENT

1. Environment

The terrain shown in the Figure 3 is created by Raffetto (2004). The dark yellow in the terrain depiction represents city areas; the blue regions signify bodies of water; the brown, dark and light green regions identify the desert, dense and sparse forested areas respectively; the light yellow lines show the highways and major road networks in the cities. The terrain features are associated with parameters that affect the movement speed, engagement effectiveness, and concealment of the agents. These values provide multipliers to compute the overall effective speed, kill and detection outcomes of the agents at every time step. The blue aircraft icons depict the Blue MAE and LAEs; the red icons represent the Red armored vehicles and time critical targets; the pink icons identify the neutral elements.

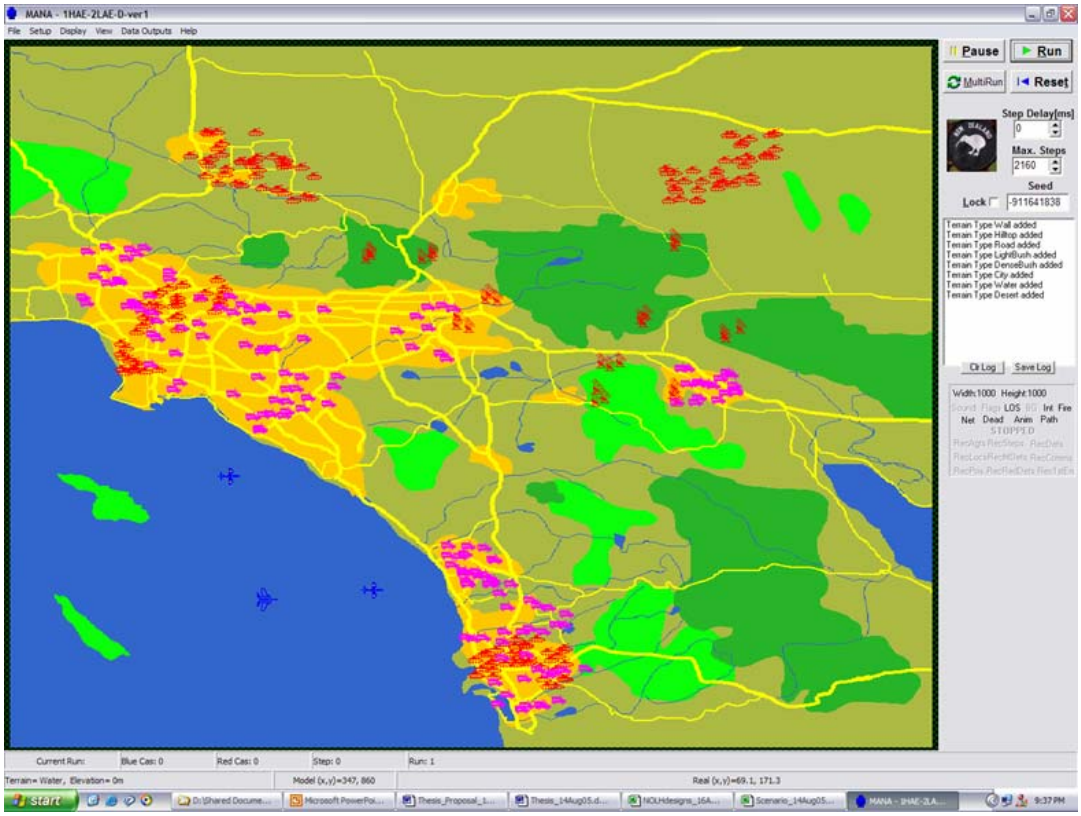

Figure 3. MANA Model for IPB Scenario [Best Viewed in Color]

The battle-space extends across 32.6 to 35.1 degrees in latitude and -118.8 to -115.6 degrees in longitude, which equates to 160 nm in width and 150 nm in height. The maximum spatial resolution that can be represented in MANA is 1000 by 1000 cells, which computes to an average of approximately 287 by 287 meters in both length and width per cell for this scenario. The model is set to elapse 10 real-time seconds for every time step taken for the simulation. Since the total amount of time for the IPB operations takes four hours, the simulation terminates after 1440 time steps have elapsed. The conversions between MANA units and real-world units are tabulated in a spreadsheet as illustrated in Figure 4 to facilitate subsequent unit conversions in the development of the models.

BATTLEFIELD SETTINGS

Real World

	Latitude	Longitude			
Lower Left	32.6	-118.8	degree	1 degree latitude =	60.00 nm
Upper Right	35.1	-115.6	degree	1 degree longitude =	49.83 nm

Width	159.46	nm
Height	150.00	nm

MANA Number of Cells

X	1000
Y	1000

Conversion Matrix

each cell is how many units...

	nm	miles	feet	km	meters
	1	1.1508	6076.1155	1.8520	1852
X	0.16	0.18	968.87	0.30	295.31
Y	0.15	0.17	911.42	0.28	277.80
X/Y	0.15	0.18	940.15	0.29	286.56

each unit is how many cells...

X	6.2713	5.4496	0.0010	3.3862	0.0034
Y	6.6667	5.7932	0.0011	3.5997	0.0036
X/Y	6.4690	5.6214	0.0011	3.4930	0.0035 <-- Used for conversion between actual and MANA

each time step is...

secs	mins	hours
10	0.1667	0.0028

each time unit is how many steps...

secs	mins	hours	
0.1	6	360	<-- Used for conversion between actual and MANA

time steps in real time...

hours	time steps
4	1440

Figure 4. Unit Conversions Between MANA Model and Real-World Units

2. Time Critical Target

Time Critical Targets (TCTs) are targets requiring immediate response because they either pose (or will soon pose) a danger to friendly forces, or they are highly lucrative, fleeting targets of opportunity with an extremely limited time window of vulnerability, the attack of which is critical to ensure the successful execution of the subsequent battle operations. The Red MLRS and ADA elements in the model, totaled 30, are classified as time critical targets as they a limited windows of vulnerability characterized by their shoot-and-scoot tactics. These targets are generally deployed in terrains where concealment to escape enemy's detection is almost perfect. The TCT comes out of its "hiding place" to a nearby operational spot only when it is ready to fire a salvo or there is a need to reload its ammunitions, and then goes right back into "hiding". The TCT only subjects itself to detection and engagement vulnerabilities during this limited period of vulnerability which generally last no longer than 30 minutes, hence acquiring and prosecuting such targets is challenging.

The TCT in the model is developed by creating a cycle of waypoints and altering the behaviors of the agents in each state. The agent moves from the current waypoint to the next during the *RunStart* state and stays in this state for a defined vulnerable duration which will eventually be data farmed. Once it reaches the next waypoint and the vulnerability duration elapses, the agents change into the *ReachFinalWaypoint* state where the concealment rate (another parameter to be data farmed) is applied to these targets to emulate the "hide" behaviors. The TCT is assumed to have the capability to detect an approaching UAV with its counter-detection sensor and evade detection by the UAV by setting the concealment rate in the *EnemyContact* state. The TCT loops through the cycle until it is detected and classified by a Blue UAV as shown in the state transition diagram of Figure 5.

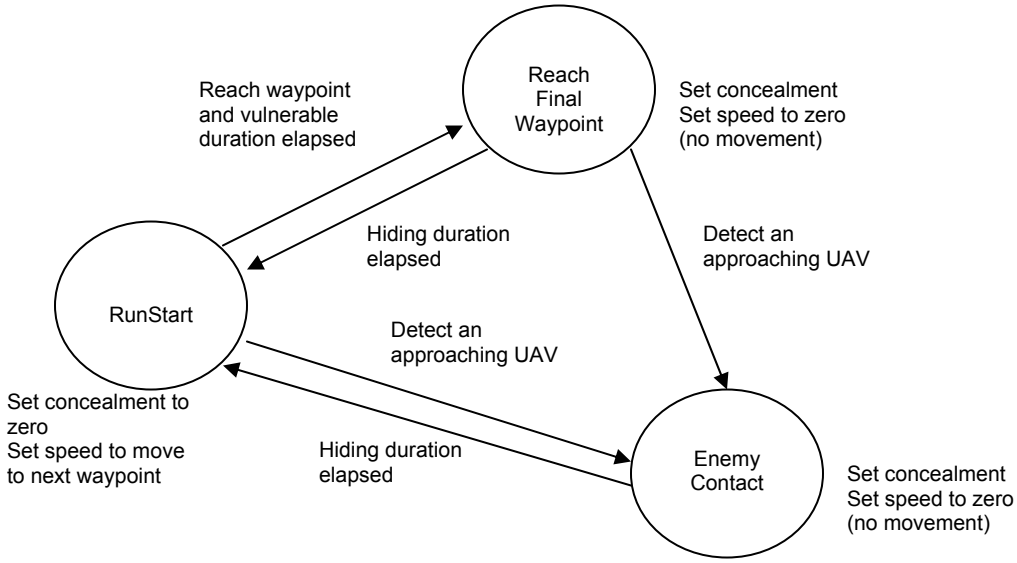

Figure 5. State Diagram of a Time Critical Target Agent

3. Armor Battalion

The model consists of four armor battalions; each is implemented as a separate squad and comprises 40 medium tanks. The three coastal battalions are scripted to follow pre-defined routes along the road axes and the last battalion is setup to patrol around the parameter of Twenty-nine Palms. The

agents are set up with propensities (or weights, as commonly known in many agent-based models) to move towards the next waypoint and to move on terrains that are easy-going, in this case, to follow the road networks whenever possible.

4. MAE and LAE UAVs

Due to the considerably limited area of operation, it is operationally infeasible to devote more than one MAE like the Predator to support the mission. However, an amphibious strike force commander may have up to five LAEs like the Pioneer at his disposal. While the MAE provides wide area surveillance and reconnaissance for the entire area of operation with poor classification capability, an LAE can provide effective close-in classification of the enemy contacts within its higher resolution sensor range. The models characterize these UAV parameters by varying the detection and classification ranges and the corresponding probabilities.

The UAVs are given a “weapon” to shoot at the targets with range and probability equal to the range and probability for sensor classification, respectively. This means that a target is “killed” when being classified to prevent repeated classification of the same target. The “weapon” is loaded with a very large amount of “ammunition” to ensure the ammunition is not depleted.

To support the analysis of the effects of LAE failure on ISR effectiveness of the cooperative sensing network, one UAV killer agent is created to “shoot” and disable a single LAE after a pre-determined time from the beginning of the scenario. The UAV killer is randomly positioned in the area of operation and remains inactive in the *Default* state until it is time for an LAE to fail. It then switches to another state where the “weapon” is enabled and “fires” a single shot with a probability of kill equal to 1.0 at the nearest LAE, hence disabling that LAE. The MAE in the model is assumed to be 100% reliable over the four-hour IPB operation, as MAEs are generally designed for longer endurance missions and with longer mean-time-to-failure parameters.

The movements and interactions of the UAV are characterized by a set of propensities in the model. Each UAV's responsiveness to either an incoming contact from another UAV or a newly sighted enemy contact determines its tendency to be diverted from its original route. The propensity for each UAV to move towards the next waypoint is set to 50. By changing the propensities to move *towards enemy* in the Agent SA properties, and move *towards unknown* in the Inorganic SA, the reactivity of the UAV to such targeting information can be explored. Additionally, the airspace deconfliction parameter which determines the spatial separation of the UAVs in flight is varied by changing the propensities to move *away from friends* in the models. Further details on how these propensities are data farmed will be discussed in Chapter III.

It should also be noted that the effectiveness of enemy contact detection and classification are very sensitive to the routes taken by the UAVs due to the relatively small UAV sensor coverage compared to the area of operation. If no UAV flies near a target, there will be neither a detection nor a classification. The routes for the LAEs are developed based on intuitive justifications after analyzing the terrain and target profiles. Refer to Appendix A for the design rationale and snapshots of the set of MAE and LAE routes. For the development of these routes, the author consulted with Captain Starr King, USN, NWDC-Sponsored Chair of Warfare Innovation and Chair of Applied Systems Analysis of the Naval Postgraduate School and Captain Kevin McMindes, a USMC pilot; both consider them reasonable and sufficiently detailed for the purpose of modeling and analysis to answer the questions of interest. However, one should not preclude other alternative routes based on various operational judgments and objectives.

5. UAV Communications Network

A communications network is set up in MANA to facilitate the sharing of information between the MAE and the LAEs, as illustrated in Figure 6. Two types of situational awareness maps are provided in MANA: a squad map which holds direct squad contact memory, and an inorganic map which stores contact

memories provided by other squads through communications links (Galligan, et al., 2004). The contacts discovered by the MAE are sent through the communications links and updated on the inorganic map of the LAE agents, and vice versa. The data links for both MAE and LAE are C-Band/UHF and are assumed to have communications ranges sufficient for coverage throughout the entire area of operation as long as there is Line Of Sight (LOS) between the UAVs. Although modern communications technologies offer superb link quality and availability from a technical view, communications degradation is, none the less, an important consideration in most military networks in which the systems are deployed due to the adverse operating environments and weather conditions. Hence, factors related to communications degradation are considered in the models by changing the values corresponding to message delay and link reliability over each communications link.

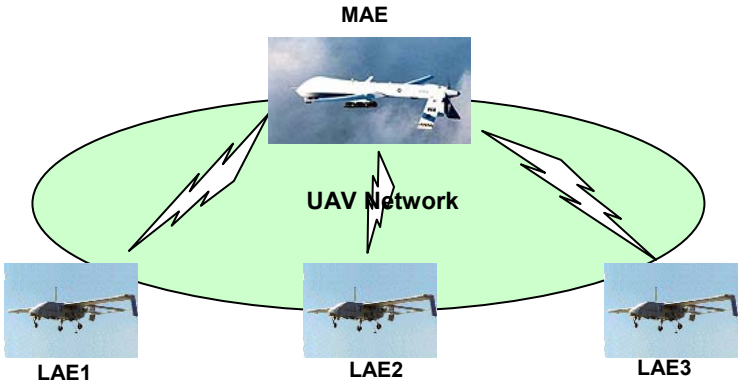

Figure 6. Information Flow Between the MAE and the LAEs in the UAV Network for Shared Situation Awareness

In actual operational environments, message latency represents the delay from the time a message is sent from the source UAV to the time it is received at the destination UAV, and varies depending on the distance between the two nodes and the current loading on the network. The link reliability in the model emulates the availability of the communications links for transmissions. There could be times where the LOS between two UAVs for transmission is not

available, in particular, when they are flying at low altitudes across rough terrains. Another major threat to link reliability could be the enemy's act of electronic attack, which is a prevalent form of interdiction in modern warfare.

C. MEASURES OF EFFECTIVENESS

The DMSO defines a Measure of Effectiveness (MOE) as "a qualitative or quantitative measure of the performance of a model or simulation or a characteristic that indicates the degree to which it performs the task or meets an operational objective or requirement under specified conditions" (Defense Modeling and Simulation Office Online M&S Glossary, 2005). This study measures the expected proportion of Red TCT and armor entities classified at the end of the four-hour IPB to assess the effectiveness of employing cooperative sensing to detect each type of targets. The MOEs distinguish between different target types; this could potentially provide insights to the decision makers about appropriate ways to apply different UAV tactics and behaviors depending on the target characteristics and their deployment profiles in the presence of a cooperative sensing environment. For instance, when an LAE establishes a new armor contact, it may be inclined to follow the contact knowing that armors tend to operate in formation. This could result in a higher classification rate. In contrast, following a TCT contact may not result in a higher classification rate since TCTs tend to deploy in isolation.

THIS PAGE INTENTIONALLY LEFT BLANK

III. DESIGN OF EXPERIMENT

A. EXPERIMENTAL FACTORS

1. Controllable Factors – Blue ISR Parameters

The number of factors affecting a cooperative sensing network's effectiveness is large, and each factor may have a wide variation of potential levels (i.e., settings). The factors are often confounded and some even exhibit conflicting interactions among them. For instance, it may appear obvious that a faster UAV is desirable because it can cover a larger sweep area in a fixed duration of time. However, in most sensor systems involving human operators, a minimum integration time is needed for a target to "remain visible" within the sensor field of view to be considered a positive detection. As the UAV travels faster, the probability of detection and classification decreases since the time available for the sensor to look at the target reduces. From an endurance standpoint, a faster UAV is generally less fuel efficient, thus has less endurance than a slower UAV. Another case for conflicting interactions between factors includes the optimal use of MAE and LAE UAVs. The MAEs, in general, provide wider sensor coverage than the LAEs due to their higher operational altitudes. In reality, higher altitudes are associated with reduced signal strengths, reduced angular resolutions, and increased interferences; all of these are culprits for driving down the probabilities of detection and classification. Similarly, it may appear desirable to have a wider Field Of View (FOV) in compensation for lower altitude flights to have an equivalent sweep area. Again, one would quickly end up sliding on the tradeoff curve between a wide FOV with low resolution and narrow FOV with high resolution, and imagery resolutions have direct impact on the target classification abilities. These illustrations clearly present the case that many of these factors are closely interrelated; the analysis of their interactions is not trivial.

Factors are classified as *controllable* in the simulation experiments if they represent action options to decision makers for the real-world problems. For this reason, controllable factors are also commonly known as *decision factors*. In concert with cooperative sensing, the decision factors that potentially contribute to the effectiveness of the sensing network in performing ISR-related missions, thus having direct relevance to gaining insights in our analysis, include:

Factors related to sensing network configurations

- Number of LAEs to one MAE

Factors related to UAV parameters

- Airspeed
- Detection range
- Classification range
- Classification probability

Factors related to network parameters

- Link reliability
- Message latency

Factors related to UAV routing behaviors

- Reactivity to friendly UAV SA versus tendency to follow a planned route
- Reactivity to a newly sighted enemy contact versus tendency to follow a planned route

Factors related to airspace deconfliction

- Minimum separation between UAVs

The UAVs selected for the study are not intended to be homogeneous but broadly classified into two categories, namely the MAE and LAE. The simultaneous investigation over the two categories of UAVs allows one to identify factors which are deemed important to the questions to be expounded, therefore provides further design considerations for architecting a cooperative sensing network for operational deployment. The factors include UAV airspeed, ranges for detection and classification, and detection and classification probabilities. To ensure the model is valid, the factors are varied with ballpark values based on current to near-future published technologies. These materials can be easily found from open-source literatures and databases such as The JANES Defense databases, The UAV Forum and Federation of American Scientist websites. The MAEs in the model have operational airspeed ranging from 60 to 100 knots and sensor detection range from 5,000 to 12,000 meters. The LAEs have operational airspeed ranging from 40 to 65 knots and sensor detection range from 2,000 to 7,000 meters. In the model, the classification range is set no farther than the detection range by taking values from 0.6 to 1.0 of the detection range.

It should be obvious that the ability of a UAV to detect and classify ground targets is dependent on its sensor coverage. The sensor coverage for a specified FOV increases with the UAV flight altitude as shown in Figure 7. The MAEs in the model have an operational altitudes ranging from 20,000 to 35,000 ft above ground level (AGL) while the LAEs from 5,000 to 20,000 ft AGL. The explored range of sensor FOV stretches from 30^0 to 60^0. Figure 7 displays the resulting range of possible sensor coverage considered in the study. As an illustration, a tactical LAE flying at 15,000 ft AGL carrying an EO payload with a 60^0 FOV has circular sensor coverage with radius 2,640 meters (i.e., 8,660 ft). If, on detecting an unknown target, the same sensor decides to close in and lower its altitude to 10,000 ft AGL and switch the EO camera to a 30^0 FOV in order to classify the target, it then has a sensor coverage radius of 817 meters.

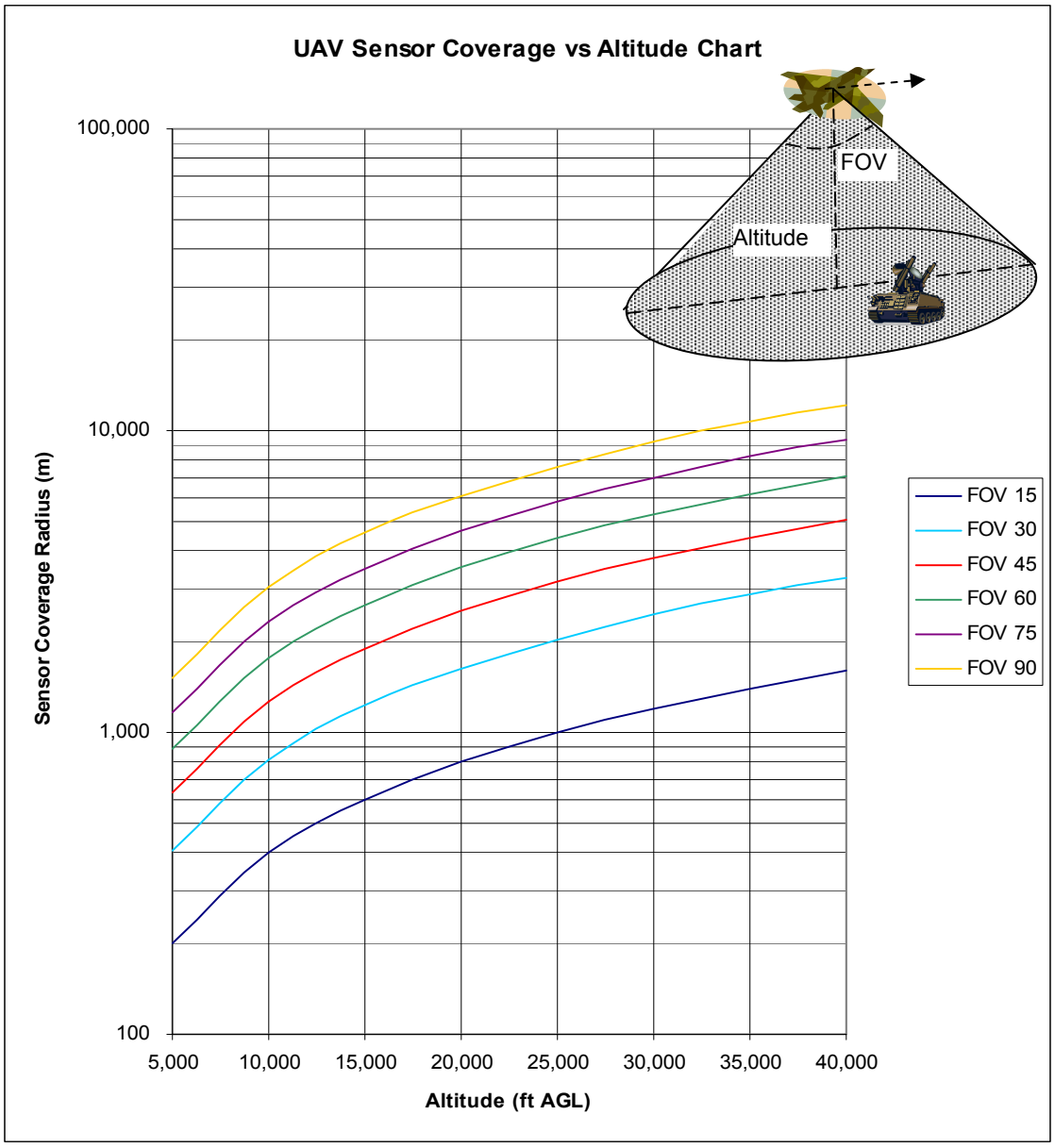

Figure 7. Graph of UAV Detection Range As a Function of Altitude and Field of View [Best Viewed in Color]

A complex and detailed representation that mimics a real world sensor in the model is viewed unnecessary, in the author's opinion, for this analysis. It is not the intent of the study to focus on highly-detailed and cumbersome physical-based modeling to give point estimate results. Instead, a simple model facilitates rapid execution to tap the power of agent-based distillations to provide insights

on the outcomes for varying model inputs. In this regard, cookie cutter models are assumed sufficient for detecting or classifying targets; targets falling within the sensor coverage have equal chance of being detected or classified. The LAE classification probability has values from 0.3 to 1.0. The MAE classification probability takes on values from 0.1 to 0.8 of the LAE classification probability to ensure that the latter is always lower than the former for every simulation run.

One of the objectives as part of the study involves finding good sensing network configurations to support swift maneuver and precision engagement by the MEB. In the model, a single MAE having large sensor coverage for effective initial detection is supplemented by multiple LAEs to enable effective close-in target classification. The number of LAEs employed affects how much area can be covered and how long it takes to complete the search. An upper limit of five LAEs has been selected for the study. Although Raffetto suggests that it is unlikely that the Marine Corps will have the resources and personnel to employ more than three UAVs simultaneously as a current standard operating procedure for a MEB size area of operation (Raffetto, 2004), the addition of a fourth and fifth LAE is envisioned for future ISR capability extension due to constant reduction in the cost of acquiring and manning UAVs. The additional LAEs allow evaluation of overall ISR effectiveness as the number of LAEs increases in a cooperative sensing environment.

The communications network forms the essential backbone for sharing detection information between the MAE and the LAEs. Degraded communications will inevitably shortchange the full potential one can harness from a cooperative sensing network to achieve high ISR capability. As discussed in the preceding chapter, electronic attack is becoming more prevalent in modern warfare. Coupled with the adverse weather and environmental conditions that these UAV networks are likely to operate in, the transmission reliability and accuracy of such information over the network must be considered. Link reliability and message delay are considered in the model to emulate such degradation in the communications network. While link reliability takes on values from 0% to

100%, the latency at which messages are transmitted from one UAV to another varies from 0 to 10 time steps in MANA, which corresponds to 0 to 100 seconds in real time.

The interactions and behaviors amongst UAVs within the network are expected to have significant impacts on the effectiveness of a cooperative sensing network. The responsiveness of a UAV to other UAV SA determines how much the UAV's next course of action is influenced by incoming targeting information from the network with respect to its original course of action. In MANA, this is achieved by changing the movement propensities of the UAV agents in response to an unknown contact in the inorganic SA. The ranges of weightings for these propensities vary from 0 to 100, and the responsiveness to the other UAV SA is computed as:

(Move toward unknown – Follow waypoint) / (Follow waypoint)

In the model, the follow waypoint weight is fixed at a value of 50; hence the responsiveness to other UAV SA ratio amounts to a range of -1.0 (completely unresponsive) to +1.0 (completely responsive).

The other parameter that affects the behavior of a UAV is its reactivity to a newly sighted enemy contact. In reality, this defines the ISR tactics that permit dynamic redirection of UAVs from their intended routes toward newly detected hostile targets. In MANA, this is implemented by varying the movement propensity of the UAV agent towards unknown targets with respect to its propensity to follow waypoints. As in the previous metric, the response to a newly sighted target is computed as:

(Move toward enemy – Follow waypoint) / (Follow waypoint)

The weight for moving toward an enemy ranges from 0 to 100, giving the responsiveness to a newly sighted enemy contact ratio of -1.0 (completely unresponsive) to +1.0 (completely responsive).

The UAVs in the scenario are separated in time and space. This models the tactical airspace control rules that necessitate UAV controllers to plan for airspace deconfliction in any UAV operations. The analysis investigates the effects far and close airspace separations have on the effectiveness of cooperative sensing by modifying the UAV agent's propensity to move toward or away from uninjured friends in MANA. A value of 0 corresponds to closer allowable airspace separation, while -100 leads to farther separation. These values represent the agents' propensities to move toward or away from one another, and not the actual minimum separation distances between them.

2. Uncontrollable Factors – Red Target Parameters

Just as controllable factors are important in gaining insights about how they impact the ISR effectiveness of a cooperative sensing network, uncontrollable factors, which are often overlooked by operational analysts and decision makers, are of equal importance in this analysis, particularly since simulation is employed. In a mathematical modeling activity such as simulation one does, after all, get to control everything whether or not it is actually controllable in the real world. By exploring over ranges of settings for the uncontrollable factors, also known as *noise factors*, one could benefit by observing the influences these factors have on the system outcomes. These insights make the analyst more capable of deriving settings for the controllable factors that make the system more robust to a wider background variation, instead of one that optimizes decision factors after fixing each noise factor to a single value which is likely to deviate from reality. The robust design approach was first advocated by Taguchi for quality planning and engineering product design activities, and focuses on minimizing variation and sensitivity to noise (Taguchi and Wu, 1980). Sanchez (2000) suggests the following benefits of using a robust design approach for simulation:

- Fewer surprises when decision is implemented

- Improved communication between analyst and “client” via expected loss
- Ability to evaluate trade-offs between noise reduction costs and performance quality
- Facilitates continuous improvement by seeking to reduce variability of response, not just achieving targeted value, and
- Insights gained allow simultaneous improvement in performance and reduction in costs

In the case of this analysis, valuable insights pertaining to the robustness of the cooperative sensing network can be achieved by varying those factors affecting the behaviors of the enemy’s forces. In particular, the TCT’s shoot-and-scoot tactics are perceived to have significant impact on the UAVs’ detection and classification capability. The set of target parameters that contributes to its susceptibility to UAV detection include:

- Concealment factor
- Vulnerability time window
- Sensor range for detecting nearby UAVs

The target concealment factor has a range of 0% to 100%. The latter signifies that the target is completely invisible to passing UAVs; the former adds no additional reduction factor to the detection probability other than those already imposed by the terrain. The vulnerability time window describes the time duration for which a TCT exposes itself as it moves from its hiding position to its firing position or next deployment, thereby being vulnerable to UAV detections. The vulnerability duration varies from 10 to 30 real time minutes or 60 to 180 MANA time steps. The TCTs are assumed to have the capabilities to detect incoming UAVs and take positions for concealment thus reducing the signatures susceptible to detection. Whether the target can successfully take cover depends

largely on its sensor range for detecting nearby UAVs to provide sufficient response time for concealment. The TCT onboard sensor range varies from 0 to 10 kilometers.

One's intuition suggests the reliability of UAVs may significantly impact the robustness of a cooperative sensing network. In addition to the base case, the overall classification effectiveness is explored for situations when a UAV fails or crashes, thus becoming unavailable in the IPB process. As the MAE in the sensing network is a critical node connecting and coordinating the ISR efforts amongst the LAEs, it is assumed in this study that the MAE has a long mean time to failure and the likelihood of its failure during the four hour IPB operation is negligible. Instead, the study expounds on the degree the ISR capability is degraded should a single LAE fail after some time into the operation, and evaluates how cooperative sensing could mitigate the "hole" in ISR plan. The model emulates a random failure to one of the LAEs at the zero, first, second, third and fourth hour. It should be noted that an LAE failure at the beginning of the IPB is nearly equivalent to the configuration of having one less LAE from the start, but will have a different and varied set of UAV routings since the failed LAE is chosen at random. Also, an LAE failing at the fourth hour has no effect on the classification outcome for the IPB since it fails right at the end of the scenario. This is a computationally efficient way to obtain some insights about the effects of LAE reliability without having to go into the details of modeling UAV breakdowns.

The ranges of factors in both real world and MANA representations are depicted in Figure 8.

REAL WORLD & MANA METRICS

Factors	MANA Names	Units	Actual		MANA	
			Low	High	Low	High
Sensing Network Config						
# LAE	# LAE	-	1	5	1	5
UAV Parameters						
MAE airspeed	MAE Airspeed	knot	60	100	108	180
LAE airspeed	LAE Airspeed	knot	40	65	72	117
MAE detection range	MAE Detect Range	km	5	12	17	42
LAE detection range	LAE Detect Range	km	2	7	7	24
MAE classification range	MAE Class Range	km	3	12	10	42
LAE classification range	LAE Class Range	km	1.8	7	6	24
MAE classification probability	MAE Class Prob	-	0.1	0.8	0.1	0.8
LAE classification probability	LAE Class Prob	-	0.3	1.0	0.3	1.0
Network Parameters						
Link reliability	Comms Reliability	percent	0	100	0	100
Message latency	Comms Latency	second	0	100	0	10
UAV Routing Behaviors						
Reactivity to friendly UAV SA versus tendency to follow a planned route	React Inorg SA	-	-1	+1	0	100
Reactivity to a newly sighted enemy contact versus tendency to follow a planned route	React En Contact	-	-1	+1	0	100
Airspace Deconfliction						
UAV airspace separation	Move Toward Friend	-	far	near	-100	0
TCT Parameters						
Concealment factor	TCT Conceal	percent	0	100	0	100
Vulnerability time window	TCT Vul Duration	minute	10	30	60	180
Sensor range for detecting UAV	TCT Detect Range	km	0	10	0	35

Figure 8. Experimental Factors and Levels in Both Real World Metrics and MANA Representations

B. ORTHOGONAL LATIN HYPERCUBE DESIGN

In simulation, experimental design provides a way of deciding before the runs are made which particular configurations to simulate so that the desired information can be obtained with the least amount of simulating. Carefully designed experiments are much more efficient than a “hit-or-miss” sequence of runs in which one simply tries a number of alternative configurations unsystematically to see what happens. Factorial and fractional factorial experimental designs are particularly useful in the early stages of experimentation, when one is pretty much in the dark about which factors

(parameters under investigation which are deemed to contribute to the effects of an experimental outcome) are important and how they might affect the responses. As the model's behavior is gradually understood and a set of more specific goals are determined, a whole variety of specific experimental techniques can then be used to seek optimal combinations of factor levels that maximize understanding toward these goals (Law and Kelton, 2000).

The full factorial experimental design quickly becomes unmanageable because the number of simulation runs needed escalates exponentially with increasing number of factors and factor levels. In this exploration of the use of multiple cooperative UAVs for ISR missions, the total number of factors in consideration is 19 with some factors having as many as 10 levels. It works out that 10^{19} (10 quintillion) design points are needed to study all possible factor-level combinations. If it is desirable to make 10 replications per design point, certainly a modest sample size from a statistical viewpoint, the total number of simulation runs would sum up to 10^{20} (100 quintillion). If every replication takes a computing cluster one second to complete, the simulation would not finish even when the sun goes out and the earth dies; a problem one would not even think of solving.

Fractional factorial designs provide a way to get good estimates of only the main effects and perhaps two-way interactions at a fraction of the computational effort required by a full factorial design. Basically, a 2^{k-p} fractional factorial design is constructed by choosing $1/2^p$ of all the possible design points and then running simulations for only these chosen points. Clearly, one would like p to be large from a computational efficiency viewpoint, but a larger p may also result in less information from the experiment, as one might suspect. Furthermore, the 2^{k-p} fractional factorial experimental design does not allow the investigation of non-linearity effects.

A smarter design of experiment is desired. The Orthogonal Latin Hypercube (OLH) design was pursued for its efficiency, excellent space filling properties and design flexibility. Excellent space filling results in low correlation between input factors; design flexibility imposes few restrictions on the number of

factors and levels, and thus provides the ability to identify nonlinear relationships. The Nearly Orthogonal Latin Hypercube (NOLH) has nearly the same properties but a small amount of orthogonality is allowed in order to get better space-filling. A good space-filling design is one in which the design points are scattered throughout the experimental region with minimal unsampled regions; that is, the voided regions are relatively small. This means that the design points are not concentrated in clusters or solely at corner points of the region, as can happen with two-level factorial designs (Cioppa, 2002; Cioppa and Lucas, 2006). For a general discussion of designing simulation experiments, see Kleijnen et al. (2005).

To construct the NOLH for this analysis, we used a Microsoft Excel spreadsheet created by Professor Susan Sanchez (Sanchez, 2005). The NOLH design considers 18 factors with 129 levels for each factor. Figure 9 is an extract of the NOLH design that depicts the first 50 of the 129 design points.

low level	0	0	0	0	0	0	0	108	72	17	7	0.6	0.6	0.3
high level	10	100	100	100	100	100	100	180	117	42	24	1	1	1
decimals	0	0	0	0	0	0	0	0	0	0	0	1	1	1
	[1]	[2]	[3]	[4]	[5]	[6]	[7]	[8]	[9]	[10]	[11]	[12]	[13]	[14]
factor name	Comms Latency	Comms Reliability	MAE Reactivity to Inorgan SA	LAE Reactivity to Inorgan SA	MAE Re-directivity to New Sighting	LAE Re-directivity to New Sighting	Air-space Separation	MAE Airspeed	LAE Airspeed	MAE Detect Range	LAE Detect Range	MAE Class to Detect Range Ratio	LAE Class to Detect Range Ratio	LAE Class Prob
	2	45	45	34	69	56	76	148	114	36	20	0.8	1	1
	9	30	46	9	45	42	20	142	89	40	17	0.8	1	0.8
	4	76	27	41	16	75	65	152	98	29	10	0.8	0.9	1
	7	89	37	44	76	7	41	127	93	27	13	0.7	1	0.8
	0	39	23	10	53	36	93	180	100	20	24	0.9	0.7	0.6
	7	43	1	40	33	59	4	126	77	21	24	0.9	0.8	0.5
	4	100	29	16	23	24	94	177	105	35	9	0.6	0.6	0.6
	6	70	6	34	92	87	2	130	81	29	8	0.7	0.7	0.5
	0	5	20	20	98	73	43	160	110	36	12	0.8	0.7	1
	10	8	27	12	10	20	55	122	78	29	9	0.9	0.6	0.9
	0	98	28	31	7	77	22	152	109	21	16	0.7	0.7	0.8
	9	98	38	14	100	51	91	128	86	23	18	0.7	0.8	0.9
	5	26	18	41	72	5	36	155	112	17	11	1	0.9	0.5
	8	22	35	9	23	91	54	123	90	17	12	0.9	1	0.6
	3	52	23	47	21	3	14	179	108	38	20	0.7	0.8	0.5
	8	75	3	17	52	98	73	125	91	41	17	0.7	0.8	0.5
	2	18	74	4	70	69	49	123	99	33	17	0.7	1	0.3
	10	35	78	42	20	15	48	161	74	32	19	0.8	0.8	0.4
	2	77	52	21	3	68	53	125	113	25	15	0.9	1	0.3
	6	97	75	13	80	34	16	147	83	18	15	0.9	0.8	0.3
	3	20	95	49	66	30	100	115	101	21	24	0.6	0.8	0.9
	6	27	92	38	13	86	27	178	97	18	17	0.6	0.7	0.7
	2	72	98	33	34	5	95	111	111	37	8	1	0.8	0.9
	7	62	98	19	63	81	28	179	90	33	9	1	0.7	0.8
	3	23	61	32	99	47	26	140	109	31	14	0.7	0.6	0.3
	9	1	57	15	29	38	81	153	85	33	13	0.6	0.7	0.6
	2	71	100	5	12	60	30	129	110	29	19	0.8	0.7	0.6
	10	94	70	16	75	28	59	178	74	24	21	0.8	0.6	0.7
	3	45	55	36	54	0	38	131	93	18	8	0.6	0.9	0.8
	6	46	70	48	42	74	91	149	88	25	10	0.7	0.9	1
	5	73	76	7	39	4	1	117	111	40	21	0.8	0.9	0.7
	5	63	89	13	73	66	77	164	73	35	19	0.9	0.9	0.8
	1	36	34	55	49	91	56	173	95	39	20	0.8	0.9	0.8
	9	48	9	54	40	38	3	132	96	40	23	0.8	0.9	0.9
	4	93	41	73	15	94	82	146	91	23	13	0.7	0.9	0.7
	5	87	44	63	95	11	13	137	108	24	9	0.7	0.8	0.8
	1	32	10	77	84	48	66	150	72	22	20	0.9	0.7	0.6
	8	15	40	99	30	59	61	114	107	21	19	1	0.7	0.6
	3	95	16	71	5	22	85	157	76	32	14	0.8	0.8	0.4
	9	84	34	94	86	99	37	119	107	34	16	0.7	0.7	0.4
	3	49	20	80	68	55	10	169	83	39	8	1	0.7	0.9
	8	38	12	73	52	2	71	121	104	39	10	0.9	0.6	0.7
	5	67	31	72	27	90	11	168	87	26	20	0.7	0.8	1
	6	81	14	62	74	23	92	129	102	19	21	0.7	0.8	0.7
	2	4	41	82	56	29	55	174	87	22	8	1	0.9	0.4
	9	42	9	65	2	52	67	138	110	26	10	0.8	1	0.5
	0	79	47	77	13	17	16	168	73	32	15	0.6	1	0.4
	6	88	17	97	78	70	98	141	105	32	18	0.8	0.9	0.4
	5	41	96	74	96	88	95	137	83	41	14	0.7	0.9	0.4
	8	9	58	78	41	16	40	176	109	31	17	0.6	0.9	0.5

Figure 9. Nearly Orthogonal Latin Hypercube of the Design of Experiment

Figure 10 plots the design points derived from the 18 factor NOLH crossed with a single-factor, five-level design for the number of LAEs to each MAE to yield a total of 645 design points. An individual dot on each grid represents a design point with levels corresponding to the factors denoted on the row and the column. The pairwise scatter plot shows good space filling properties. The design points are highly orthogonal (all correlation values lower than 0.05), with the exception of the LAE classification and detection range pair, the MAE classification and detection range pair, as well as the LAE and MAE classification probability pair. These pairs of factors are deliberately constrained such that one factor is expressed as a random fraction of the other for every design point while creating the NOLH. For instance, the LAE classification range is restricted to a

varying fraction of the LAE detection range since it is illogical to have the former parameter larger than the latter for the same sensor system on an LAE. The 645 design points are run for 50 replications each, which results in a total of 32,250 MANA runs.

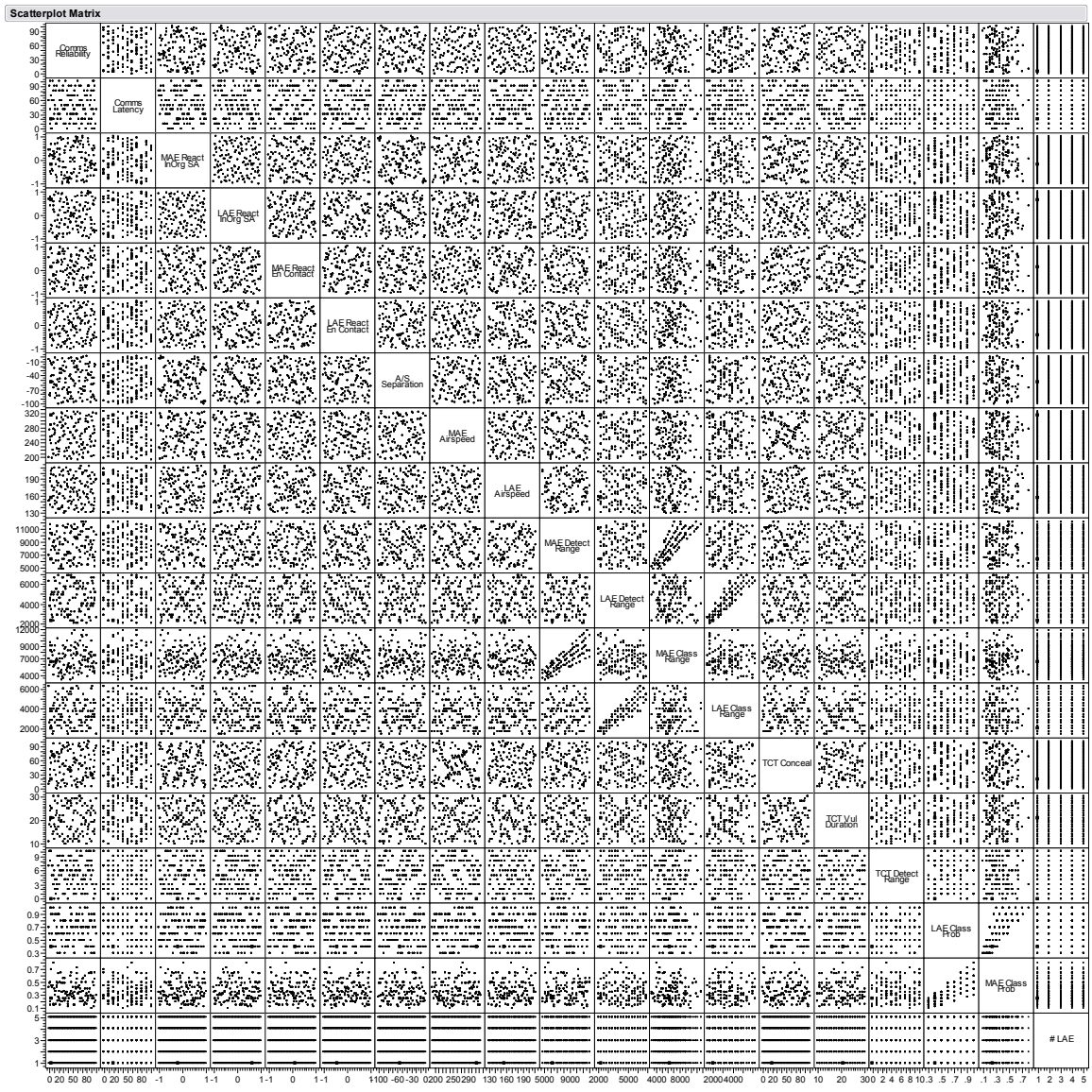

Figure 10. Pairwise Scatter Plot of Design Points Using a Nearly Orthogonal Latin Hypercube Crossed With a Single-Factor

The Tiller is a software tool in the Project Albert's toolkit that allows the setup of XML study files comprising a large number of design points based on the experimental design. The study files provide the sequence of changing values for the associated MANA parameters, thus enabling batch processing without the need to load each simulation run manually. The study files, together with the base case simulation model file, are then submitted to the computing clusters in the MAUI High Performance Computing Center (MHPCC) hosted by the Air Force Research Laboratory Center, and managed by the University of Hawaii (Maui High Performance Computing Center, 2005).

THIS PAGE INTENTIONALLY LEFT BLANK

IV. DATA ANALYSIS

A. DATA PRE-PROCESSING

The output data generated from the MHPCC is in either the Comma Separated Value (CSV) or the Microsoft Data Base (MCB) file format. The data file contains the excursion number for each design point and a random index representing the replication number in each design point, as well as the settings for factors that vary in the NOLH design. Each row in the data file includes the number of Blue and Red killed, the numbers of agents injured and killed per squad, the time steps for completing the simulation run, and a few other values. The only data of interest in the output files are the total number of Red killed and those relating to squads corresponding to the TCTs and armor battalions, and obviously, those parameter values that are varied in each simulation run. These data are then imported into the JMP IN Statistical Software (JMP Statistical Discovery Software website, 2005) on which data analysis is performed. The JMP Statistical Software provides many valuable analytical tools with a superior graphical user interface so there is a relatively short learning curve in using the basic features sufficient for most analytical use. The software is also selected for its powerful data pre-processing capability and its ability to handle extremely large data sets.

The number of Red agents killed represents the number of Red targets that are classified by the Blue UAVs at the end of the simulation run. The expected proportion of targets classified for each target type is derived by summarizing the data over the replications for each design point and dividing the mean number of targets classified by their start-off total. These expected proportions of targets classified provide the MOEs for analyzing the effectiveness of the cooperative sensing network and the effects the factors in consideration

have on such sensing capability. The MANA parameters are also transformed back to their real-world representations before analyzing the data in order to ease interpretation of the results.

B. ANALYSIS TOOLS AND METHODOLOGIES

Several analytical tools and methodologies are applied to the model outputs. These sift out trends intrinsic within the data to help answer the questions of interest and provide useful insights and operational guidance relevant to the employment of cooperative sensing for military ISR purposes. The paragraphs below give brief descriptions of the main techniques used throughout the analysis. These techniques should by no means be used in exclusion of the others; using all in a complementary manner can provide better perspectives and operational insights.

1. Data Partitioning

Data partitioning is a form of exploratory modeling (sometimes known as data mining). It is a process of exploring a large amount of data, usually using an automated method, to find patterns and discoveries. Data partitioning is used to recursively partition a data set, automatically splitting the data at optimum points to maximize the difference in the values of the response variables between the branches of the split. The result is a decision tree that classifies each observation into a group (Sall et al., 2005). The technique is often used for exploring relationships without having a good prior model. It can handle large problems with relative ease and the results are very interpretable.

2. Multiple Linear Regression

Multiple Linear Regression is the technique of fitting or predicting a response variable from a linear combination of several other variables. The fitting principle is least squares, which finds a line through the data points that

minimizes the sum of squared distances to the line of fit (Sall et al., 2005). It is not the intend of this analysis to use the regression technique in the conventional way of deriving a mathematical model for predicting the proportion of Red targets classified given a set of cooperative sensing parameters; the agent-based distillation models are not set up for such details. However, the technique is used to provide valuable insights into the factors of significance, their interactions with one another, and the discovery of any non-linearities that might exist. Pareto plots are often used to visually plot bars emphasizing the order of importance of the factors from the most importance to the least. The prediction profiler in JMP IN presents a useful interface to show the predicted response for each combination of factor settings. It provides a handy way to look at the effect on the predicted response of changing one factor setting while holding the others constant, which can be useful for judging the contribution of each factor to the response.

C. RESULTS OF ANALYSIS

1. Sensing Network Configurations

To investigate the impact the number of LAEs have on the proportion of targets classified, regression analysis is performed to obtain the best fit for the proportion of total Red targets, TCTs and armor targets classified against the number of LAEs respectively. Refer to the bivariate fits in Section 1 of Appendix B. The regression models show that the quadratic effects are significant for the proportions of total Red target and armor classifications (p-value < 0.001), but not for the proportion of TCT classification (p-value = 0.2870).

For ease of illustration, the proportions of targets classified are grouped by the number of LAEs to obtain the average proportions of targets classified for each configuration with various numbers of LAEs. A quadratic curve is fitted for the proportion of total Red target classifications as shown in Figure 11; a line and a curve are fitted for the proportions of TCT and armor classifications

respectively, as depicted in Figure 12. An initial look at the results depicted by the curve in Figure 11 seems to suggest that one MAE and four LAEs is the most cost-effective cooperative sensing network configuration for the scenario in consideration. However, the detailed breakdown of the proportion of targets classified into the types of targets shown in Figure 12 reveals that while the classification rate for armor targets saturates when number of LAEs reaches four, the classification rate for TCT targets continues to increase with more than five LAEs. TCTs are less susceptible to UAV detections due to their higher concealment abilities. Armor battalions have strong detection signatures and are easily classified by relatively fewer LAEs, or even by the MAE itself which has a less superior classification capability. These imply that an investment of more sensing resources is required to detect TCTs. Another reason for the differences in the number of LAEs associated with diminishing returns could be due to the fleeing characteristics of TCTs and their ability to evade detections, thus a denser LAE concentration is required in the entire area of operation to defeat their counter-detection capability and limited windows of vulnerability. One would have completely missed these observations without looking at the detailed target classification proportions by types. This illustrates the importance of defining the correct set of MOEs.

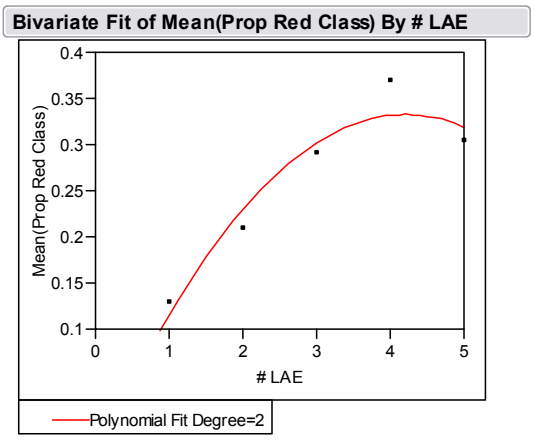

Figure 11. Quadratic Fit for the Average Proportion of Red Targets Classified Against the Number of LAEs

The sudden drop in the proportion of armor targets classified for five LAEs is found to be attributed to the distribution of routes. When the fifth LAE is introduced, it misses most of the armor elements in Area 1 as the convoy proceeds northward. This observation further demonstrates the sensitivity of the MOEs to variation in UAV routings, as anticipated during the model development phase and discussed in Chapter II.

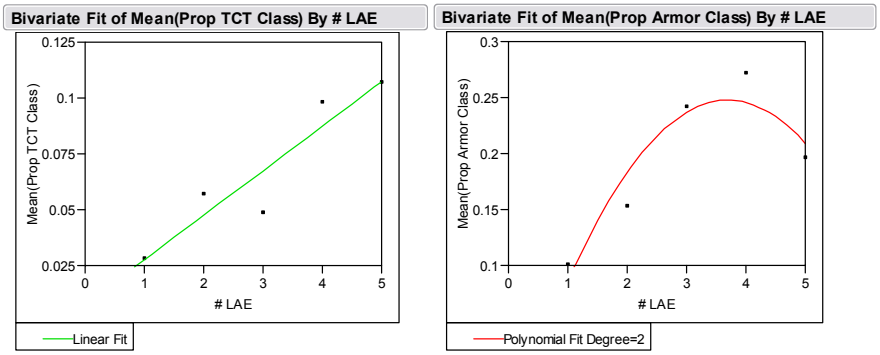

Figure 12. Linear and Quadratic Fits for the Average Proportion of TCT and Armor Targets Classified Against the Number of LAEs

The histogram plots depicted in Figure 13 allow further exploration of the proportions of TCT and armor targets classified for each MAE-LAE configuration. These reveal high frequencies at low classification rate for both types of targets, even though the means and the modes generally increase with the number of LAEs. Two categorical response variables are defined for the proportions of TCT and armor classification lower than 0.05 and 0.1 respectively. A logistic regression model is fitted for each of these response variables to investigate the rationales for the low classification rates. The details of the logistic regression models are shown in Appendix B. The analysis identifies LAE classification range and LAE responsiveness to MAE cueing as common factors of significance that contribute both to the low TCT and armor classification rates amongst few other factors. In the case of classifying TCTs, the TCT ability to conceal and its sensor range to evade UAV detection are important factors explaining the low classification rates. The partitioning analysis (refer to the partitioning tree in

Appendix B, Section 1) also suggests that LAE classification ranges less than 3,200 and 2,600 meters can only classify an average of only 4% and 6% of the total TCT and armor targets, respectively.

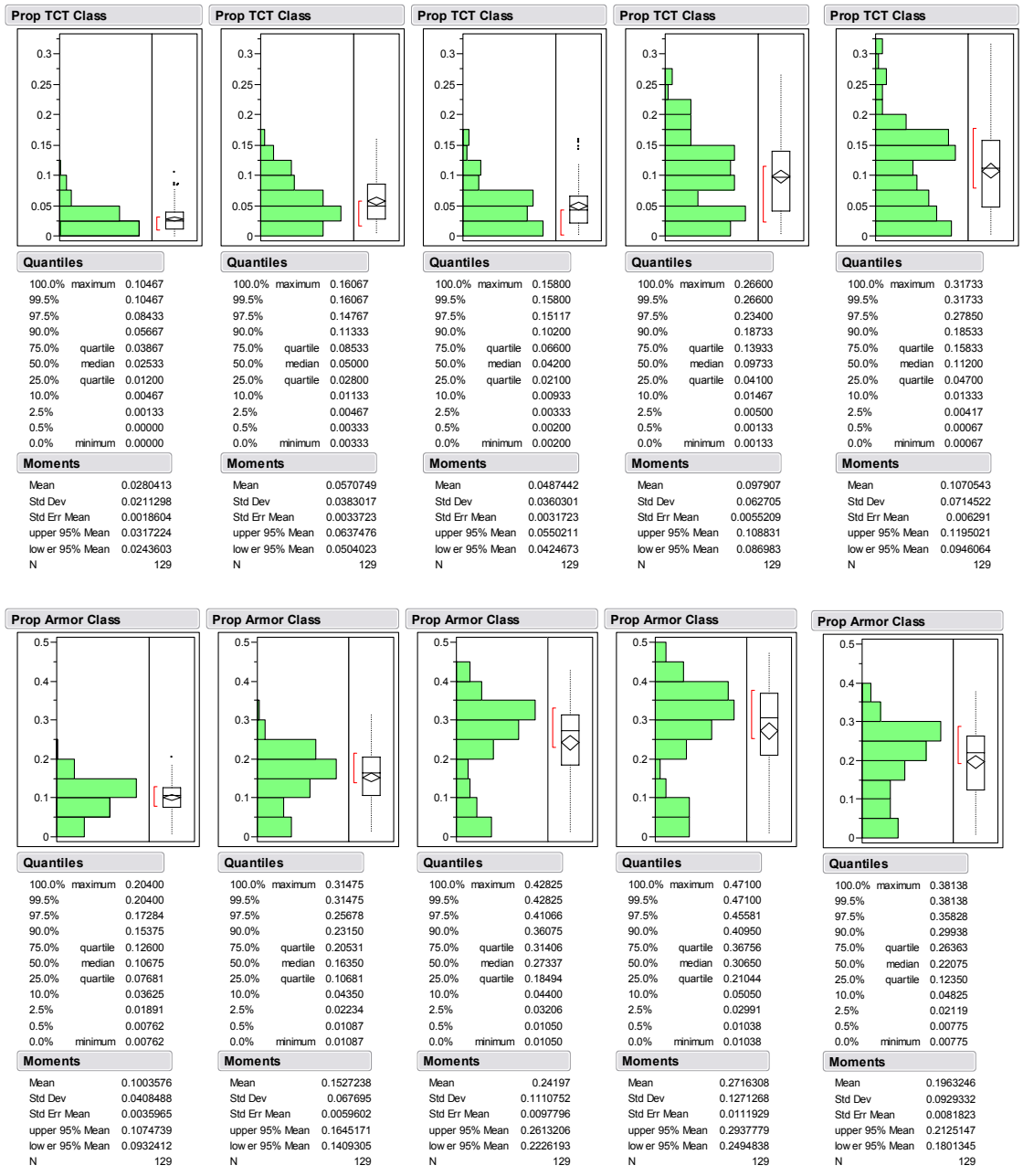

Figure 13. Distributions of the Average Proportion of TCT (Top Row) and Armor (Bottom Row) Targets Classified for One LAE (Left) to Five LAEs (Right)

2. Factors of Significance

The Multiple Linear Regression technique is used to determine factors that are significant to the proportion of targets classified during the four-hour IPB with the cooperative sensing network. Separate analysis are conducted for the TCT and armor targets, as distinctive differences exist between the two arrays of targets in terms of their target profiles and operational characteristics.

Three stepwise linear regression models are fitted for the proportion of TCT classified with consideration of simply the main effects, the main and quadratic effects, and including the two-way interactions (Refer to Appendix B for the detailed models). The adjusted R-square values, instead of the standard R-square values, are considered when comparing the models to take into account the number of terms used to achieve the explanatory power of the models. The quadratic and interaction terms in the full model account for approximately 20% of explanatory power and are therefore included in the model for subsequent analysis. There are seven main effects, two quadratics and five interaction terms in the selected model as depicted in Figure 14. These fourteen terms explain 73% of the total variability, based on the adjusted R-square value.

Response Prop TCT Class

Summary of Fit

RSquare	0.731611
RSquare Adj	0.725647
Root Mean Square Error	0.030259
Mean of Response	0.067764
Observations (or Sum Wgts)	645

Analysis of Variance

Source	DF	Sum of Squares	Mean Square	F Ratio
Model	14	1.5723599	0.112311	122.6672
Error	630	0.5768141	0.000916	Prob > F
C. Total	644	2.1491740		<.0001

Parameter Estimates

Term	Estimate	Std Error	t Ratio	Prob>|t|
Intercept	-0.062471	0.007717	-8.10	<.0001
LAE React InOrg SA	0.0120452	0.002049	5.88	<.0001
MAE Class Range	0.0000039	6.059e-7	6.50	<.0001
LAE Class Range	0.0000212	9.586e-7	22.09	<.0001
LAE Class Prob	0.0503922	0.005722	8.81	<.0001
TCT Conceal	-0.000549	0.000041	-13.40	<.0001
TCT Detect Range	-0.003615	0.000397	-9.11	<.0001
# LAE	0.0198858	0.000842	23.60	<.0001
(LAE React InOrg SA-0.00031)*(LAE Class Range-3569.77)	0.0000076	0.000002	4.38	<.0001
(LAE Class Range-3569.77)*(# LAE-3)	0.000006	6.537e-7	9.19	<.0001
(LAE Class Prob-0.65039)*(# LAE-3)	0.0137356	0.004044	3.40	0.0007
(TCT Conceal-50.0155)*(TCT Detect Range-5.08527)	-0.000093	0.000016	-5.85	<.0001
(TCT Conceal-50.0155)*(# LAE-3)	-0.000156	0.000029	-5.39	<.0001
(LAE Class Range-3569.77)*(LAE Class Range-3569.77)	-7.013e-9	7e-10	-10.02	<.0001
(TCT Conceal-50.0155)*(TCT Conceal-50.0155)	-0.000008	0.000002	-5.05	<.0001

Figure 14. Multiple Linear Regression Model for the Proportion of TCT Classification

The Pareto plot in Figure 15 ranks the factors in the full model in descending order of importance. The number of LAEs is listed as having the greatest impact on TCT classification rate. The prediction profiler in Figure 16 highlights a substantial increase in the proportion of TCTs classified – from 0.047 to 0.126 (approximately 2.5 times) – as the number of LAEs in the sensing network increases from one to five with all the other factors held constant.

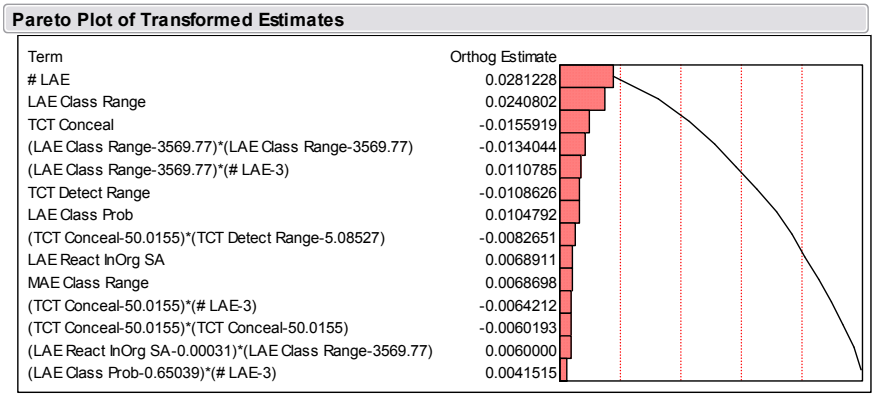

Figure 15. Pareto Plot of Factors Significant to the Classification of TCTs

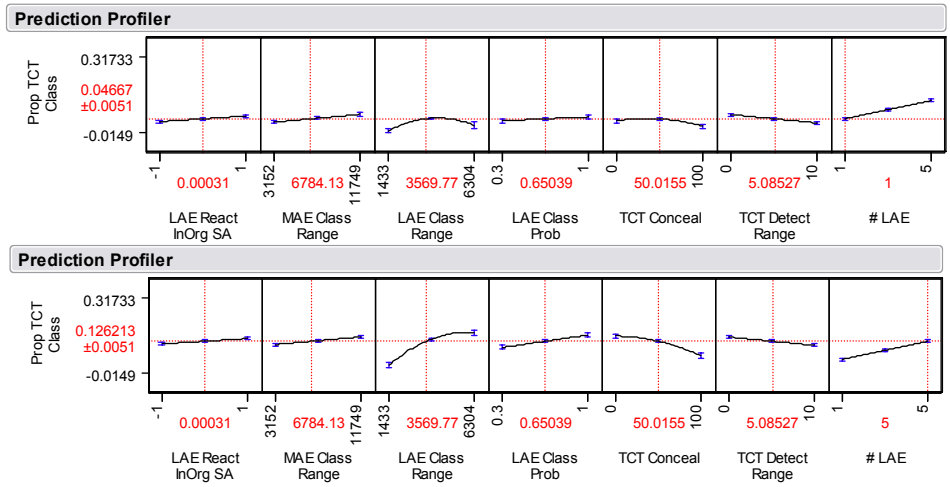

Figure 16. Prediction Profiler Showing Approximately 2.5 Times Improvement in TCT Classification By Increasing the Number of LAEs From One to Five

It is also apparent that improving the LAE sensor qualities (from the aspects of classification range and classification probability) contributes considerably to the increase in the overall effectiveness of classifying the TCTs.

The MAE is generally inferior in its ability to classify targets due to the high flight altitude and wide sensor FOV in order to satisfy the wide area coverage requirement. In contrast, the LAEs have lower flight altitudes and more focused sensors that enable them to see targets with better resolutions, so though LAEs are myopic in their coverage, they have much better chances of classifying targets. The overall classification effectiveness of the cooperative sensing network increases when the LAEs are more responsive to the MAE cueing instead of following their pre-assigned routes. The interaction plot in Figure 17, however, shows an adverse effect when the LAEs have short classification ranges while being responsive to the MAE cueing. An LAE with small classification coverage, on being cued by the MAE, might take so long to fly close towards the TCT that it will miss its limited vulnerability window and lose the target completely. Even if the LAE arrives before the TCT again takes cover, a short classification range means the LAE has a limited number of classification opportunities, hence a low chance of successfully classifying the contact during its time on target. This wasteful trip can cost the LAE classification opportunities which would have arisen if it kept following its pre-assigned route. The results also show that extending the MAE classification range has a small but positive impact in the performance. This increases the number of classification opportunities during the MAE's time on target and helps compensate for the poor classification probability per attempt. Note that the benefits of having higher classification probabilities for LAEs are greater when there are more LAEs than when there are fewer.

The negative coefficients associated with the TCT concealment and TCT detection range factors present the obvious case that TCTs which are well concealed with longer counter-detection sensor ranges are better able to evade incoming UAVs and avoid detection and classification. However, the interaction profiler (Figure 16) points out that the drop in the proportion of classification with increasing TCT concealment ability is more substantial for larger number of LAEs. On top of that, it is also observed that enhancing the two TCT's

parameters simultaneously has a synergistic effect in reducing their susceptibility to UAV classification. This makes perfect sense, as it is not helpful for a TCT to be forewarned by its counter-detection sensor of an approaching UAV if it does not have an effective concealment capability.

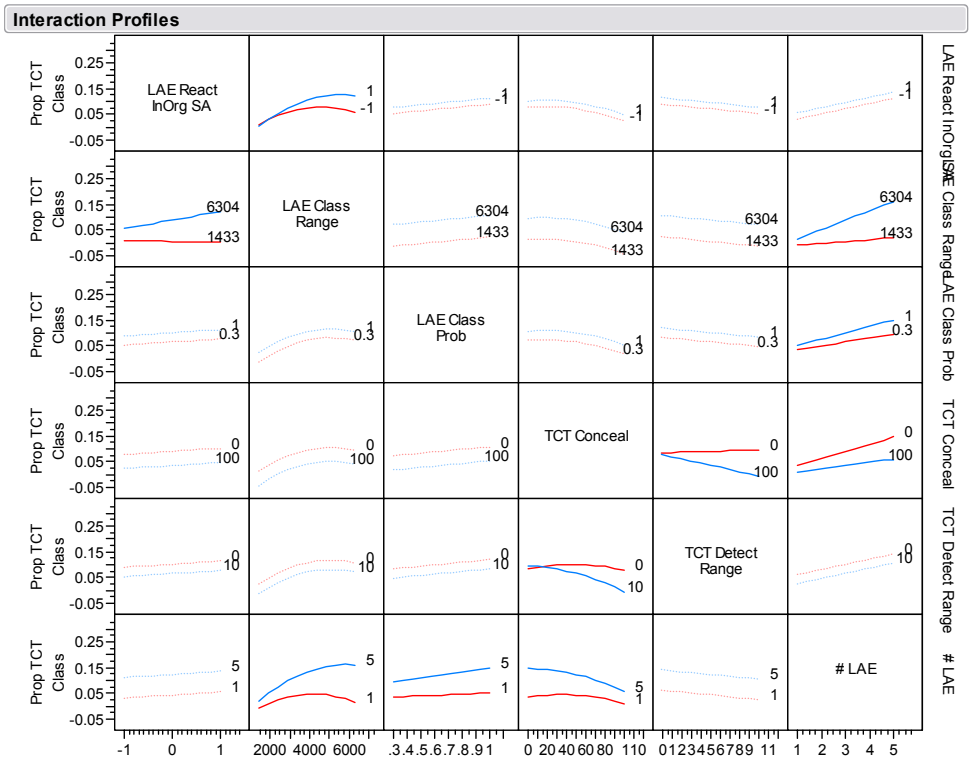

Figure 17. Interaction Plot of Factors Significant to the Classification of TCTs

Figure 18 shows the partitioning tree for the proportion of TCTs classified. The number of LAEs is the first break point for this model, which indicates the number of LAEs has a substantial impact on effectiveness; this is consistent with the results presented from the regression analysis. The tree displays a mean proportion of TCT classification of only 4.5% with fewer than four LAEs and 10.2% with four or more LAEs (refer to Appendix B for the full partitioning tree). Moving down the right branch (i.e., using four or more LAEs), only 3.8% of the TCTs are classified if the LAE classification range is less than 2,866 meters. So it is futile to invest in more LAEs alone but it is important to invest in more LAEs that have sensors with longer classification ranges. Note, however, that despite

the investment one might devote into the cooperative sensing network, the increment in classification effectiveness against very well-concealed TCTs is negligible.

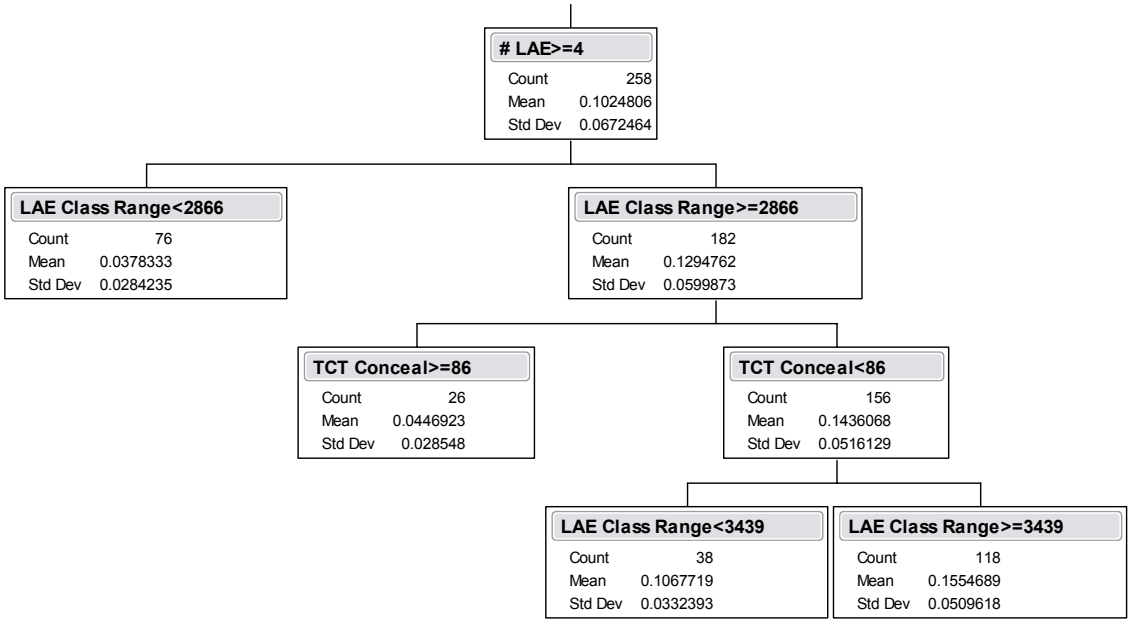

Figure 18. Right Branch of the Partitioning Tree for Proportion of TCT Classification With Four or More LAEs

While partitioning trees are useful for exploring relationships without having a good prior model and inherently a powerful tool for capturing interactions, McMindes (2005) highlights a few drawbacks associated to such form of exploratory modeling. There is no sense of relative importance between the factors other than the hierarchical representation of the tree structure. For instance, Figure 18 shows the number of LAEs is more important than LAE classification range, but how much more important? There is also no sense of indication of the sensitivity of a split. The LAE classification range is best split at 2,866 meters, which is something absolutely not controllable in practice. So how much is lost if the splitting is shifted to the left or right by 50 meters? The break points also tend to be somewhat unstable, especially as the groups become

small. For these reasons, partitioning trees are used in conjunction with results from other techniques, such as Multiple Linear Regression, and to provide qualitative insights.

A similar stepwise linear regression approach is again conducted for the proportion of armor targets classification. Three models were constructed using three sets of potential terms: the first model involved only the main effects, the second model involved both main and quadratic effects, and the third (full) model also included the two-way interactions. Here, the full model explains 80% of the total variability while the quadratic model already explains a notable 77%. The interaction terms account for less than 4% of the explanatory power in the full model, so the simpler model is chosen for subsequent analyses (refer to Appendix B for the detailed models). The seven main effects and two quadratic terms in the selected model are highlighted in Figure 19. These nine terms explain 77% of the total data variability.

Response Prop Armor Class

Summary of Fit

RSquare	0.777112
RSquare Adj	0.773953
Root Mean Square Error	0.052919
Mean of Response	0.192601
Observations (or Sum Wgts)	645

Analysis of Variance

Source	DF	Sum of Squares	Mean Square	F Ratio
Model	9	6.1999396	0.688882	245.9965
Error	635	1.7782373	0.002800	Prob > F
C. Total	644	7.9781769		<.0001

Parameter Estimates

Term	Estimate	Std Error	t Ratio	Prob>|t|
Intercept	-0.218018	0.019501	-11.18	<.0001
LAE React InOrg SA	-0.014634	0.003583	-4.08	<.0001
LAE React En Contact	0.0154657	0.003583	4.32	<.0001
LAE Airspeed	0.000569	0.000088	6.45	<.0001
MAE Class Range	0.0000054	0.000001	5.14	<.0001
LAE Class Range	0.0000567	0.000002	33.85	<.0001
LAE Class Prob	0.0964538	0.010006	9.64	<.0001
# LAE	0.0310841	0.001473	21.10	<.0001
(LAE Class Range-3569.77)*(LAE Class Range-3569.77)	-2.196e-8	1.187e-9	-18.49	<.0001
(# LAE-3)*(# LAE-3)	-0.022495	0.001245	-18.06	<.0001

Figure 19. Multiple Linear Regression Model for the Proportion of Armor Classification

The LAE classification range and the number of LAEs are ranked as the two most important factors that affect the proportion of armor classification, as

the Pareto plot in Figure 20 illustrates. The quadratics of the two main effects are next on the list, and indicate strong non-linear effects; the negative regression coefficients for the quadratic terms with positive corresponding main effect coefficients indicate that increasing either the LAE classification range or the number of LAEs will eventually lead to diminishing returns. This is illustrated clearly in the prediction profiler graphs in Figure 21. In fact, the proportion of armor classification shoots up from 0.053 to 0.311 (almost a fivefold improvement) as the LAE classification range extends from 1,433 to 4,900 meters, and enlarging the LAE classification footprint beyond this upper limit reduces the overall classification effectiveness of the sensing network. Visually watching a few simulation runs suggests why this occurs. An LAE with long classification range is easily distracted by the surrounding neutral vehicles within the sensor footprint, and this renders the LAE ineffective in its mission to search out the Red targets. As discussed in the earlier section, the drop in the proportion of armor classification for five LAEs is attributed to the distribution of routes when the fifth LAE is introduced, since these routes miss most of the armor elements in Area 1.

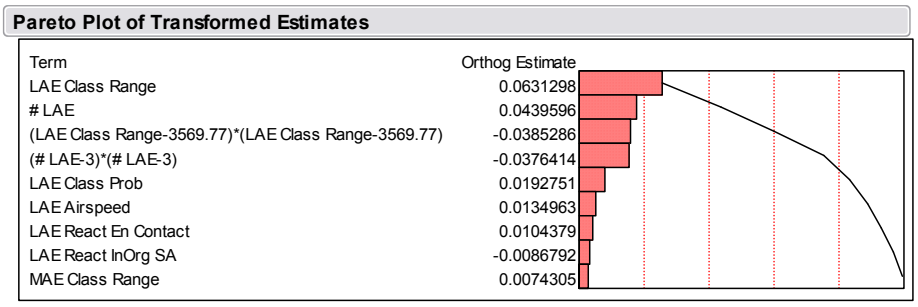

Figure 20. Pareto Plot of Factors Significant to the Classification of Armor Targets

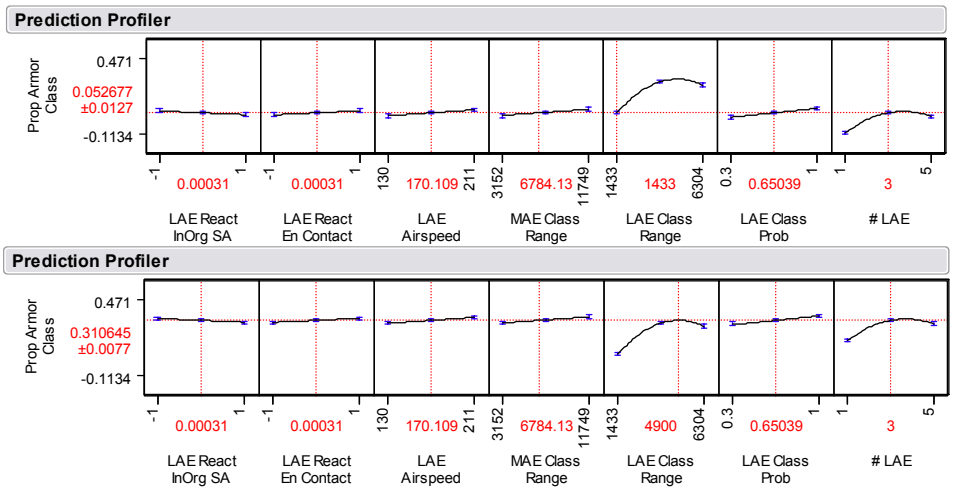

Figure 21. Prediction Profiler Showing Almost 5 Times Improvement in Armor Classification By Increasing LAEs Classification Range Less Than 3.5 Times

As in the case of TCT classification, better quality LAE sensors (in terms of higher classification probabilities) enhance the classification effectiveness against the armor targets. Increasing the MAE classification range leads to a marginal improvement on the classification effectiveness as well, perhaps because it also increases the number of classification opportunities. In contrast, increasing the MAE classification probability was not shown to have an impact. The probability of an MAE successfully classifying an intended target in each opportunity is too low to make significant contribution to the overall effectiveness even at the highest range, and therefore not a significant factor. To find more of the highly mobile armors that are commonly deployed in a formation, a faster LAE does contribute to a higher classification success. This is not true for detecting the TCTs in this scenario, as they generally move over shorter distances.

Unlike classifying TCTs, an LAE should lean towards being more responsive to follow a newly classified armor element since the discovery of one is likely to lead to the entire formation. Such LAE behaviors would not benefit TCT classification since they are mostly sparsely deployed in isolation. Being

responsive to the MAE cueing, in this case, may result in lower proportion of armor classification, but higher TCT discovery.

The partitioning tree for the proportion of armor classified (Figure 22) shows LAE classification range to be the first break point for this model, which is consistent with the results presented from the regression analysis. The tree presents a mean proportion of armor classification of 23.2% when the LAE classification range is at least 2,579 meters and 5.8% below that. The next two levels of partitioning are based on the number of LAEs on both branches, thus indicating a non-linear relationship between the number of LAEs and the response variable with the best values around three to four LAEs. As discussed earlier, the introduction of the fifth LAE misses most of the armor elements in Area 1 due to its pre-assigned routing. A faster LAE could, however, mitigate this by reaching the area of responsibility earlier before the armor battalion moves away.

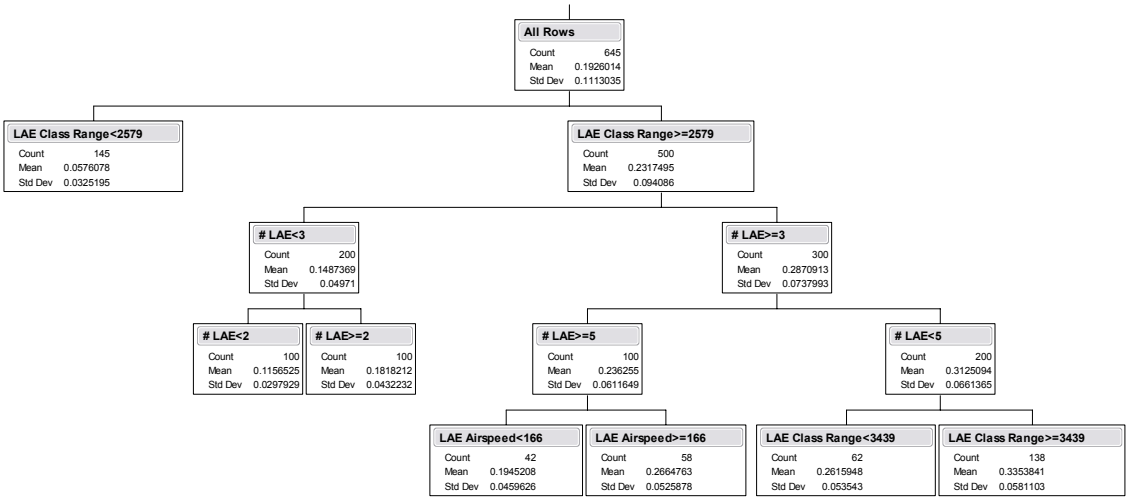

Figure 22. Partitioning Tree for Proportion of Armor Classification

3. UAV Behaviors

The contour plots in Figure 23 depict the contours for the proportions of TCT and armor classification with respect to the LAE responsiveness toward new enemy contacts they make (labeled “LAE React En Contact” on the Y-axis) and

MAE redirections (labeled “LAE React Inorg SA” on the X-axis). The dark blue patches represent higher proportions of classification in contrast to the light blue patches. The points on the plots indicate combinations of these two factors that appeared among the experiments.

The plot shows a higher concentration of dark blue patches on the right half of the plot, thus suggesting better classification effectiveness against the TCTs when the LAEs have better responsiveness towards the MAE cueing. However, LAE response to a newly classified enemy contact does not seem to matter in achieving better overall classification performance. The result is intuitive since the TCTs are mostly sparsely distributed in this scenario. It is more likely that they are first detected by the MAE with the wide area sensor which then cues the LAEs to perform a close-in classification of these targets. Since the TCTs are sparsely located, having the LAEs follow newly discovered contacts is unlikely to lead to another TCT detection.

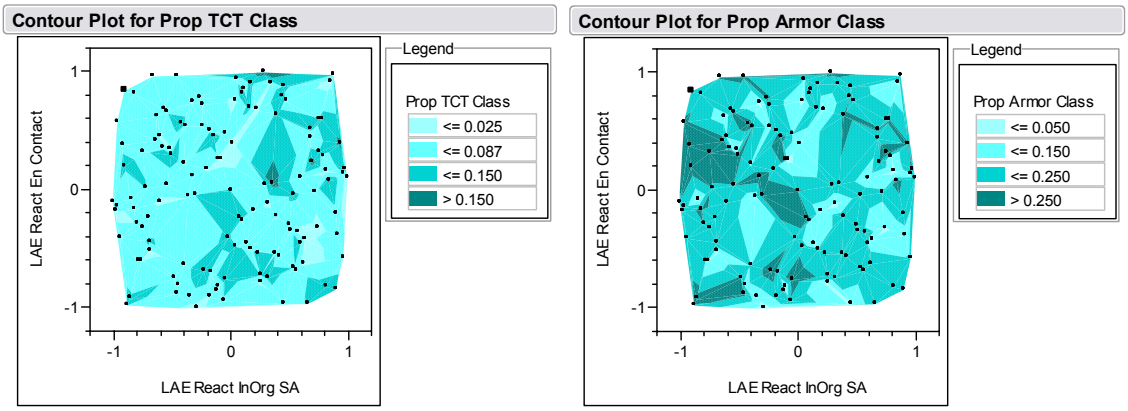

Figure 23. Contour Plots Showing Proportions of TCT (Left) and Armor (Right) Classification With Respect to LAE responsiveness Toward New Enemy Contacts and MAE Redirections [Best Viewed in Color]

For classifying armor targets, the dark blue patches clustering around the top left of the plot suggest that having LAEs that are more responsive towards a newly classified enemy contact and less towards the MAE cueing significantly improves the overall classification effectiveness against armor targets. As armor elements tend to appear in formations, following a newly classified armor

element is likely to lead to the discovery of more armor elements in close neighborhood. However, once an LAE has found a cluster of targets, being too responsive to the MAE cueing might distract the LAE from making its kill and result in a lower overall proportion of armor classification.

4. Impact of LAE Failure

To examine how an LAE failure during the four-hour IPB operation might affect the overall classification performance – and how a cooperative sensing network could mitigate this performance degradation – the scenario with four LAEs is modified slightly so that one LAE is randomly selected to fail. Successive sets of experiments are conducted where this LAE fails immediately from the start of the scenario, and at the first, the second, and the third, and the last hour of the operation. When an LAE fails, the other UAVs continue on with the pre-assigned routes unless otherwise influenced by their responses to UAV redirections; there is no re-planning of the UAV routes. A few other factor ranges are modified based on the results described earlier in this chapter. First, only two discrete levels are used for link reliability: 0 represents no cooperation and 100 represents full cooperation. The ranges of reactivity to other UAV SA for both the MAE and LAEs are also modified to take on values between 0 to +1. This represents that the UAVs are at least as reactive to redirection as to following their pre-assigned routes. The new NOLH is then crossed with the LAE lifetime (i.e., number of hours before a randomly selected LAE fails) to obtain the new experimental design matrix.

The graphs in Figure 24 show the average proportions of TCT and armor classification when an LAE fails at various time instances with and without cooperative sensing capability. The graphs again clearly illustrate that cooperation does help in classifying TCTs but not armor targets. However, for both target types, having a failed LAE significantly degrades classification performance – as much as 21% in the four-hour operation, comparing an LAE failing at the start and the end of the operation. Although the improvement gained

in classification proportion for TCTs is constant regardless of the time of LAE failure, an improvement of 0.012 from a base of 0.065 to 0.087 is worth noting.

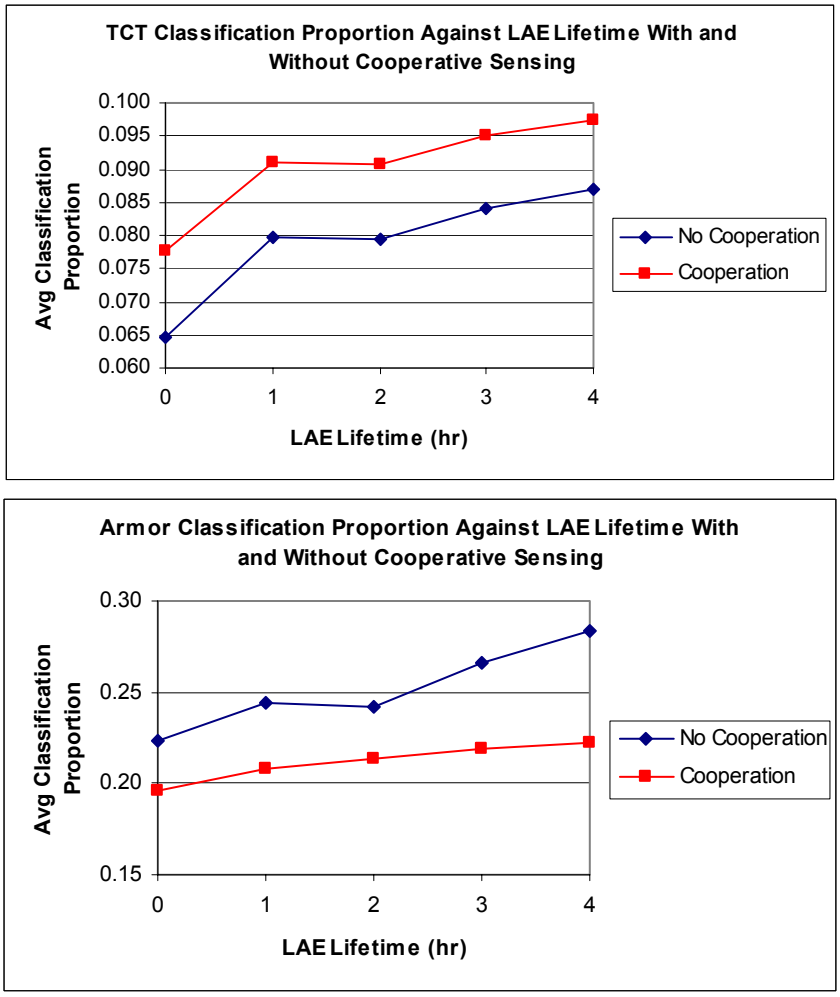

Figure 24. Graphs Depicting Average Proportions of TCT and Armor Classification Against LAE Lifetime With and Without Cooperative Sensing Capability

In contrast, the gentler slope in the armor classification proportion when the LAE lifetime drops from four to zero hours shows that less degradation in classification performance occurs when the UAVs are part of a cooperative sensing network. This indicates that although cooperative sensing does not help in the overall armor classification in this particular scenario, it may provide a more robust solution in some scenarios.

In conjunction with the earlier observations, one should note that while it is undesirable for an LAE to be responsive to MAE redirection for a while once an armor entity is found, but instead follow the new contact which will likely lead to the discovery of more armor targets, at other times it may be worthwhile to react to an MAE redirection before the LAE has even made its initial classification. This suggests that appropriate switching between these behaviors during different phases of an LAE operation is necessary. In summary, being responsive to MAE cueing may not always give the best overall classification results; reacting to a cueing request may lead to the classification of other potential targets but risk the opportunity of a greater payoff by remaining in its path. Prior intelligence of the enemy's courses of action and deployments is important for deciding appropriate redirections of LAEs even in the presence of cooperative sensing. Following a fixed set of standard operating tactics regardless of the targets of interest and enemy's courses of action is not an effective way to deploy a cooperative sensing network.

THIS PAGE INTENTIONALLY LEFT BLANK

V. CONCLUSIONS AND RECOMMENDATIONS

A. KEY OPERATIONAL INSIGHTS

The overall effectiveness of the cooperative sensing network for classifying TCTs and armor targets with four LAEs stand at relatively low mean percentages of 9.8% and 27.2%, respectively. The low classification proportions are attributed to the limited time frame the UAVs have for the IPB operation and the modestly large number of neutral vehicles. Depending on the setup of the UAV behaviors and sensor parameters, the UAVs may be distracted by this clutter around interesting targets, thus unable to complete the routes they were initially designated. However, based on the author's past experiences with intelligence collection experiments, the results fall within the respectable range from an operational standpoint, given the short-range optical sensory assets searching in a considerably large area of operations. The relative classification performance of approximately one TCT to three armor targets makes reasonable sense as the armor targets have unlimited durations of vulnerability and the movement of an armor battalion generally emits strong signatures which leads to easy detection. They are also closely clustered which means the acquisition of one tank gives away the others in the formation. However, the TCTs are direct opposites in their operations; they are well concealed, operate individually and have limited periods of vulnerability, thus making them hard targets to catch.

Two out of the seven main effects filtered out as factors of significance by the regression analysis describe Red TCT characteristics that are beyond the control of Blue forces. These two factors are the TCT concealment factor which dictates their ability to conceal themselves to avoid UAV detection and classification, and the counter-detection sensor range which determines their ability to detect approaching UAVs and hence evade UAV detection and classification. While TCT counter-detection sensor range does not show a steep impact on the UAV classification performance – and can be overcome with better LAE sensors with longer classification ranges and higher classification

probabilities – well-camouflaged TCTs reduce the overall UAV classification capability substantially. This suggests that mounting an EO sensor alone on the LAEs is not an effective solution to the problem of locating well-camouflaged TCTs. Perhaps a more viable option for classifying TCTs in densely forested areas is to equip the LAEs with IR sensors as well, to allow the targets to be tracked based on heat emissions instead of solely on optical detection. In this way, the classification opportunities are no longer limited to the windows of vulnerabilities when the TCT appears.

The increase in the LAE responsiveness to an MAE redirection versus its tendency to follow its pre-assigned routes has a marginal positive effect on the proportion of TCT classification in the scenario. The MAE, which is designed to provide global initial detection, cues all the LAEs to perform a close-in classification when it finds suspicious contacts. Once the first LAE to arrive has successfully classified the contacts, the modeling approach used in this thesis makes certain that all other responding LAEs are turned back. However, such LAE behavior deters effective overall classification performance on armor targets. Instead, an LAE should adopt the tactics to follow a newly classified armor contact which would likely lead to the acquisition of more armor elements in the formation. An LAE that is responsive to the MAE cueing may benefit the first successful armor classification. However, if this LAE is frequently distracted by subsequent MAE redirections, and the associated traveling times are long because the cues are dispersed, then it may spend time traveling between unclassified targets that could otherwise be more effectively used to acquire more armor elements clustering around the first.

Communication parameters such as link reliability and message latency are notably absent from the regression models that depict factors of significance in a cooperative sensing network deployment. The author opines the observation does correctly reflect the actual environment in that the range of message latency between 0 to 100 seconds is short compared to the LAE flight time to the suspicious contact in response to an MAE redirection, thus does not impact the

overall classification effectiveness of the sensing network. The relatively low tempo of MAE redirections during the short four-hour IPB operation might also give the MAE sufficient opportunities for retransmissions even in the presence of poor link availability. Note also that the airspace separation between the UAVs does not play a significant role in determining the overall classification proportions of the targets. The separations between the MAE and the LAEs in practice are not a concern since they tend to fly at different altitudes. Similarly, the separations between the LAEs are of little concern in this scenario since their flight plans have already ensured no two LAEs are close to each other at any point in time. On an MAE redirection, all other responding LAEs are turned back after the first LAE to arrive has successfully classified the contact; the likelihood of having two LAEs closing into the same target is small. It is obvious in retrospect that airspace separation has little impact, if not none at all, on this particular sensing network performance.

While much is discussed about the behaviors of the UAVs in response to the presence of shared SA in a cooperative sensing environment in the earlier observations, many of the factors that contribute directly or indirectly to the extent of overall coverage of the sensing network appear in the analysis as significant. Factors such as MAE classification range, LAE classification range and number of LAEs show general trends of improving classification capabilities for both target types as their values increase. However, the increase in classification proportion for increasing LAE classification range tapers off, and even tips downwards around the 5,000 meters range. In this scenario, the surrounding neutral vehicles easily distract an LAE with a large classification footprint. This renders the LAE ineffective in its mission to search out the Red targets. In addition, the overall classification performance of the sensing network is very sensitive to the routings of the UAVs, which suggests that it is worthwhile to devote much time and effort into collecting information regarding the enemy's target profiles, position and terrain prior to preparing the UAV search paths to provide the greatest ground coverage in areas of suspected operation. The

analysis reveals that while much is invested into netting UAVs together for interaction and cooperation, the traditional emphasis of investing in building better quality sensors that see further and clearer is as important.

Cooperative sensing does provide a more robust solution in this scenario in terms of the classification performance should an LAE fail or be shot down during the four-hour operation. Without cooperation, an LAE failure will result in a "hole" in the ISR coverage of the entire area of operation unless a spare LAE is dispatched. The detrimental effect is mitigated to a certain extent with cooperative sensing in that another LAE may be redirected to patch this "hole." However, an LAE being responsive to an MAE cueing may not always give the best overall classification results; reacting to a cueing request may lead to the classification of other potential targets but risk the opportunity of a greater payoff by remaining in its path. Prior intelligence of the enemy's courses of action and deployments is important for deciding appropriate redirections of LAEs even in the presence of cooperative sensing. Following a fixed set of standard operating tactics regardless of the targets of interest and enemy's courses of action is not the way forward in employing a cooperative sensing network.

B. RECOMMENDATIONS FOR FUTURE WORK

As with all exploratory investigations, the thesis has led to more questions and identified other relevant areas of interest for follow-on work. The ensuing paragraphs recommend some possible aspects that merit further research.

The analysis highlights the sensitivity of the models and the MOEs to variations in the UAV routings. While the routings in this research are based on an intuitive justification which was deemed appropriate and sufficient for the study by subject matter experts, other routings would also be justifiable with differing operational considerations and other prior intelligence on the adversary courses of action, targets and terrains. Designing an experiment that explores various routing guidance and options, based on a broader number of scenarios

with possible enemy configurations (deployment plans and courses of action) to plan a robust set of routes, could yield a more accurate sense of the design of a cooperative sensing network and a robust solution.

Based on the findings from the analysis, the responsiveness of an LAE to an MAE redirection should vary depending on the current status and recent types of targets classified. For instance, an LAE which has recently made an armor classification might not want to respond to an incoming MAE cueing, but follow the newly classified contact which is likely to lead to more armor target acquisitions. On the contrary, an idling LAE flying on its designated flight plan or one that has just made a TCT classification might get better payoff by being very responsive to an MAE redirection. This prompts another area that is worth further exploration: using an agent-based simulation model to derive more “intelligent” means of cooperation, taking into account the LAE status and the type of recent classification.

Although MANA has been commonly used for evaluating ISR-related problems in a number of studies, such as those presented in the Background Work Section of Chapter I, it is seldom used for modeling cooperative sensing where information passing across a communications network could influence the behaviors of the agents. There is currently no accurate way to verify the models, except by visual inspection of a few instances of the model and by the justification of the set of average classification proportions of the targets falling within ballpark ranges. Porting the models over to another agent-based platform, like PYTHAGORAS (another agent-based distillation model in the Project Albert suite of models), would be beneficial for cross-validating the results of this analysis. This cross-validation is particularly useful to ensure that certain complex behaviors are not modeled incorrectly, or that insights obtained from the analysis are not due to artifacts of a specific modeling platform. However, one should be cautious to avoid focusing on specific numerical comparisons based on the model output data since different simulations yield different set of results.

Instead, a cross-validation process would reveal whether the two sets of model outputs yield qualitatively similar insights.

Another advantage of porting the models over to PYTHAGORAS would be to leverage the power and versatility of its sensor setup. An agent in PYTHAGORAS may carry up to three sensors, and each sensor may have different detection parameters with different detectability on various terrain features (Bitinas, 2004). This flexible sensor setup enables the exploration of a cooperative sensing network configured for multiple sensors, such as an EO and a FOPEN, on a UAV. The effects of having a mix of sensor-bearing UAVs in the area of operation could also be explored. The inclusion of FOPEN or even the multi-modal SAR sensors could facilitate exploration of the improvement in the overall classification performance of the sensing network. However, the downside of using PYTHAGORAS is its simplicity in modeling communications with the rudimentary broadcast mechanism. The broadcast mechanism does not permit the considerations of message latency and link reliability as implemented in the MANA models, but simply exchanges SA information among the UAVs. By studying similar models in MANA and PYTHAGORAS, an analyst could attempt to exploit the strengths of each specific modeling platform to gain better understanding of how a broader variety of sensors, cooperative information sharing, and UAV tactics influence the mission effectiveness.

To gain deeper insights on the effectiveness of a cooperative sensing network for ISR operations, scenarios where multiple local LAEs operate independently in the absence of a coordinating component like the MAE should be investigated. A greater challenge is modeling the effects of UAV swarming, where the deployment of a larger concentration of small UAVs with myopic sensors operating in a distributed yet cooperative manner could be explored.

C. SUMMARY

The success of a battle is increasingly reliant on more accurate and timely collection of the battle-space intelligence. Unmanned systems, and certainly UAVs, are widely used in today's military ISR operations and will be more prevalent in the next generation military as war-fighting concepts such as Network Centric Warfare and Distributed Operation emerge. Tighter integration and tactics development to enhance cooperation between these intelligence collection assets is one of the current focuses among the military intelligence community, and the motivation for this thesis.

The use of agent-based simulation is definitely appropriate to seek insights relating to the tactics and behaviors in using a cooperative sensing network for military ISR. The models are easy to construct and consume relatively less computing power than most conventional simulation models. They can be executed for tens of thousands of replications to exhaust many possible representations of real-life situations. By applying suitable experimental designs, one can move from a realm of impossibility when the number of variations to be investigated is insurmountably large to a problem that can be realistically tackled within days or weeks. The simulation also provides ways to analyze a much wider variety of settings than time and cost would permit in a field experiment. The insights from agent-based simulation models may also provide guidance for setting up future higher-resolution simulation experiments or field tests.

In this thesis, the author has built a number of agent-based models intended to capture the essential details of UAV performance for the purpose of answering the questions that might be of interest for system designers and operators to implement a cooperative sensing network for the military. However, with careful considerations, appropriate assumptions are also made to keep the model manageable within the identified scope. The data collected from the simulations are analyzed and investigated using a wide array of complementary analytical tools and techniques. The study has successfully led to several operational insights pertaining to the design and use of cooperative sensing for

ISR purposes, including the importance of having good UAV sensor capabilities and “intelligent” application of UAV cooperation tactics based on the interested target characteristics, to achieve high overall effectiveness. The study has also spawned further questions and identified relevant areas for follow-on work.

APPENDIX A. UAV ROUTINGS

This appendix presents snapshots of the UAV routings for each MAE-LAE configuration as well as the rationales that led to these routings. During the development of these routes, the author consulted with Captain Starr King, USN, NWDC-Sponsored Chair of Warfare Innovation and Chair of Applied Systems Analysis of the Naval Postgraduate School and Captain Kevin McMindes, a USMC pilot. Both consider the routings reasonable and sufficiently detailed for the purpose of modeling and analysis to answer the questions of interest. However, one should not preclude other alternative routes based on various operational judgments and objectives.

1. MAE ROUTING

The routing of the MAE is planned with the operational objective to provide a detection coverage that is as extensive as possible over the entire area of operation. The MAE performs the classic outward spiral search pattern by following the waypoints as depicted in Figure A-1. Note that the agents in MANA always start their movement from the waypoint with the largest index and proceed to the one with index zero in a reverse numerical order. In the models, the MAE is intended to loop around the waypoints such that it flies back to the starting waypoint once the last one is reached.

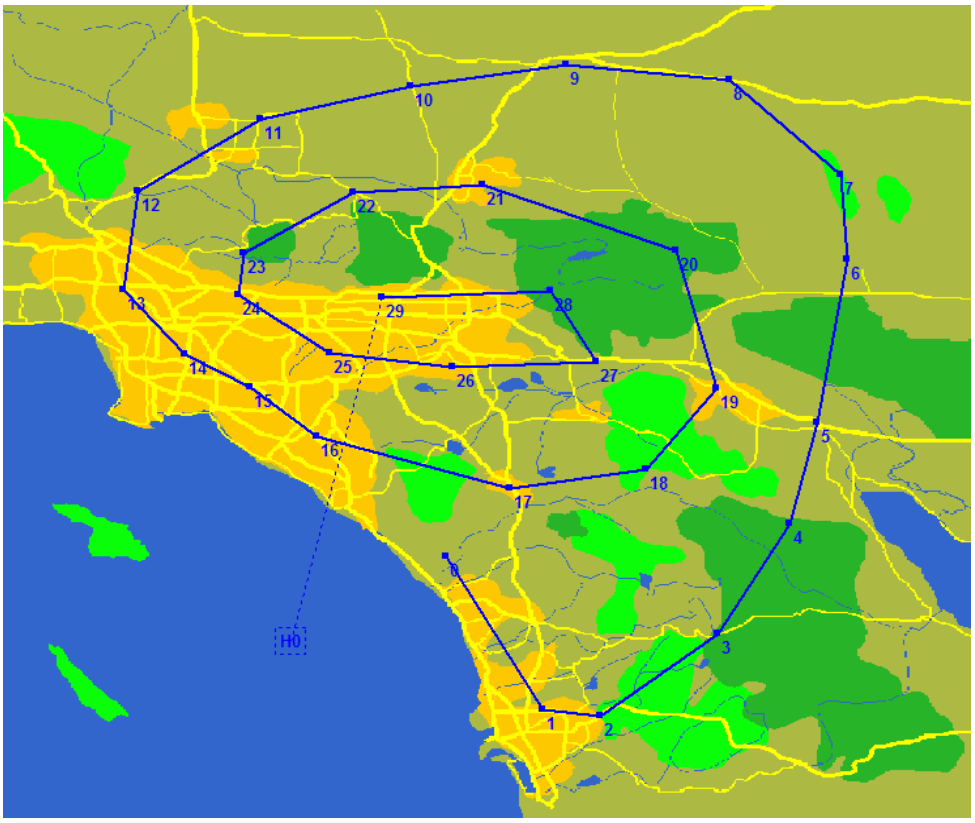

Figure A-1 Routing of the MAE

2. ONE-LAE ROUTING

In the One-LAE configuration shown in Figure A-2, the one and only LAE is allocated to provide surveillance around the parameter of the Red objective, Twenty-nine Palms, where critical Red activities are deemed to be of most interest to the MEB commander.

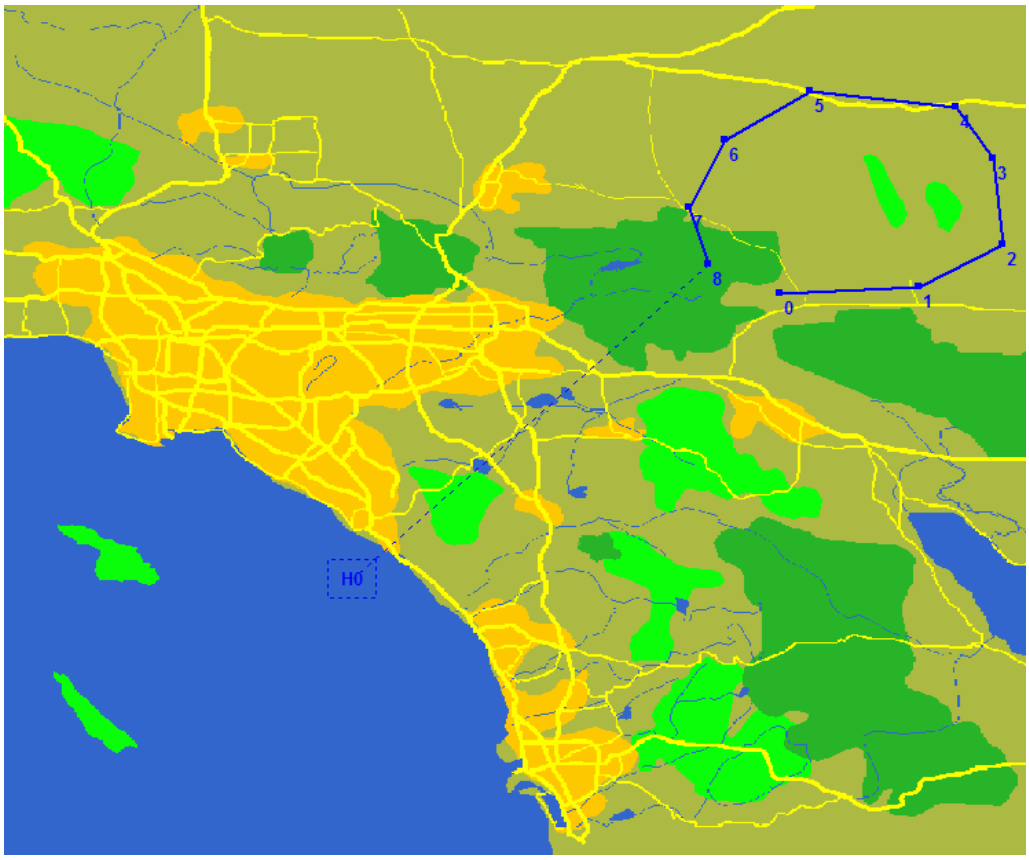

Figure A-2 Routing of One LAE

3. TWO-LAE ROUTINGS

On availability of a second LAE, it is assigned to provide coverage over the larger of the two cities, Los Angeles and its suburbs, while leaving the first LAE to continue its surveillance of Twenty-nine Palms. The only intuitive justification for giving priority to the cities over the forested and mountainous areas when allocating areas of responsibilities to the LAE assets is based on the assumption that the developed areas are considered to be more accessible by well-developed road networks and infrastructures that facilitate deployment of large Red forces. The routes of the two LAEs are shown in Figure A-3.

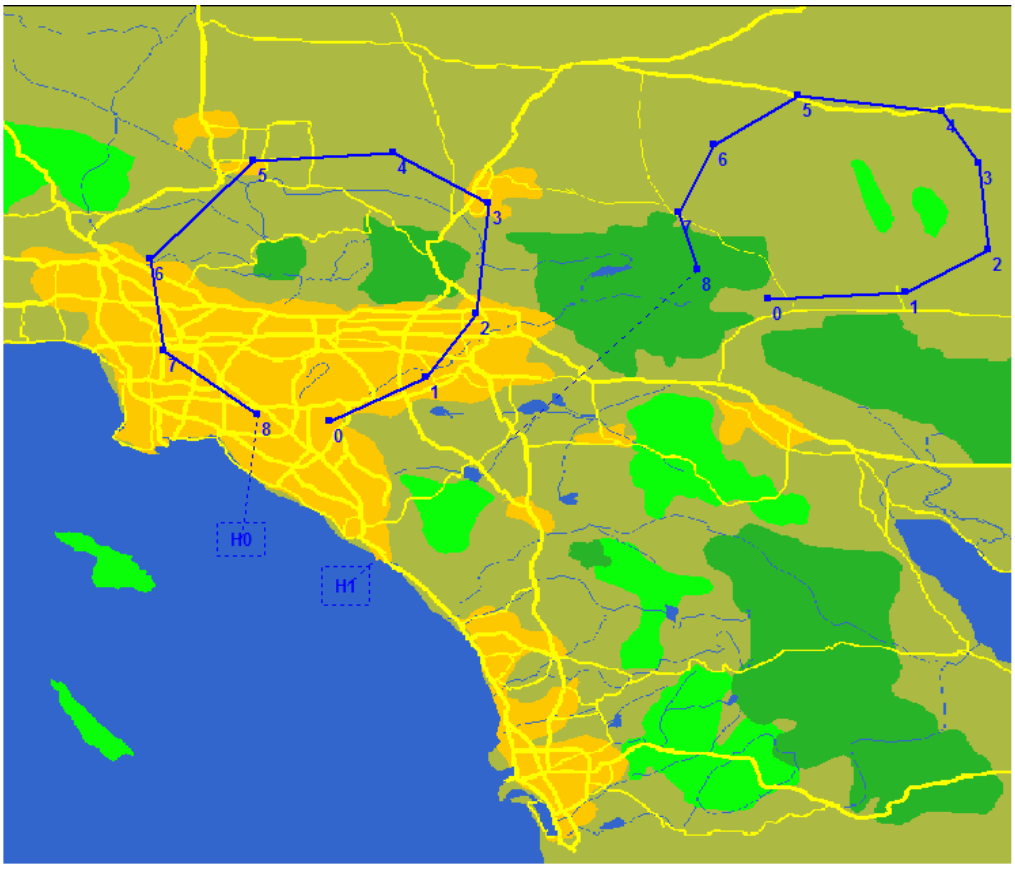

Figure A-3 Routing of Two LAEs

4. THREE-LAE ROUTINGS

With the third LAE, it is desired to extend the ISR coverage to the next larger city, San Diego, while focusing LAE assets on the regions that are in a direct path from the amphibious landing to the Red objective. The routings are shown in Figure A-4. The area of coverage may appear ambitious for a local sensor capability as an LAE, but it is considered important to establish situational awareness in these regions where many Red air defense elements and time critical targets are expected to operate to defend Twenty-nine Palms against the Blue attack.

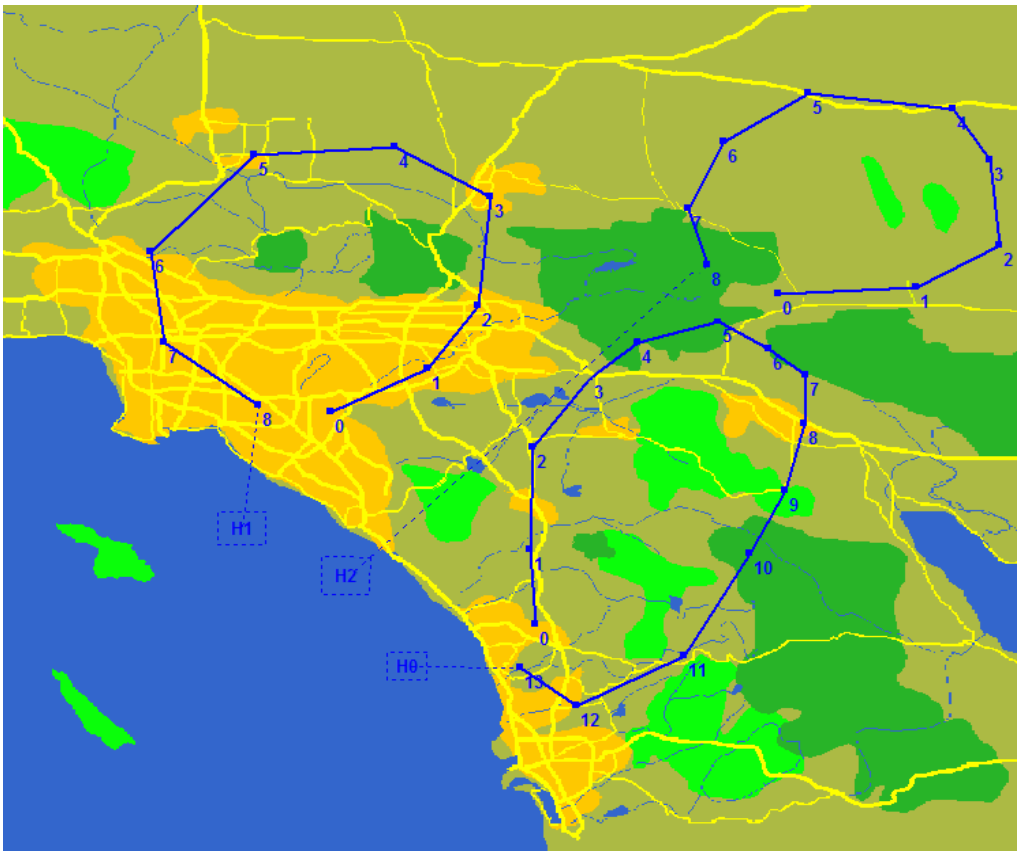

Figure A-4 Routing of Three LAEs

5. FOUR-LAE ROUTINGS

The addition of the fourth LAE provides more effective ISR coverage of the Los Angeles loop whose area of responsibility is initially very large for a single LAE. The original area of responsibility is now broken into two halves: the western and eastern loop, each allocated to an LAE as illustrated in Figure A-5.

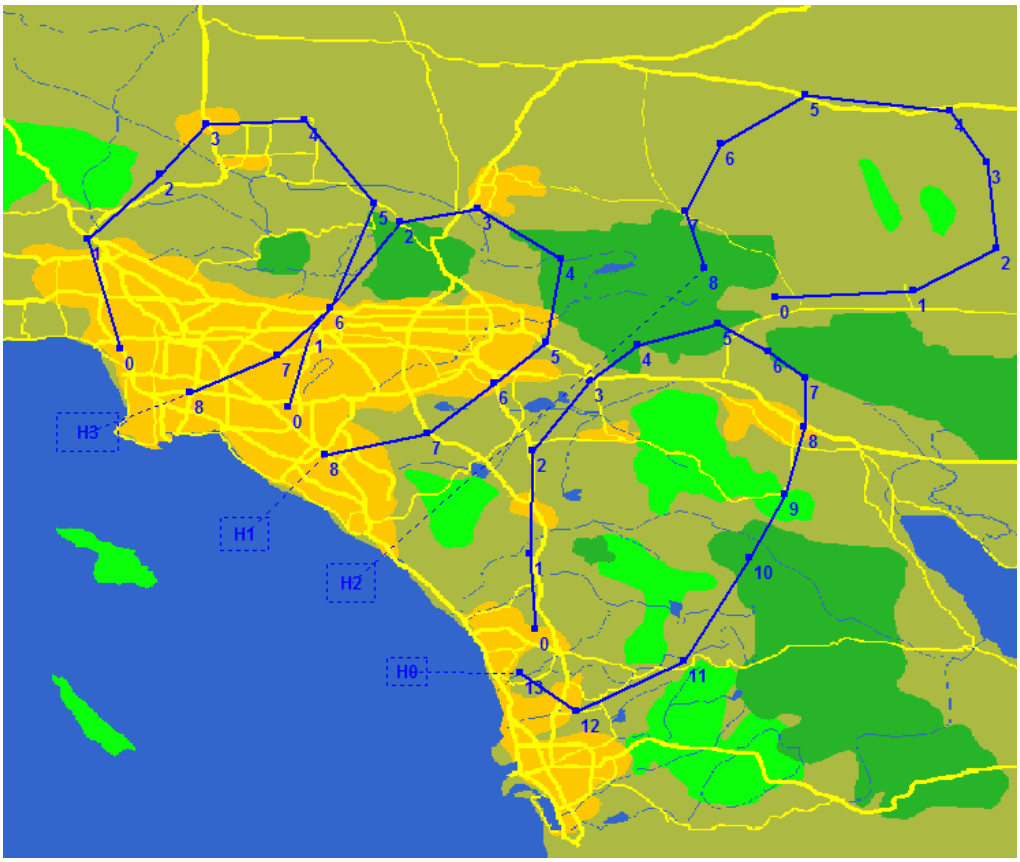

Figure A-5 Routing of Four LAEs

6. FIVE-LAE ROUTINGS

With five LAEs, the large San Diego loop is now divided into a northern and southern loop as depicted in Figure A-6. A single LAE is responsible for the ISR coverage of each loop.

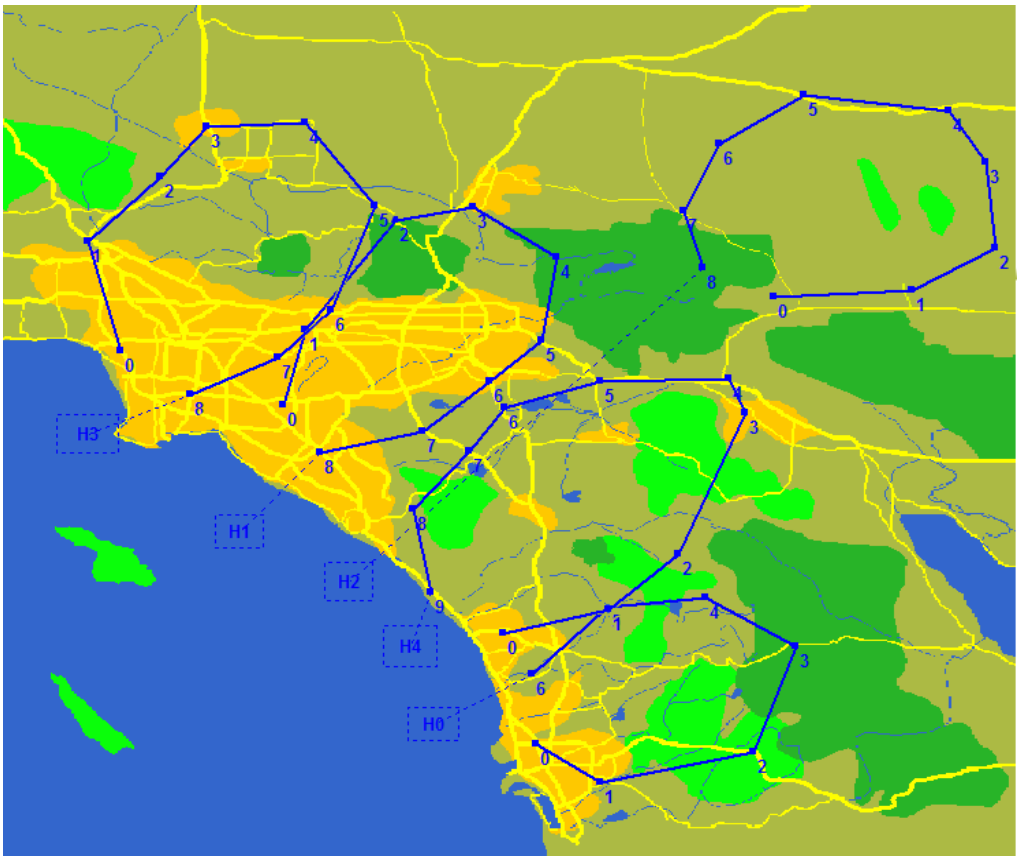

Figure A-6 Routing of Five LAEs

THIS PAGE INTENTIONALLY LEFT BLANK

APPENDIX B. LINEAR REGRESSIONS, PARTITIONING TREES, GRAPHS AND PLOTS FOR ANALYSIS

This appendix contains the linear regression outputs, partitioning trees, prediction profiler graphs and other plots used in the complete analytical effort. The materials are arranged according to their relevance to the analytical focus provided by the initial questions of interest.

1. SENSING NETWORK CONFIGURATIONS

Distributions of the proportion of total red targets classified for one (leftmost) to five (rightmost) LAEs show a general trend of better average classification results as the number of LAEs increases. Note that poor results can occur for all situations.

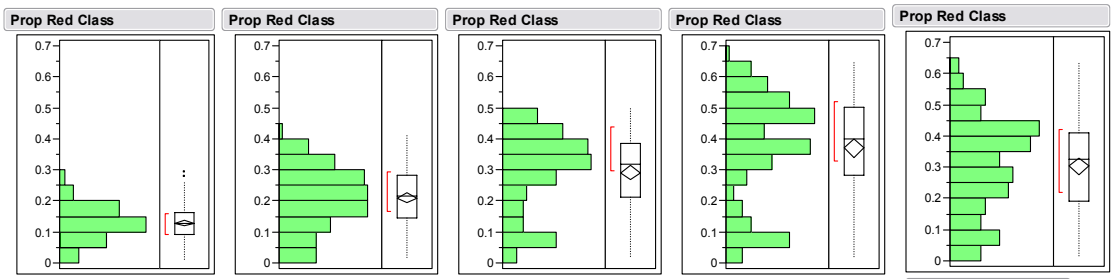

Quantiles		
100.0%	maximum	0.29067
99.5%		0.29067
97.5%		0.25535
90.0%		0.19229
75.0%	quartile	0.16321
50.0%	median	0.12787
25.0%	quartile	0.09300
10.0%		0.05650
2.5%		0.02931
0.5%		0.00762
0.0%	minimum	0.00762

Moments	
Mean	0.1283989
Std Dev	0.0544607
Std Err Mean	0.004795
upper 95% Mean	0.1378866
lower 95% Mean	0.1189112
N	129

Quantiles		
100.0%	maximum	0.41567
99.5%		0.41567
97.5%		0.39072
90.0%		0.33525
75.0%	quartile	0.28296
50.0%	median	0.21529
25.0%	quartile	0.14577
10.0%		0.05717
2.5%		0.03253
0.5%		0.01621
0.0%	minimum	0.01621

Moments	
Mean	0.2097988
Std Dev	0.0968781
Std Err Mean	0.0085296
upper 95% Mean	0.2266761
lower 95% Mean	0.1929214
N	129

Quantiles		
100.0%	maximum	0.49825
99.5%		0.49825
97.5%		0.47098
90.0%		0.43888
75.0%	quartile	0.38650
50.0%	median	0.31754
25.0%	quartile	0.21233
10.0%		0.06538
2.5%		0.04371
0.5%		0.01383
0.0%	minimum	0.01383

Moments	
Mean	0.2907141
Std Dev	0.1298252
Std Err Mean	0.0114305
upper 95% Mean	0.3133313
lower 95% Mean	0.268097
N	129

Quantiles		
100.0%	maximum	0.65075
99.5%		0.65075
97.5%		0.63798
90.0%		0.56854
75.0%	quartile	0.50042
50.0%	median	0.39787
25.0%	quartile	0.28419
10.0%		0.07300
2.5%		0.04621
0.5%		0.01504
0.0%	minimum	0.01504

Moments	
Mean	0.3695378
Std Dev	0.1756173
Std Err Mean	0.0154622
upper 95% Mean	0.4001325
lower 95% Mean	0.3389431
N	129

Quantiles		
100.0%	maximum	0.63787
99.5%		0.63787
97.5%		0.57714
90.0%		0.50738
75.0%	quartile	0.41085
50.0%	median	0.32542
25.0%	quartile	0.19258
10.0%		0.06571
2.5%		0.03285
0.5%		0.01242
0.0%	minimum	0.01242

Moments	
Mean	0.3033789
Std Dev	0.1526812
Std Err Mean	0.0134428
upper 95% Mean	0.3299778
lower 95% Mean	0.2767799
N	129

Distributions of the proportion of TCT classified for one (leftmost) to five (rightmost) LAEs show a general trend of better classification results as the number of LAEs increases. Once again, poor outcomes can occur even when the number of LAEs is large.

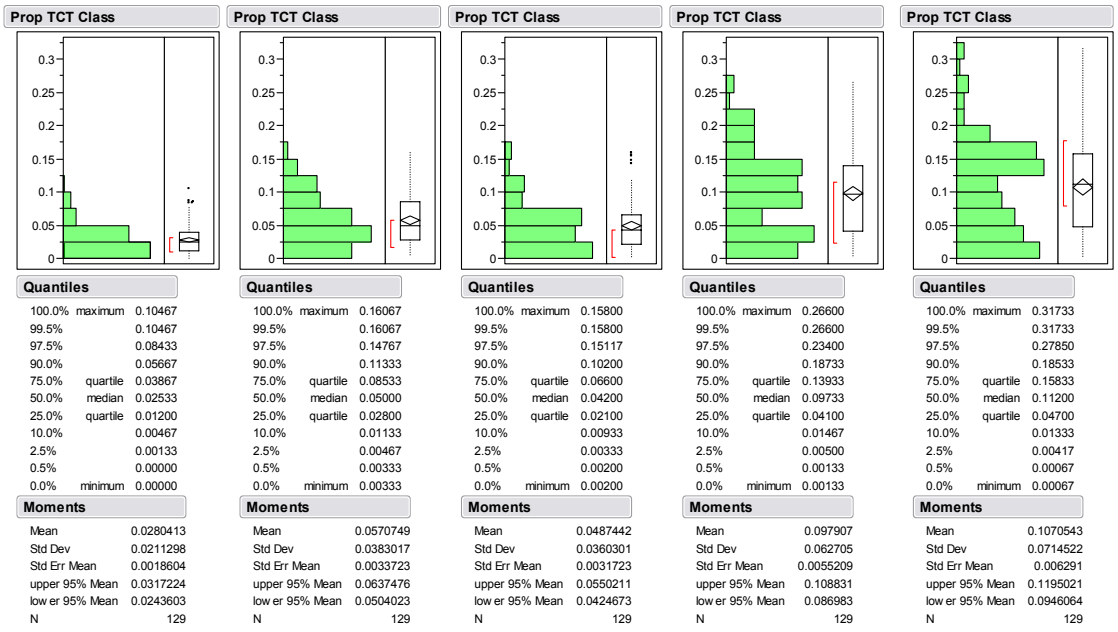

Quantiles		
100.0%	maximum	0.10467
99.5%		0.10467
97.5%		0.08433
90.0%		0.05667
75.0%	quartile	0.03867
50.0%	median	0.02533
25.0%	quartile	0.01200
10.0%		0.00467
2.5%		0.00133
0.5%		0.00000
0.0%	minimum	0.00000

Moments	
Mean	0.0280413
Std Dev	0.0211298
Std Err Mean	0.0018604
upper 95% Mean	0.0317224
low er 95% Mean	0.0243603
N	129

Quantiles		
100.0%	maximum	0.16067
99.5%		0.16067
97.5%		0.14767
90.0%		0.11333
75.0%	quartile	0.08533
50.0%	median	0.05000
25.0%	quartile	0.02800
10.0%		0.01133
2.5%		0.00467
0.5%		0.00333
0.0%	minimum	0.00333

Moments	
Mean	0.0570749
Std Dev	0.0383017
Std Err Mean	0.0033723
upper 95% Mean	0.0637476
low er 95% Mean	0.0504023
N	129

Quantiles		
100.0%	maximum	0.15800
99.5%		0.15800
97.5%		0.15117
90.0%		0.10200
75.0%	quartile	0.06600
50.0%	median	0.04200
25.0%	quartile	0.02100
10.0%		0.00933
2.5%		0.00333
0.5%		0.00200
0.0%	minimum	0.00200

Moments	
Mean	0.0487442
Std Dev	0.0360301
Std Err Mean	0.0031723
upper 95% Mean	0.0550211
low er 95% Mean	0.0424673
N	129

Quantiles		
100.0%	maximum	0.26600
99.5%		0.26600
97.5%		0.23400
90.0%		0.18733
75.0%	quartile	0.13933
50.0%	median	0.09733
25.0%	quartile	0.04100
10.0%		0.01467
2.5%		0.00500
0.5%		0.00133
0.0%	minimum	0.00133

Moments	
Mean	0.097907
Std Dev	0.062705
Std Err Mean	0.0055209
upper 95% Mean	0.108831
low er 95% Mean	0.086983
N	129

Quantiles		
100.0%	maximum	0.31733
99.5%		0.31733
97.5%		0.27850
90.0%		0.18533
75.0%	quartile	0.15833
50.0%	median	0.11200
25.0%	quartile	0.04700
10.0%		0.01333
2.5%		0.00417
0.5%		0.00067
0.0%	minimum	0.00067

Moments	
Mean	0.1070543
Std Dev	0.0714522
Std Err Mean	0.006291
upper 95% Mean	0.1195021
low er 95% Mean	0.0946064
N	129

Distributions of the proportion of armor classified for one (leftmost) to five (rightmost) LAEs show a general trend of better classification results as the number of LAEs increases. The exception observed for the scenario with five LAEs is attributed to the distribution of routes when the fifth LAE is introduced which misses most of the armor elements in Area 1 as the convoy moves northwards.

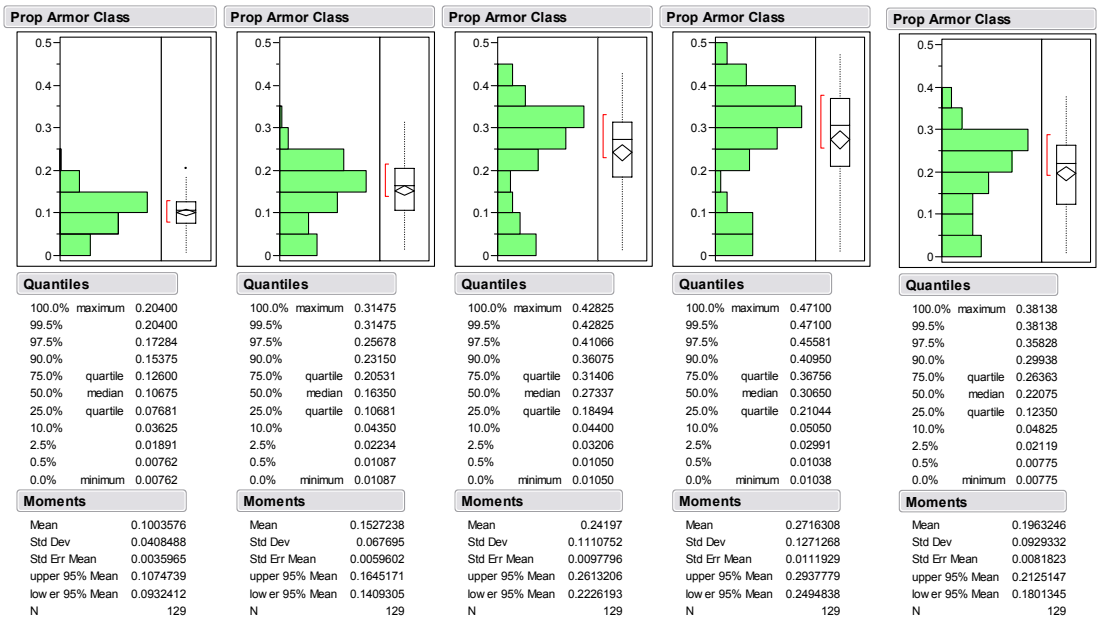

The bivariate fits for the proportion of target classification by the number of LAEs show that the quadratic terms are statistically significant in the models for the total red and armor targets but not in the model for the TCT targets.

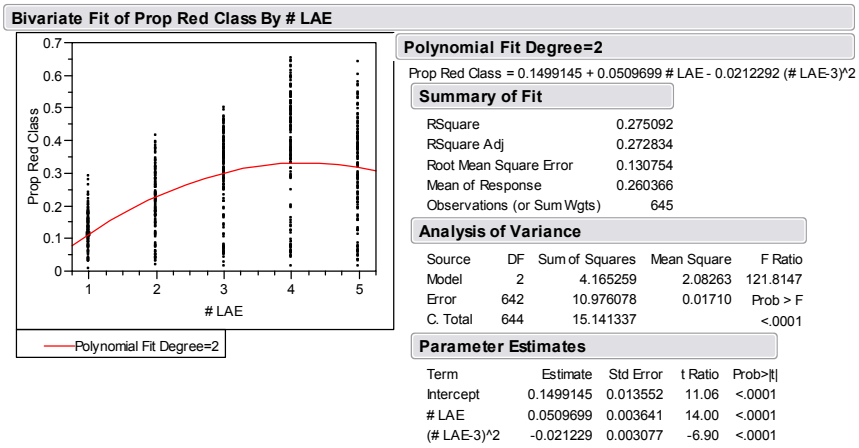

Bivariate Fit of Prop TCT Class By # LAE

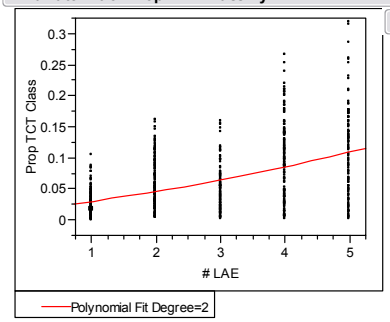

Polynomial Fit Degree=2

Prop TCT Class = 0.0055754 + 0.0198858 # LAE + 0.0012658 (# LAE-3)^2

Summary of Fit

RSquare	0.238704
RSquare Adj	0.236333
Root Mean Square Error	0.050483
Mean of Response	0.067764
Observations (or Sum Wgts)	645

Analysis of Variance

Source	DF	Sum of Squares	Mean Square	F Ratio
Model	2	0.5130171	0.256509	100.6496
Error	642	1.6361569	0.002549	Prob > F
C. Total	644	2.1491740		<.0001

Parameter Estimates

Term	Estimate	Std Error	t Ratio	Prob>|t|
Intercept	0.0055754	0.005232	1.07	0.2870
# LAE	0.0198858	0.001406	14.15	<.0001
(# LAE-3)^2	0.0012658	0.001188	1.07	0.2870

Bivariate Fit of Prop Armor Class By # LAE

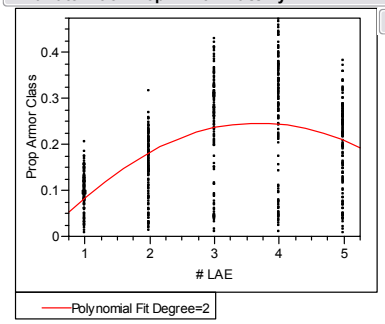

Polynomial Fit Degree=2

Prop Armor Class = 0.1443391 + 0.0310841 # LAE - 0.022495 (# LAE-3)^2

Summary of Fit

RSquare	0.270777
RSquare Adj	0.268506
Root Mean Square Error	0.095195
Mean of Response	0.192601
Observations (or Sum Wgts)	645

Analysis of Variance

Source	DF	Sum of Squares	Mean Square	F Ratio
Model	2	2.1603087	1.08015	119.1947
Error	642	5.8178682	0.00906	Prob > F
C. Total	644	7.9781769		<.0001

Parameter Estimates

Term	Estimate	Std Error	t Ratio	Prob>|t|
Intercept	0.1443391	0.009866	14.63	<.0001
# LAE	0.0310841	0.00265	11.73	<.0001
(# LAE-3)^2	-0.022495	0.00224	-10.04	<.0001

A stepwise logistic regression model is fitted for the categorical response variable *lowTCTclass* to investigate the rationale for high frequencies clustering around the low value as depicted in the distribution graphs.

$$lowTCTclass = \begin{cases} 1 & if\ \ proportion\ of\ \ TCT\ \ classified < 0.05 \\ 0 & otherwise \end{cases}$$

Nominal Logistic Fit for Low TCT Class

Whole Model Test

Model	-LogLikelihood	DF	ChiSquare	Prob>ChiSq
Difference	109.95633	6	219.9127	<.0001
Full	337.11662			
Reduced	447.07295			

RSquare (U)	0.2459
Observations (or Sum Wgts)	645

Converged by Gradient

Lack Of Fit

Source	DF	-LogLikelihood	ChiSquare
Lack Of Fit	122	104.84869	209.6974
Saturated	128	232.26793	Prob>ChiSq
Fitted	6	337.11662	<.0001

Parameter Estimates

Term	Estimate	Std Error	ChiSquare	Prob>ChiSq
Intercept	-4.0189294	0.6504023	38.18	<.0001
LAE React InOrg SA	0.48629692	0.1619628	9.02	0.0027
MAE Detect Range	0.00019502	0.0000467	17.44	<.0001
LAE Class Range	0.00087507	0.00009	94.48	<.0001
LAE Class Prob	1.79752337	0.4586052	15.36	<.0001
TCT Conceal	-0.0241628	0.0033894	50.82	<.0001
TCT Detect Range	-0.138945	0.0320138	18.84	<.0001

For log odds of 0/1

The model reveals that the factors of significance for the low classification rates are LAE classification range and classification probability, LAE responsiveness to other UAV SA, MAE detection range, TCT concealment and TCT evasion detection range.

The prediction profiler graph for the logistic regression model suggests that the LAE classification range is the most influential factor given that all others are kept constant at their nominal values.

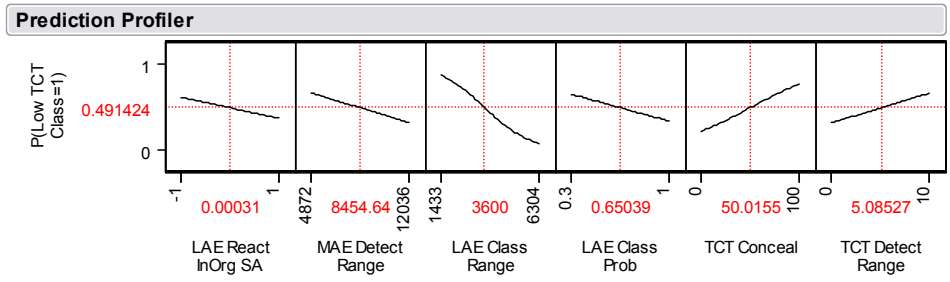

The partitioning tree for the proportion of TCT targets further suggests that an LAE with classification range less than approximately 3,200 meters has a mean classification proportion of only 0.04. Even if the LAE has better classification capabilities, the TCT classification rate is even worse if the TCT concealment is above 85%.

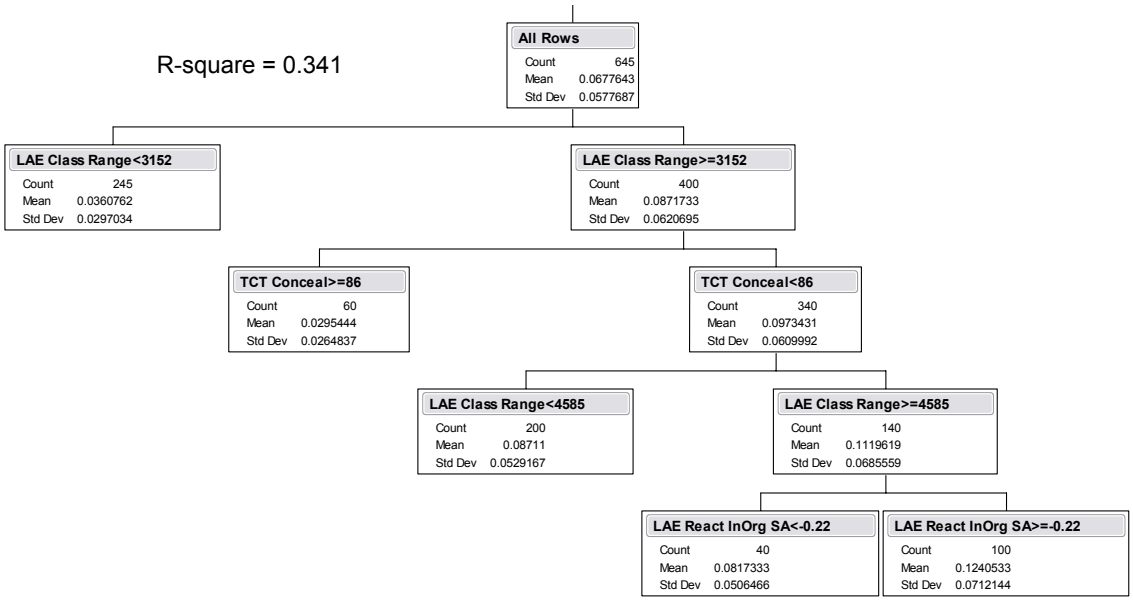

A similar analytical approach is also conducted to investigate the rationale for the low proportion of armor classified. The categorical response variable *lowARMORclass* is defined as follows.

$$lowARMORclass = \begin{cases} 1 & if\ \ proportion\ of\ \ armor\ classified < 0.1 \\ 0 & otherwise \end{cases}$$

Nominal Logistic Fit for Low Armor Class

Whole Model Test

Model	-LogLikelihood	DF	ChiSquare	Prob>ChiSq
Difference	197.73733	4	395.4747	<.0001
Full	166.87878			
Reduced	364.61611			

RSquare (U)	0.5423
Observations (or Sum Wgts)	645

Converged by Gradient

Lack Of Fit

Source	DF	-LogLikelihood	ChiSquare
Lack Of Fit	124	73.35416	146.7083
Saturated	128	93.52462	Prob>ChiSq
Fitted	4	166.87878	0.0802

Parameter Estimates

Term	Estimate	Std Error	ChiSquare	Prob>ChiSq
Intercept	-10.494934	1.089704	92.76	<.0001
LAE React InOrg SA	-0.5623604	0.2333648	5.81	0.0160
MAE Class Range	0.00027273	0.0000733	13.86	0.0002
LAE Class Range	0.00267633	0.0002349	129.79	<.0001
MAE Class Prob	5.50551346	1.0309848	28.52	<.0001

For log odds of 0/1

The model suggests that LAE classification range, LAE responsiveness to other UAV SA, MAE classification range and classification probability are significant determinants of the low classification rates for armor targets.

The LAE classification range is again identified by the prediction profiler as the most significant factor given that all others are kept at their nominal levels.

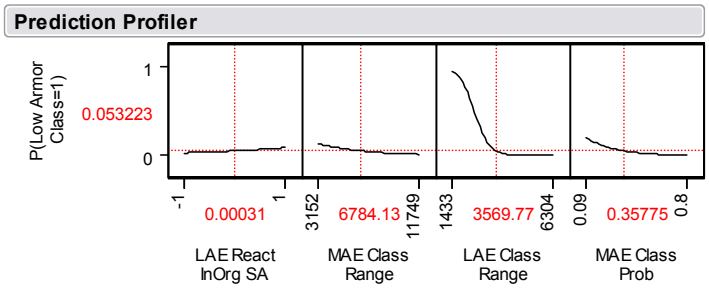

The partitioning tree shows that an LAE with classification range of less than 2,600 meters has a mean proportion of armor targets classified of about 0.06.

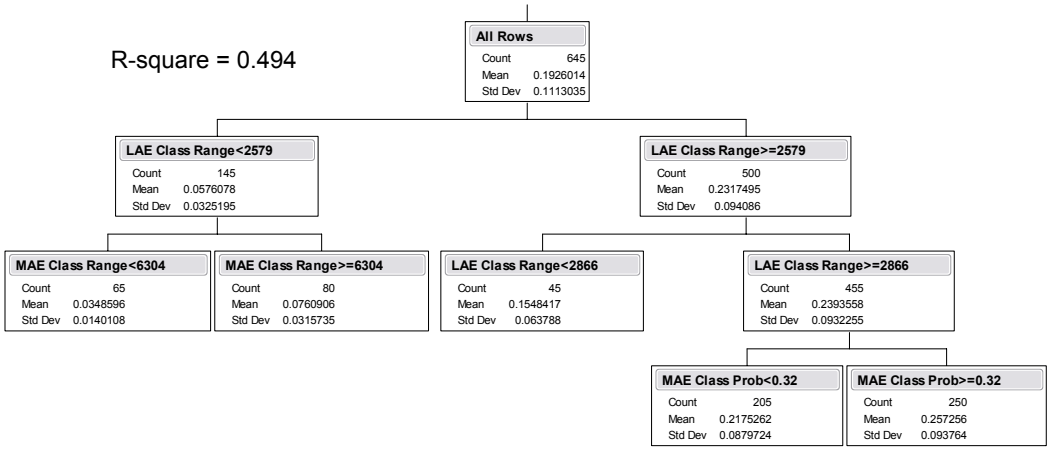

2. FACTORS OF SIGNIFICANCE

Next, Multiple Linear Regression models are provided for the proportion of TCT classified with consideration of only the main effects (top left), the main and quadratic effects (top right) and including the two-way interactions (bottom).

Response Prop TCT Class

Summary of Fit

RSquare	0.581127
RSquare Adj	0.576524
Root Mean Square Error	0.037593
Mean of Response	0.067764
Observations (or Sum Wgts)	645

Analysis of Variance

Source	DF	Sum of Squares	Mean Square	F Ratio
Model	7	1.2489432	0.178420	126.2497
Error	637	0.9002308	0.001413	Prob > F
C. Total	644	2.1491740		<.0001

Parameter Estimates

Term	Estimate	Std Error	t Ratio	Prob>|t|
Intercept	-0.07178	0.009439	-7.60	<.0001
LAE React InOrg SA	0.011604	0.002545	4.56	<.0001
MAE Class Range	0.0000039	7.521e-7	5.24	<.0001
LAE Class Range	0.0000185	0.000001	16.12	<.0001
LAE Class Prob	0.0492387	0.007107	6.93	<.0001
TCT Conceal	-0.000533	0.000051	-10.47	<.0001
TCT Detect Range	-0.003614	0.000492	-7.34	<.0001
# LAE	0.0198858	0.001047	19.00	<.0001

Response Prop TCT Class

Summary of Fit

RSquare	0.650138
RSquare Adj	0.645179
Root Mean Square Error	0.034441
Mean of Response	0.067764
Observations (or Sum Wgts)	645

Analysis of Variance

Source	DF	Sum of Squares	Mean Square	F Ratio
Model	9	1.3972599	0.155251	131.1113
Error	635	0.7519141	0.001184	Prob > F
C. Total	644	2.1491740		<.0001

Parameter Estimates

Term	Estimate	Std Error	t Ratio	Prob>|t|
Intercept	-0.06237	0.008775	-7.11	<.0001
LAE React InOrg SA	0.0117325	0.00233	5.04	<.0001
MAE Class Range	0.000004	6.888e-7	5.84	<.0001
LAE Class Range	0.0000212	0.000001	19.46	<.0001
LAE Class Prob	0.0503286	0.006507	7.74	<.0001
TCT Conceal	-0.000549	0.000047	-11.78	<.0001
TCT Detect Range	-0.003587	0.000451	-7.96	<.0001
# LAE	0.0198858	0.000958	20.76	<.0001
(LAE Class Range-3569.77)*(LAE Class Range-3569.77)	-6.907e-9	7.86e-10	-8.79	<.0001
(TCT Conceal-50.0155)*(TCT Conceal-50.0155)	-0.000009	0.000002	-5.19	<.0001

Response Prop TCT Class

Summary of Fit

RSquare	0.731611
RSquare Adj	0.725647
Root Mean Square Error	0.030259
Mean of Response	0.067764
Observations (or Sum Wgts)	645

Analysis of Variance

Source	DF	Sum of Squares	Mean Square	F Ratio
Model	14	1.5723599	0.112311	122.6672
Error	630	0.5768141	0.000916	Prob > F
C. Total	644	2.1491740		<.0001

Parameter Estimates

Term	Estimate	Std Error	t Ratio	Prob>|t|
Intercept	-0.062471	0.007717	-8.10	<.0001
LAE React InOrg SA	0.0120452	0.002049	5.88	<.0001
MAE Class Range	0.0000039	6.059e-7	6.50	<.0001
LAE Class Range	0.0000212	9.586e-7	22.09	<.0001
LAE Class Prob	0.0503922	0.005722	8.81	<.0001
TCT Conceal	-0.000549	0.000041	-13.40	<.0001
TCT Detect Range	-0.003615	0.000397	-9.11	<.0001
# LAE	0.0198858	0.000842	23.60	<.0001
(LAE React InOrg SA-0.00031)*(LAE Class Range-3569.77)	0.0000076	0.000002	4.38	<.0001
(LAE Class Range-3569.77)*(# LAE-3)	0.000006	6.537e-7	9.19	<.0001
(LAE Class Prob-0.65039)*(# LAE-3)	0.0137356	0.004044	3.40	0.0007
(TCT Conceal-50.0155)*(TCT Detect Range-5.08527)	-0.000093	0.000016	-5.85	<.0001
(TCT Conceal-50.0155)*(# LAE-3)	-0.000156	0.000029	-5.39	<.0001
(LAE Class Range-3569.77)*(LAE Class Range-3569.77)	-7.013e-9	7e-10	-10.02	<.0001
(TCT Conceal-50.0155)*(TCT Conceal-50.0155)	-0.000008	0.000002	-5.05	<.0001

Note that the ratios used in the experimental design and their basic parameters (for example, ratio of MAE/LAE classification probabilities, MAE classification probability, and LAE classification probability) are all included as potential terms in the model selection process. However, none of the ratios appeared in any of the stepwise models, while some of the basic parameters (for example, LAE classification probability) are included in the selected model.

The adjusted R-squares as opposed to the standard R-squares for the three models are considered when selecting the appropriate base model for analysis so that the matrices are normalized against the number of terms used in the models. The full model (includes the quadratic and interaction terms) explains 73% of the variability, while the main effect model and quadratic model explain only 58% and 65% respectively. The quadratic and interaction terms account for about 20% of the explanatory power in the full model. These terms are therefore deemed important and the full model is used a baseline model for analysis.

The actual by predicted plot on the left shows the lower tail of the distribution being cut off as the actual proportion can only take on values between zero and one. Similarly, there are no negative residuals when the predicted value is less than or equal zero, hence the residual by predicted plot appears capped by the 45 degree boundary on the bottom left of the plot. This departure from the regression assumption of additive constant variance noise would be of more concern if we were interested in making accurate numerical predictions of classification capabilities, rather than in identifying those factors that have the greatest impact on classification capability. It also shows the value of obtaining qualitatively similar results from several different analysis methods, such as partitioning trees, Multiple Linear Regression, and logistic regression.

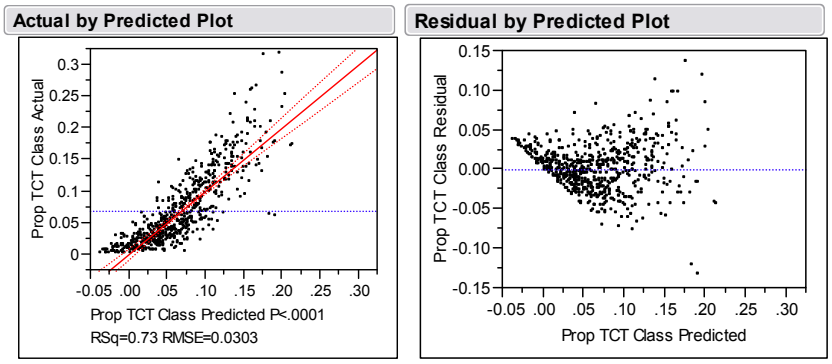

The Pareto plot displays the factors of significance in descending order in accordance to their effects on the proportion of TCT classified.

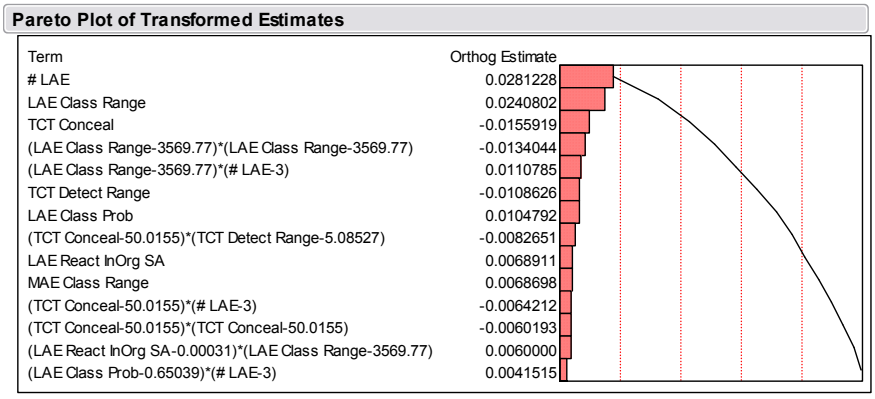

The prediction profiler graph shows a significant increasing linear relationship between the response variable and the number of LAEs, which also appears in the Pareto plot as the factor with the greatest impact. The graph also illustrates the non-linear relationships of the response variable with both LAE classification range and TCT concealment ability.

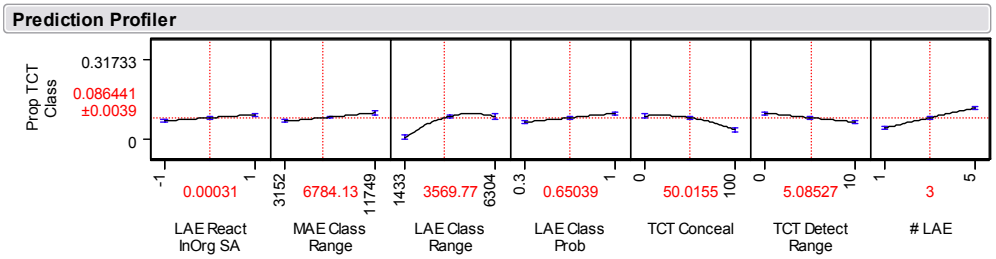

The interaction plot highlights the statistically significant interactions in solid lines.

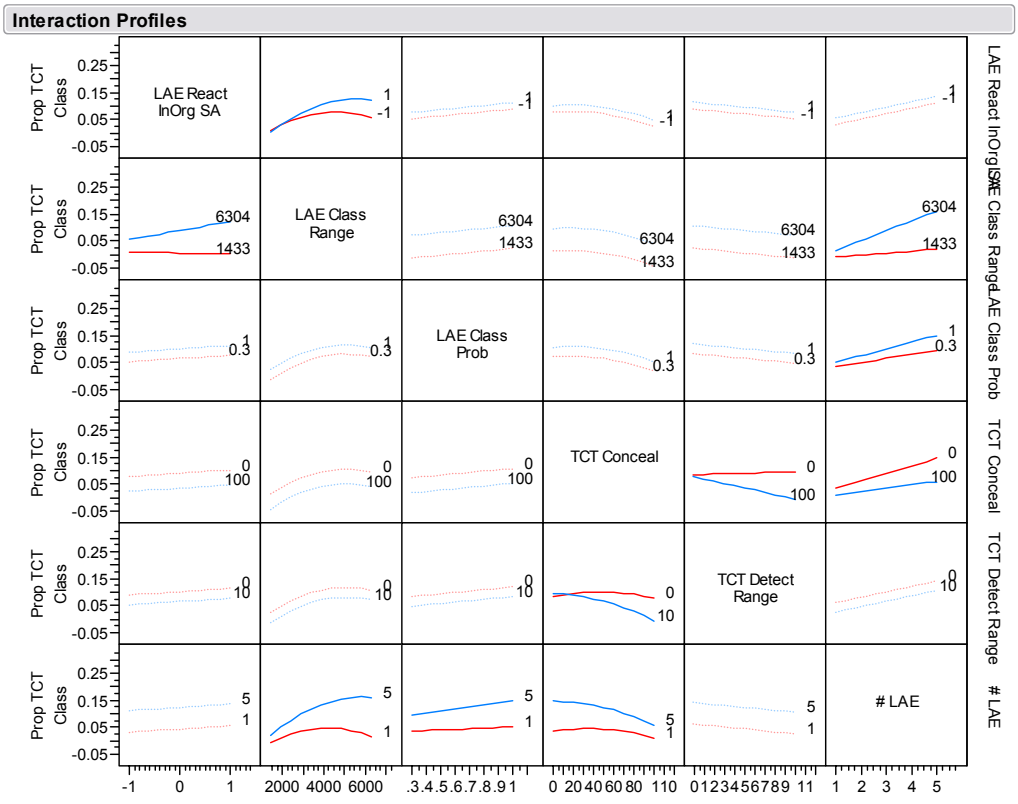

The partitioning tree shows a partition of the mean proportion of TCT classification that explains approximately 68.5% of the response variability. The right branch of each partition represents the split that offers a higher mean classification rate than the left branch. The first few tiers of the tree depict the most significant factors. The results are consistent with those suggested by the earlier observations.

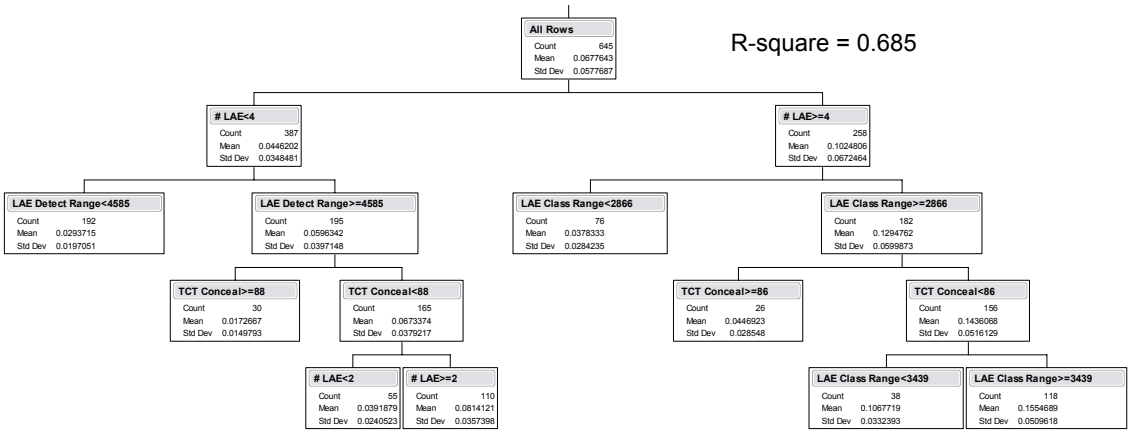

The Multiple Linear Regression models are also provided for the proportion of armor classified with consideration of only the main effects (left), the main and quadratic effects (right) and including the two-way interactions (next page).

Response Prop Armor Class

Summary of Fit

RSquare	0.546679
RSquare Adj	0.541697
Root Mean Square Error	0.07535
Mean of Response	0.192601
Observations (or Sum Wgts)	645

Analysis of Variance

Source	DF	Sum of Squares	Mean Square	F Ratio
Model	7	4.3614987	0.623071	109.7406
Error	637	3.6166781	0.005678	Prob > F
C. Total	644	7.9781769		<.0001

Parameter Estimates

Term	Estimate	Std Error	t Ratio	Prob>|t|
Intercept	-0.282286	0.028265	-9.99	<.0001
LAE React En Contact	0.0175678	0.005101	3.44	0.0006
LAE Airspeed	0.000538	0.000126	4.28	<.0001
MAE Detect Range	0.0000049	0.000001	3.42	0.0007
LAE Detect Range	0.0000168	0.000005	3.61	0.0003
LAE Class Range	0.000032	0.000005	6.25	<.0001
LAE Class Prob	0.0926305	0.01425	6.50	<.0001
# LAE	0.0310841	0.002098	14.82	<.0001

Response Prop Armor Class

Summary of Fit

RSquare	0.777112
RSquare Adj	0.773953
Root Mean Square Error	0.052919
Mean of Response	0.192601
Observations (or Sum Wgts)	645

Analysis of Variance

Source	DF	Sum of Squares	Mean Square	F Ratio
Model	9	6.1999396	0.688882	245.9965
Error	635	1.7782373	0.002800	Prob > F
C. Total	644	7.9781769		<.0001

Parameter Estimates

Term	Estimate	Std Error	t Ratio	Prob>|t|
Intercept	-0.218018	0.019501	-11.18	<.0001
LAE React InOrg SA	-0.014634	0.003583	-4.08	<.0001
LAE React En Contact	0.0154657	0.003583	4.32	<.0001
LAE Airspeed	0.000569	0.000088	6.45	<.0001
MAE Class Range	0.0000054	0.000001	5.14	<.0001
LAE Class Range	0.0000567	0.000002	33.85	<.0001
LAE Class Prob	0.0964538	0.010006	9.64	<.0001
# LAE	0.0310841	0.001473	21.10	<.0001
(LAE Class Range-3569.77)*(LAE Class Range-3569.77)	-2.196e-8	1.187e-9	-18.49	<.0001
(# LAE-3)*(# LAE-3)	-0.022495	0.001245	-18.06	<.0001

Response Prop Armor Class

Summary of Fit

RSquare	0.808431
RSquare Adj	0.804814
Root Mean Square Error	0.049174
Mean of Response	0.192601
Observations (or Sum Wgts)	645

Analysis of Variance

Source	DF	Sum of Squares	Mean Square	F Ratio
Model	12	6.4499617	0.537497	222.2841
Error	632	1.5282152	0.002418	Prob > F
C. Total	644	7.9781769		<.0001

Parameter Estimates

Term	Estimate	Std Error	t Ratio	Prob>|t|
Intercept	-0.221601	0.018155	-12.21	<.0001
LAE React InOrg SA	-0.014474	0.00333	-4.35	<.0001
LAE React En Contact	0.0158282	0.003331	4.75	<.0001
LAE Airspeed	0.0005793	0.000082	7.06	<.0001
MAE Class Range	0.0000056	9.857e-7	5.72	<.0001
LAE Class Range	0.0000568	0.000002	36.48	<.0001
MAE Class Prob	0.0617215	0.01893	3.26	0.0012
LAE Class Prob	0.0626223	0.013932	4.49	<.0001
# LAE	0.0310841	0.001369	22.70	<.0001
(LAE Airspeed-170.109)*(# LAE-3)	0.0002518	0.000058	4.34	<.0001
(LAE Class Range-3569.77)*(# LAE-3)	0.0000091	0.000001	8.58	<.0001
(LAE Class Range-3569.77)*(LAE Class Range-3569.77)	-2.191e-8	1.103e-9	-19.85	<.0001
(# LAE-3)*(# LAE-3)	-0.022495	0.001157	-19.44	<.0001

As before, the full model explains 80% of the variability while the main effect model and quadratic model explain only 54% and 77% respectively. The interaction terms account for less than 4% of the explanatory power in the full model. These terms are therefore deemed insignificant and the quadratic model is the model of choice for further analysis.

The actual by predicted plot on the left shows the lower tail of the distribution being cut off as the actual proportion can only take on values between zero and one. In the same manner, there are no negative residuals when the predicted value is less than or equal to zero, hence the residual by predicted plot appears capped by the 45 degree boundary on the bottom left of the plot. These results are less pronounced that for the TCT classification model. There is also some evidence of nonlinearity, which may be due to the omission of interaction terms, or because the underlying relationships that reveal diminishing returns are not exactly quadratic.

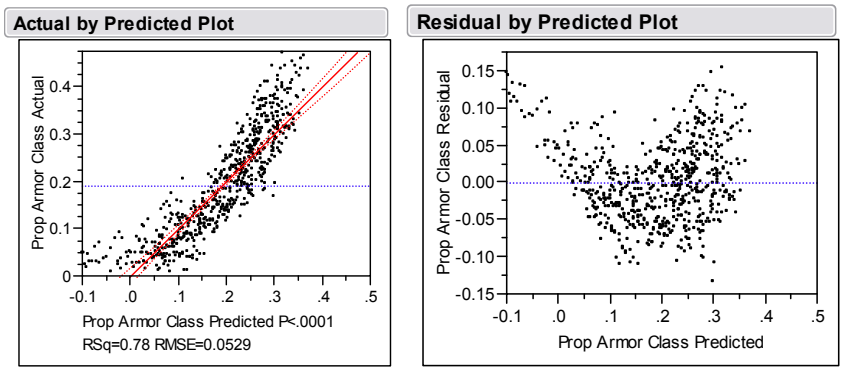

The Pareto plot displays the factors of significance in descending order in accordance to their effects on the proportion of armor targets classified.

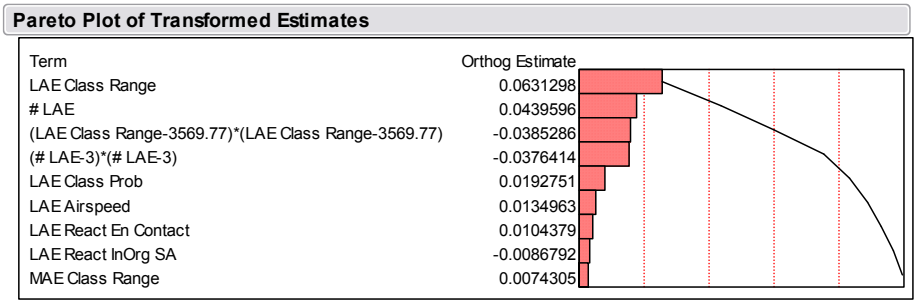

The prediction profiler graph shows significant non-linear relationships of the response variable against the number of LAEs and LAE classification range, both of these factors and their quadratics appear in the Pareto plot as the highest four factors with the most impact on the proportion of armor targets classified.

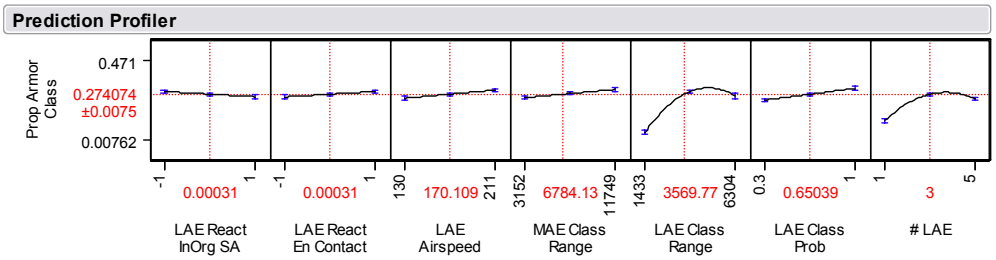

The partitioning tree depicts a partition of the mean proportion of armor classification which explains approximately 83.6% of the data variability. The first few tiers of the tree capture the non-linear relationships of the classification rate against the number of LAEs and LAE classification range as well.

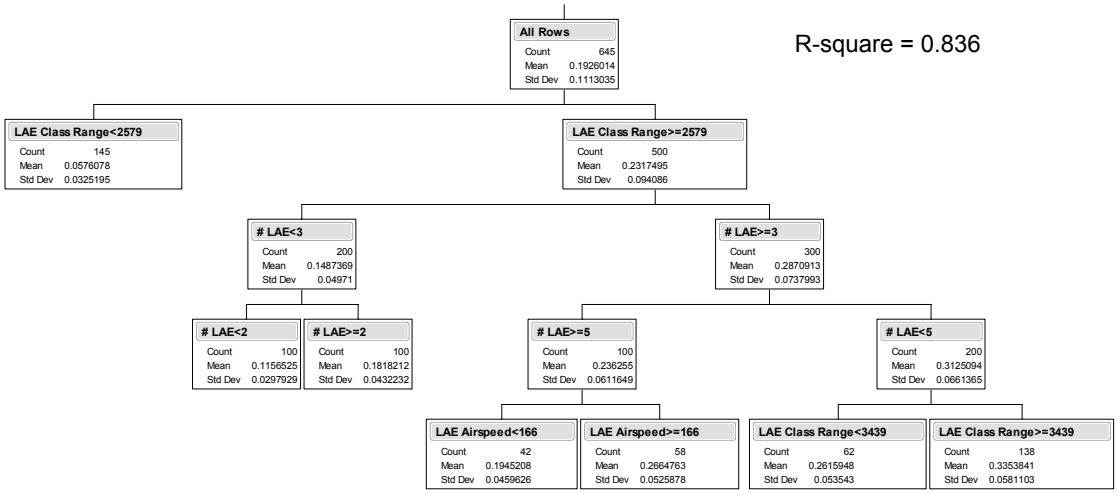

3. UAV BEHAVIORS

Contour plots showing the responsiveness of the LAEs toward newly classified enemy contacts and MAE redirections with respect to following the pre-assigned routings to support high target classification proportions.

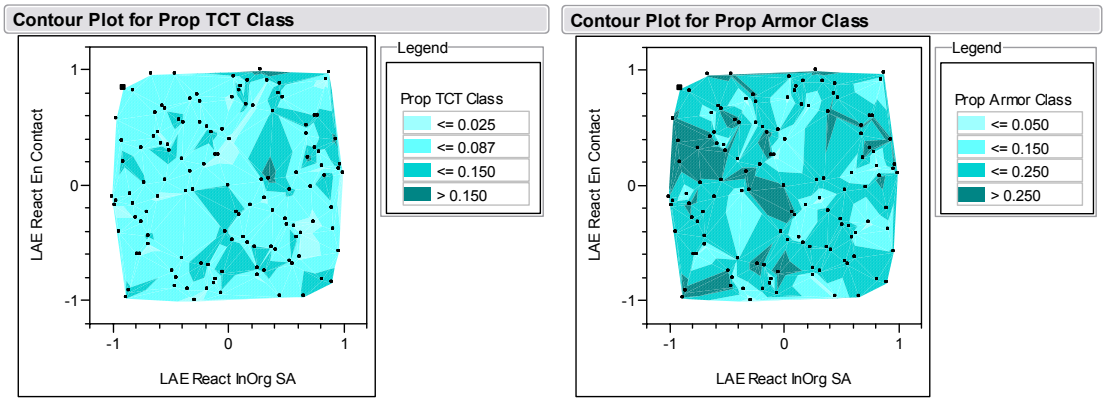

The dark blue patches show higher proportions of target classification than the light blue patches. It should be noted that the scales for the two contour plots are different. The plots show generally higher classification proportions on TCTs if an LAE is more reactive to MAE redirection, while no obvious benefit is seen by having an LAE be more reactive to a new classified enemy contact. For classifying armor targets, having LAEs react less to MAE redirection and more to a new classified enemy contact seems to improve the overall classification performance.

4. IMPACT OF LAE FAILURE

The following graphs depict the average proportions of TCT and armor classification due to the failure of an LAE at various time instances in the scenario with and without cooperative sensing capability.

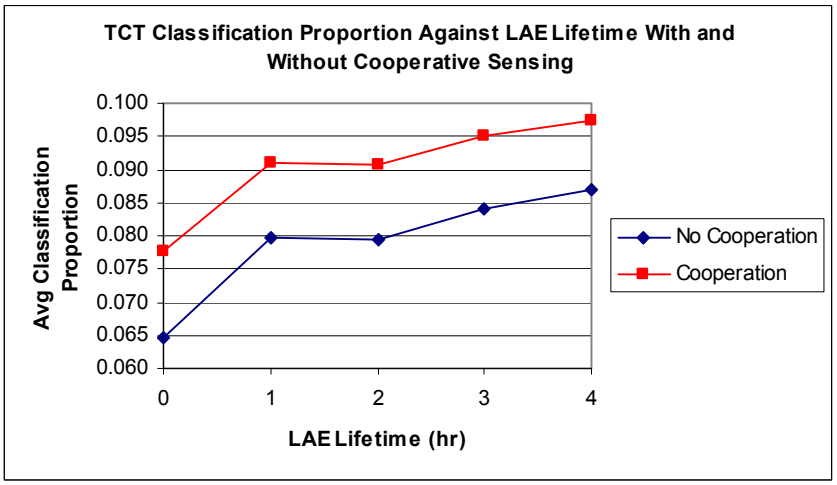

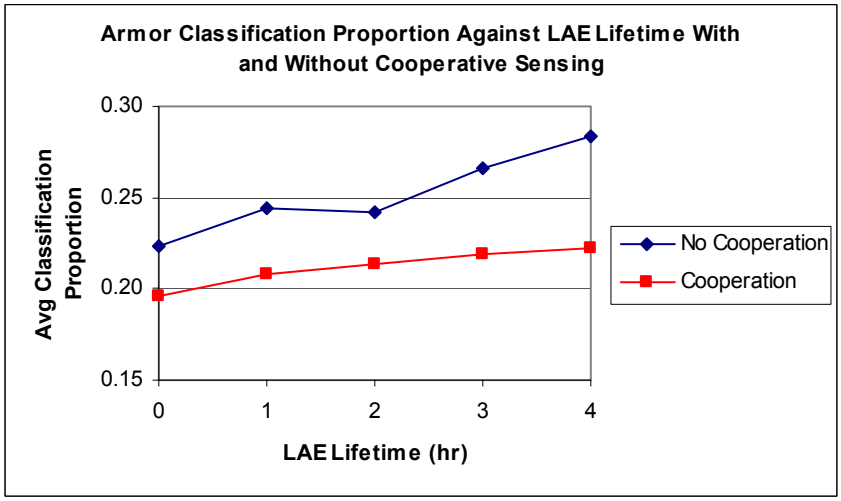

THIS PAGE INTENTIONALLY LEFT BLANK

LIST OF REFERENCES

Berner, A. R., The Effective Use of Multiple Unmanned Aerial Vehicles in Surface Search and Control. M.S. Thesis, Department of Operations Research, Naval Postgraduate School, Monterey, CA, December 2004.

Bitinas, E., PYTHAGORAS Manual - Not Published, 2004.

Bjorkman, E., Sheldon, R., Effects Based Operations Analysis of Counter Terrorism Using Agent Based Modeling. Proceedings of the 70th Military Operations Research Society Symposium, June 2002.

Cioppa, T. M., Efficient Nearly Orthogonal and Space-filling Experimental Designs for High-Dimensional Complex Models. Ph.D. Dissertation, Department of Operations Research, Naval Postgraduate School, Monterey, CA, 2002.

Cioppa, T. M., Lucas, T. W., Efficient Nearly Orthogonal and Space-filling Latin Hypercubes. Technometrics, forthcoming 2006.

Defense Modeling and Simulation Office website, <www.dmso.mil>, last accessed 17 July 2005.

Defense Modeling and Simulation Office Online M&S Glossary (DoD 5000.59-M) website, <https://www.dmso.mil/public/resources/glossary>, last accessed 21 October 2005.

Federation of American Scientists Intelligence Resource Program, Unmanned Aerial Vehicles website, <http://www.fas.org/irp/program/collect/uav.htm>, last accessed 8 July 2005.

Federation of American Scientists Military Analysis Network, X-45 Unmanned Combat Air Vehicle website, <http://www.fas.org/man/dod-101/sys/ac/ucav.htm>, last accessed 9 July 2005.

Galligan, D. P., Anderson, M. A., Lauren, M. K., Map Aware Non-uniform Automata (MANA) Users Manual, Current to MANA v3.0.37. Available for download at the MCWL website, July 2004.

Gonzales, D., Moore, L., Pernin, C., Matonick, D., Dreyer, P., Assessing the Value of Information Superiority for Ground Forces – Proof of Concept. RAND, 2001.

Hagee, W. M., General Commandant of the Marine Corps. A Concept of Distributed Operations. Headquarters USMC, Department of the Navy, Washington, DC, 25 April 2005.

JMP Statistical Discovery Software website, <http://www.jmp.com>, last accessed 1 December 2005.

Kleijnen, J. P. C., Sanchez, S. M., Lucas, T. W., Cioppa, T. M. A User's Guide to the Brave New World of Designing Simulation Experiments. INFORMS Journal on Computing, Vol. 17, No. 3, pp. 263-289. 2005.

Law, M. A., Kelton. W. D., Simulation Modeling and Analysis, Third Edition. McGraw Hill: New York, pp. 622-644. 2000.

Marine Corps Warfighting Laboratory Project Albert website, <http://www.mcwl.quantico.usmc.mil/Albert/home.cfm>, last accessed 22 July 2005.

Marine Corps Warfighting Laboratory Sea Viking website, <http://www.mcwl.quantico.usmc.mil/SV/home.cfm>, last accessed 11 August 2005.

McMindes, K. L., Unmanned Aerial Vehicle Survivability: The Impacts Of Speed, Detectability, Altitude and Enemy Capabilities. M.S. Thesis, Department of Operations Research, Naval Postgraduate School, Monterey, CA, September 2005.

Maui High Performance Computing Center website, <http://www.mhpcc.edu>, last accessed 21 October 2005.

North, M., Rimmer, M., Macal, C., Why the Navy Need TSUNAMI. Proceedings of the Seventh Annual Swarm Researchers Meeting, April 2003, <http://www.nd.edu/~swarm03/Program/Abstracts/NorthSwarm2003.pdf>, last accessed 16 November 2005.

Raffeto, M. A., Unmanned Aerial Vehicle Contributions to Intelligence, Surveillance and Reconnaissance Missions for Expeditionary Operations. M.S. Thesis, Department of Operations Research, Naval Postgraduate School, Monterey, CA, September 2004.

Sall, J., Creighton, L., Lehman, A., *JMP Start Statistics – A Guide to Statistics and Data Analysis Using JMP and JMP IN Software, Third Edition*. Thomson Brooks Cole, 2005.

Sanchez, S. M., Robust Design: Seeking the Best of All Possible Worlds. Proceedings of the 2000 Winter Simulation Conference, eds. Joines, J., Barton, R., Kang, K. Institute of Electrical and Electronic Engineers: Piscataway, NJ, pp. 69-76.

Sanchez, S. M., Simulation Experiments & Efficient Designs Lab NOLHdesigns Spreadsheet, <http://diana.cs.nps.navy.mil/SeedLab>, last accessed 20 August 2005.

Taguchi, G., Wu, Y., Introduction to Off-line Quality Control. Nagoya, Japan: Central Japan Quality Association, 1980.

The UAV Forum website, <http://www.uavforum.com/vehicles/vehicles.htm>, last accessed 8 July 2005.

Tighe, T. R., Strategic Effects of Airpower and Complex Adaptive Agents: An Initial Investigation. Air Force Institute of Technology, Wright-Patterson AFB, OH, March 1999.

US Joint Forces Command, Joint Lessons Learned: Operation Iraqi Freedom Major Combat Operations, Coordinating Draft. March 2004.

THIS PAGE INTENTIONALLY LEFT BLANK

INITIAL DISTRIBUTION LIST

1. Defense Technical Information Center
   Ft. Belvoir, Virginia

2. Dudley Knox Library
   Naval Postgraduate School
   Monterey, California

3. Professor Susan M. Sanchez
   Naval Postgraduate School
   Monterey, California

4. Professor David W. Netzer
   Naval Postgraduate School
   Monterey, California

5. LCDR Gordon Cross
   U.S. Special Operations Command
   MacDill AFB, Florida

6. Mr Erik Syvrud
   U.S. Special Operations Command
   MacDill AFB, Florida

7. Professor Tat Soon Yeo
   Temasek Defence Systems Institute
   Singapore

8. Ms Lai Poh Tan
   Temasek Defence Systems Institute
   Singapore

9. Mr Lawrence A. H. Liang
   Defence Science & Technology Agency
   Singapore